Electrical Properties Of Amorphous Semiconductor Devices

Mr D. Miles

23/8/94

ACKNOWLEDGEMENT.

I wish to thank Dr.C.P.Please for all his help and encouragement during my two years as his student. In addition, thanks to my family and friends for their support throughout my time at Southampton.

Abstract

The research in this document is based on the analysis of three specific problems of an amorphous MOS capacitor. The motivation for concentrating on this particular device is the relative simplicity of its design and operation, in addition to its diverse applications in electronic technology. The emission and capture processes of a single state, or trap, in the forbidden gap is extended to a continuous distribution to model the localised state distribution existing in amorphous semiconductors. With this concept of a continuous distribution of localised states in mind the basic semiconductor system of equations is transformed into a system that models amorphous semiconductors. These equations are well established and have been analysed by many people.

Each of the problems is concerned with a steady gate voltage being applied to an amorphous MOS capacitor. In the first problem the dopant in the semiconductor is assumed to be fully ionised and a steady solution is sought. The second problem also seeks a steady solution for the MOS capacitor, but more realistically assumes partial ionisation of the dopant atoms. In the final problem the short time transient behaviour of the MOS capacitor is analysed. The capacitor, initially in equilibrium, is subjected to a steady gate voltage, and the creation of a deep depleted region is found. However, the longer return of the device to equilibrium is not analysed.

In most devices the doping concentrations, represented by λ, are extremely large. This fact is exploited and the analyses of the problems are carried out in the limit as $\lambda \to \infty$. This greatly simplifies the problems, and the method of matched asymptotic expansions is applied. The presence of a continuous distribution of states in the forbidden gap complicates the analysis of amorphous semiconductor devices considerably. Therefore, to simplify, the concentration of the gap states is assumed small enough not to influence the semiconductor equations to highest order. Mathematically speaking, small gap state concentrations, represented by α, are assumed, and the equations are solved in the limit $\alpha \to 0$.

Contents

Chapter 1

Introduction

Much interest has arisen in the area of hydrogenated amorphous semiconductor devices, (a-Si:H to be succinct), over the past two decades. Cheapness and versatility of production of devices and their wide range of applications is the foundation for the enormous amount of work that has taken place. Perhaps the most important and well researched device is the amorphous silicon thin film transistor which was first proposed for applications by LeComber, [1], in 1979. Since then there has been extensive research resulting in the utilisation of these devices for many functions, especially in the field of large area electronics where significant market potential in low power portable computers and small televisions exists.

The properties and physics of conventional crystalline semiconductor devices are well understood. However, much research is being carried out to increase the knowledge of the equivalent amorphous devices. One of the main distinctions between these two materials is the structural order of the crystalline lattice, as opposed to the structural disorder of the amorphous state. A consequence of the disorder present in amorphous semiconductors is the existence of a continuous distribution of localised states in the forbidden gap. States in the forbidden gap also exist in crystalline semiconductors, arising from lattice defects and impurities, but occur at discrete energy levels. It is possible to reduce the discrete state concentrations, thus providing devices with more desirable properties. At present, the reduction of the gap states in amorphous materials to a suitable level has not been achieved. Endeavouring to understand both the disordered state and additional unusual behaviour of amorphous devices can only increase our knowledge of their operation. In particular, research into the instabilities, both for practical importance and fundamental insight into the basic properties, of these devices has been undertaken and will continue to take place. A major instability is the threshold voltage shift that occurs after prolonged application of a gate voltage to a thin film transistor. Charge trapping in the gate insulator and the metastable

creation of new states in the amorphous silicon has been proposed to account for this shift. Indeed, research into the creation of these new states has increased the understanding of the role of the states in the band gap and has resulted in a model for predicting the size and form of the forbidden gap states. This defect pool model is discussed in greater depth in Chapter 2.

Before entering into any detailed discussions on amorphous materials, I feel here is a good place to outline my thesis and the chapters contained within. The research in this document is based on the analysis of a Metal Oxide Silicon, or (MOS), capacitor. The motivation for concentrating on this particular device is the relative simplicity of its design and operation, in addition to its diverse applications in electronic technology. In Chapter 1 I give an introduction to some of the most well established devices used in the electronics industry. The purpose of this is to give the reader some insight into their operation, and application. The devices presented are well understood, and information on them can be found in most good general electronics texts. At the end of Chapter 1 I give a review of some of the papers written, and research undertaken, on the modelling of amorphous devices, and the problems that have been discovered. The beginning of Chapter 2 presents the reader with the most important concepts of semiconductor physics. It then proceeds to give a brief insight into the derivation of the basic semiconductor device equations. These form a well established model describing the operation of crystalline semiconductor devices. The more important recombination and generation processes are then outlined. In particular, the emission and capture processes of a single state, or trap, in the forbidden gap is illustrated. The concept of this single trap is then extended to a continuous distribution to model the localised state distribution existing in amorphous semiconductors. With this concept of a continuous distribution of localised states in mind the basic semiconductor system of equations is then transformed into a system that models amorphous semiconductors. Since the existence of this continuous distribution of states in the forbidden gap is the single most important difference between crystalline and amorphous semiconductors a detailed review and explanation of the defect pool model is given. Research into this concept has provided a model for predicting and understanding the formation of gap state distributions in amorphous semiconductors. At the end of Chapter 2 the three problems that constitute my research are presented. Each is clear. The first seeks a steady-state solution for an MOS capacitor subject to a steady gate voltage. The dopant in the semiconductor is assumed to be fully ionised. The second problem seeks a steady solution for the MOS capacitor also subject to a steady gate voltage, but more realistically assumes partial ionisation of the dopant atoms. In the final problem the short time transient behaviour of the MOS capacitor is analyzed. The capacitor, initially in equilibrium, is subjected to a steady gate voltage, and the creation of a deep depleted region is found. However, the longer return of the device to equilibrium is not analyzed. In most devices the doping concentrations, represented by λ, (explained in Chapter 2), are extremely

large. This fact is exploited and the analyses of the problems are carried out in the limit as $\lambda \rightarrow \infty$. This greatly simplifies the problems, and the method of matched asymptotic expansions is applied. The presence of a continuous distribution of states in the forbidden gap complicates the analysis of amorphous semiconductor devices considerably. Therefore, as a simplification, the concentration of the gap states is assumed small enough not to influence the semiconductor equations to highest order. Mathematically speaking, small gap state concentration, represented by α, are assumed, and the equations are solved in the limit $\alpha \rightarrow 0$. The behaviour of these gap states can then be seen from the solutions obtained in the hope of helping to give an insight into how they could influence device characteristics.

1.1 Devices and their applications

The devices that have most research interest are junction field effect transistors, (J-FET's), metal oxide silicon capacitors, (MOS capacitors), metal oxide silicon field effect transistors, (MOSFET's), thin film transistors, (TFT's), and p-type-intrinsic-n-type diodes, (PIN diodes). I now give a brief outline of each of these devices operation, unwanted behaviour and application. As mentioned previously the understanding of these devices, except for TFT's, is well established and the descriptions given can be found in most electronic texts. However, references [2], [3], and [4] are used specifically to write this section. The subsections on TFT's and PIN diodes refer in addition to [6], and [7].

1.1.1 The Junction Field Effect Transistor.

The conductance of J-FET's and MOSFET's involve predominantly one carrier type and they are referred to as unipolar devices so as to distinguish them from bipolar transistors, in which both carrier types are involved. Basically, the J-FET is a voltage controlled resistor. A simplified diagram is given in figure 1.1. In particular, consider a J-FET consisting of an n-type channel sandwiched between two p^+ layers. I could have equally chosen the converse, a J-FET with a p-type channel sandwiched between two n^+-type layers. However, there would be no additional insight into the operation of the device and I therefore only consider the former case.

The term n-type or p-type refers to a semiconductor whose electronic properties are dominated by electrons or holes, respectively. The concept of a hole, considered to be a positively charged particle, is explained in the next chapter. An n^+-type or p^+-type semiconductor has similar electronic properties to the equivalent n-type or p-type material, but the respective carrier concentration is much greater.

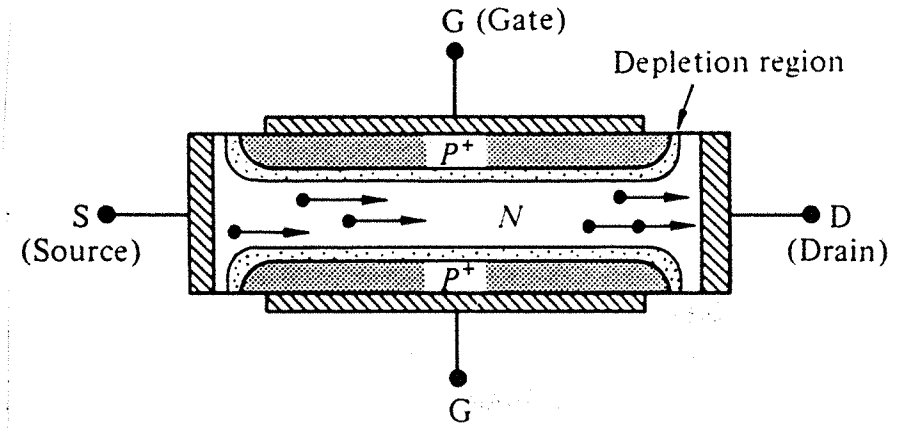

Figure 1.1: Cross section of a J-FET structure.

Consider the normal operating conditions when the two gate electrodes are tied to the same potential. I will refer to the potential of the drain relative to the source as V_D, and the potential of the gate relative to the source as V_G. Firstly, the gate electrodes are grounded, ($V_G = 0$), and the drain voltage is zero, $V_D = 0$. Under these conditions the device is in thermal equilibrium. The p^+n junctions behave like p-n diodes in equilibrium, implying the existence of small depletion widths at the top and bottom of the device. This is shown in figure 1.2 (a). When $V_D > 0$, a drain current, denoted I_D, begins to flow through the non-depleted n-region, (known as the channel). For small V_D, the thickness of the depletion region along the length of the channel is approximately constant and the device acts as a simple linear resistor, as shown in figure 1.2 (b). The operation corresponds to the linear part of the graph in figure 1.3. When V_D is increased further the approximation is no longer valid and the device enters a new phase of operation.

The voltage varies linearly across the channel from a high voltage at the drain end to a low voltage at the source end. Thus, the p-n junction near the drain end is more strongly reverse biased than the junction at the source end. Hence, the depletion width increases as one proceeds from the source to the drain, as shown in figure 1.2 (c). Thinking of the channel as a resistor, a decrease in its volume will mean an increase in its resistance. So, the widening of the depletion widths will decrease its volume and therefore increase its resistance. This is observed in the non-linear part of the characteristics, shown in the graph in figure 1.3. A drain voltage, V_{Dsat}, is reached when the upper and lower depletion regions connect, this is known as pinch off, and is shown in figure 1.2 (d). When the device is pinched off, the slope of the $I_D - V_D$ characteristic becomes approximately zero. For

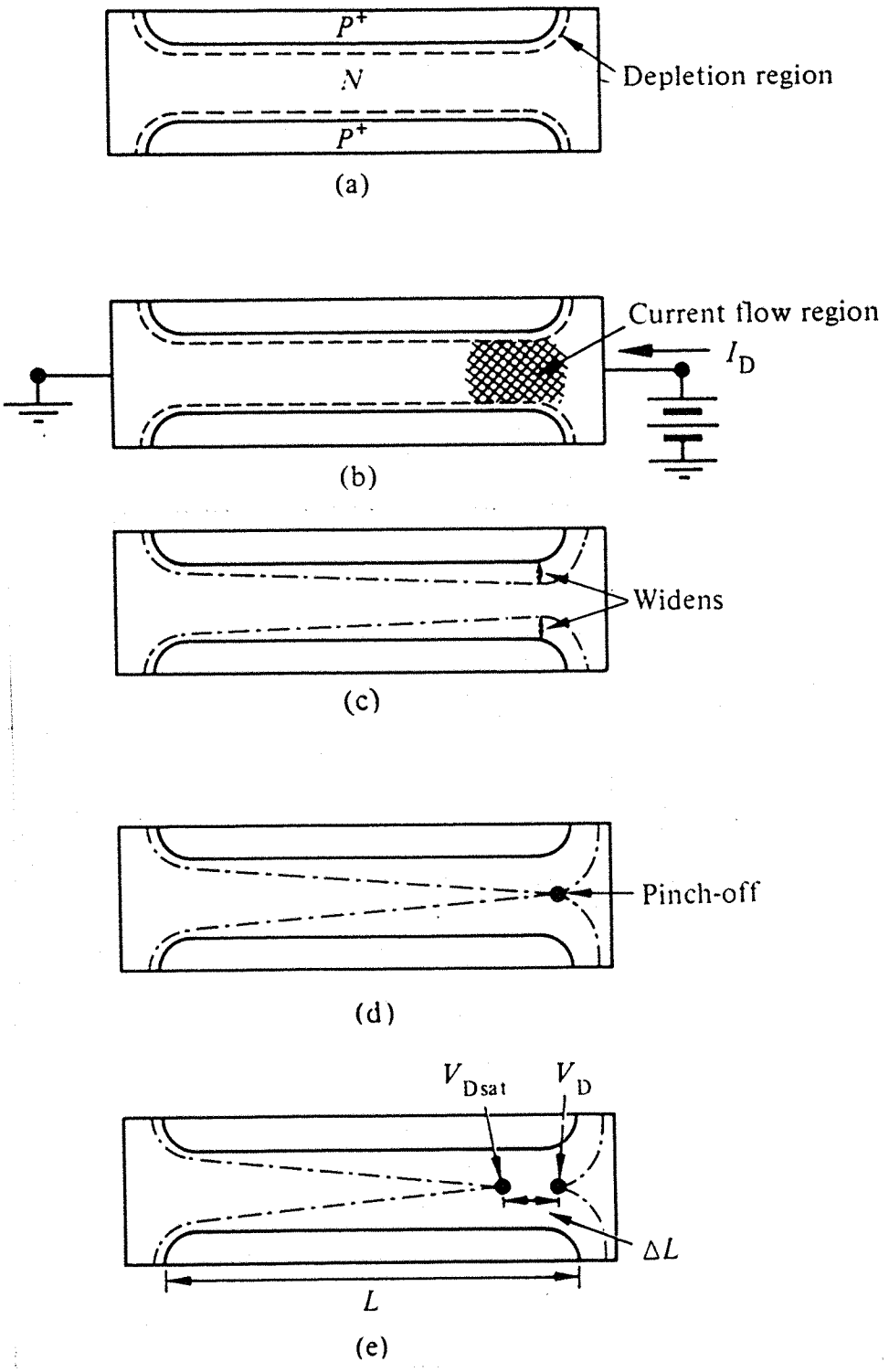

Figure 1.2: (a) A J-FET in equilibrium, (b) small V_D biasing, (c) channel narrowing under moderate V_D biasing, (d) pinch-off, and (e) post pinch-off, ($V_D > V_{Dsat}$).

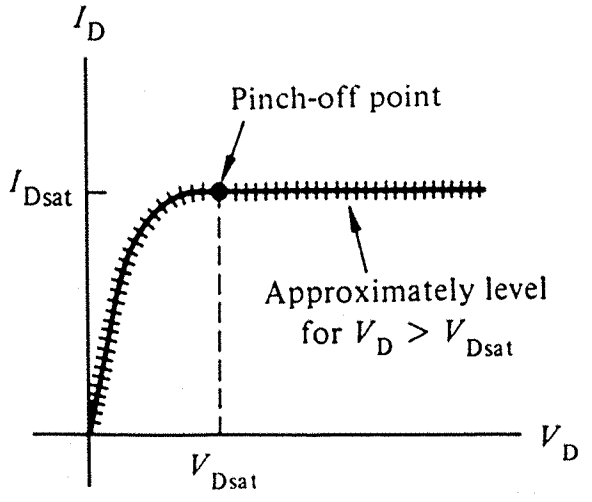

Figure 1.3: The $I_D - V_D$ characteristics when $V_G = 0$.

$V_D > V_{Dsat}$, the current, I_D, remains approximately constant at the value I_{Dsat} and is said to be saturated.

The above is a simple explanation of the device performing under zero bias conditions, i.e. when $V_G = 0$. I now consider the operation of the J-FET when $V_G < 0$. The operation of the device is similar to $V_G = 0$ operation, but with three modifications. Firstly, if $V_G < 0$ the top and bottom p^+n junctions are in reverse bias, even for $V_D = 0$. The increased depletion widths imply a thinner channel. Therefore, a larger channel resistance results. The linear mode of operation therefore has a smaller slope on the corresponding I_D-V_D characteristic, as shown in figure 1.4. Secondly, since the channel is narrower, pinch off occurs at a smaller drain bias and a smaller saturation current results.

Finally, the applied gate voltage can be decreased so much that the entire channel becomes depleted, even for zero drain voltage, as shown in figure 1.5. This voltage is known as the pinch-off gate voltage, V_P. For $V_G < V_P$, the drain current is essentially zero for all drain biases.

In the section on MOSFET's, the non-ideal behaviour described could equally apply to J-FET's. The reader is therefore referred to this section for any relevant information.

There is considerable overlap in the characteristics of MOSFET's and J-FET's. Therefore, I start with a discussion of some of the common properties possessed by both of these devices and then describe some of the characteristics unique to the J-FET.

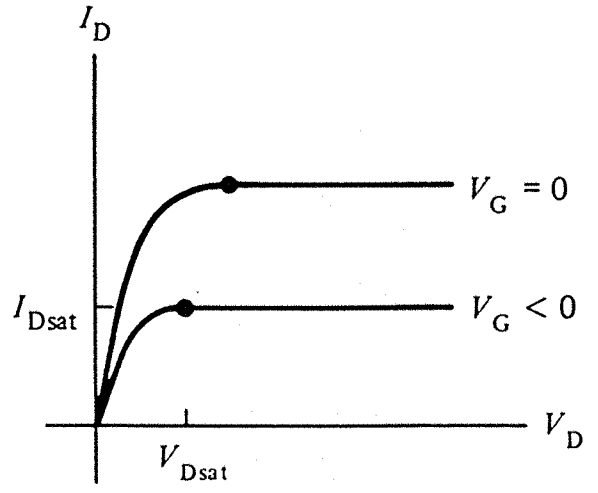

Figure 1.4: General form of the $I_D - V_D$ characteristics when $V_G < 0$.

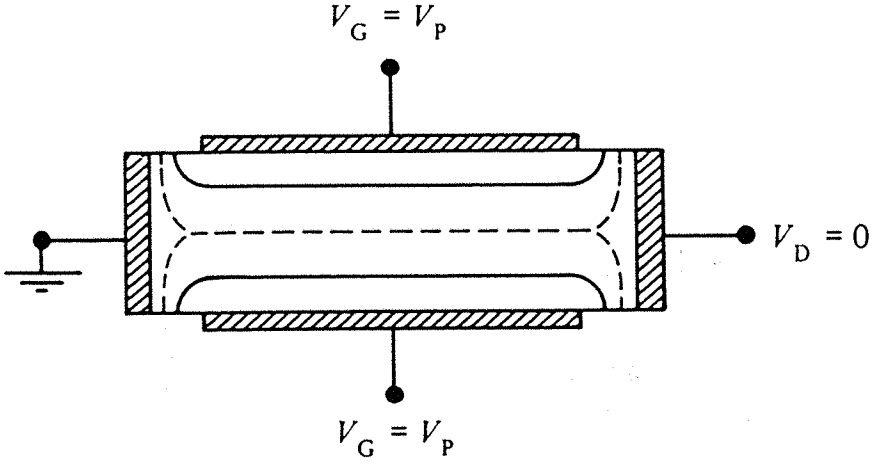

Figure 1.5: Gate pinch-off.

J-FET's and MOSFET's in general are of use in analogue switching, high input impedance amplifiers and microwaves. Noting that these devices are relatively simple, coupled with the fact their size can be easily reduced, fabrication onto densely packed circuits is possible. They have considerably higher input impedance than bipolar transistors, which allows the input of to be more readily matched to the standard microwave system. J-FET's and MOSFET's have a negative temperature coefficient at high current levels, that is, the current decreases as the temperature increases. This characteristic leads to a more uniform temperature distribution over the device area and prevents thermal run away, which occurs in the bipolar transistor. The devices are thermally stable even when the active area is large, or when many devices are connected in parallel. Because J-FET's and MOSFET's are unipolar devices, they do not suffer from minority carrier storage effects, consequently they have higher switching speeds, and higher cut off frequencies. By appropriate gate biasing, the resistance between the drain and source of a J-FET can be made very low (a few ohms as opposed to 20Ω in a bipolar transistor), or very high (a thousand megaohms as opposed to a few mega ohms in a bipolar transistor). Thus, the J-FET is well suited to being used as a switch. J-FET's are superior to bipolar transistors as regards to the input current they require. Since the gate of a J-FET is a reverse biased pn junction the dc gate current is very small indeed, so the signal power input is negligible. Although J-FET amplifiers may exhibit rather small voltage gains, their signal power gain can be very large. This means they are well suited to digital circuits, since these only need a voltage gain of 1.

1.1.2 MOS Capacitor.

The research in Chapters 3, 4 and 5 is based on mathematical analysis of the MOS capacitor. So, I undertake the task of giving a more detailed qualitative grounding in its operation, as compared with the other devices mentioned.

I consider the semiconductor substrate to be p-type. Referring to figure 1.6, it can be seen that the MOS capacitor is a simple two terminal device composed of a thin silicon oxide layer sandwiched between a silicon substrate and a metal plate. The usual plate material is aluminium or heavily doped polycrystalline silicon. The thickness of the oxide layer is between $0.01\mu m$ and $1.00\mu m$.

To simplify matters considerably a few assumptions are made about the device.

1. The metallic gate is a perfect conductor so it can be considered an equipotential.

2. The oxide is modelled as wide gap semiconductor.

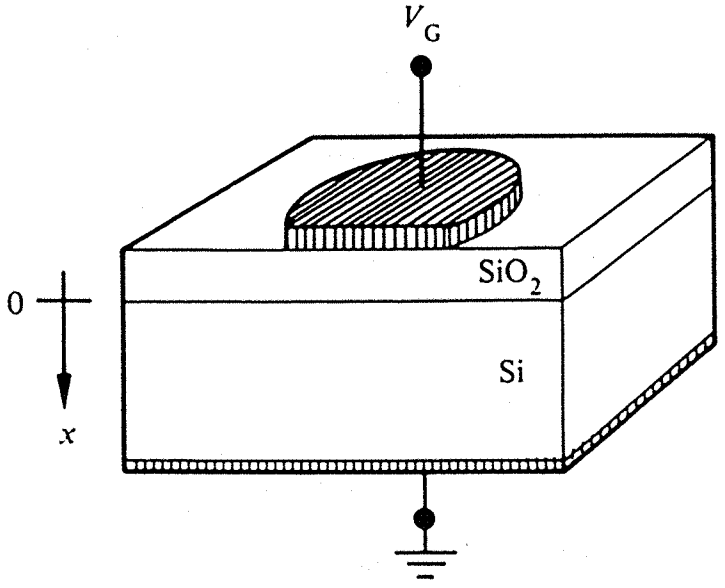

Figure 1.6: The metal-oxide-semiconductor capacitor.

3. There are no interface charge centres or charge centres in the insulator.

4. The semiconductor is long enough that a field free region is established before reaching the end of the device.

5. There is zero work function difference between the metal and semiconductor. (This will be elaborated on later in the section).

6. The analysis of the device only applies to a strip near the middle of the device, extending from the oxide-silicon interface to the back of the silicon substrate, illustrated in figure 1.6. Edge effects can therefore be ignored and the dependent variables can be considered functions of x only, (where the x co-ordinate is defined as the perpendicular distance from the oxide-silicon interface to a point inside the p-type substrate).

7. The semiconductor is uniformly doped.

8. An ohmic contact exists between the semiconductor and the metal on the back side of the device.

All of the qualitative descriptions are in terms of energy band diagrams. References [2] and [3] are good introductory text giving a good grounding in the basic concepts of energy band diagrams.

The diagram in figure 1.7 is of the resulting bands in the MOS capacitor. The dotted line at the top of the diagram, known as the vacuum level, is denoted

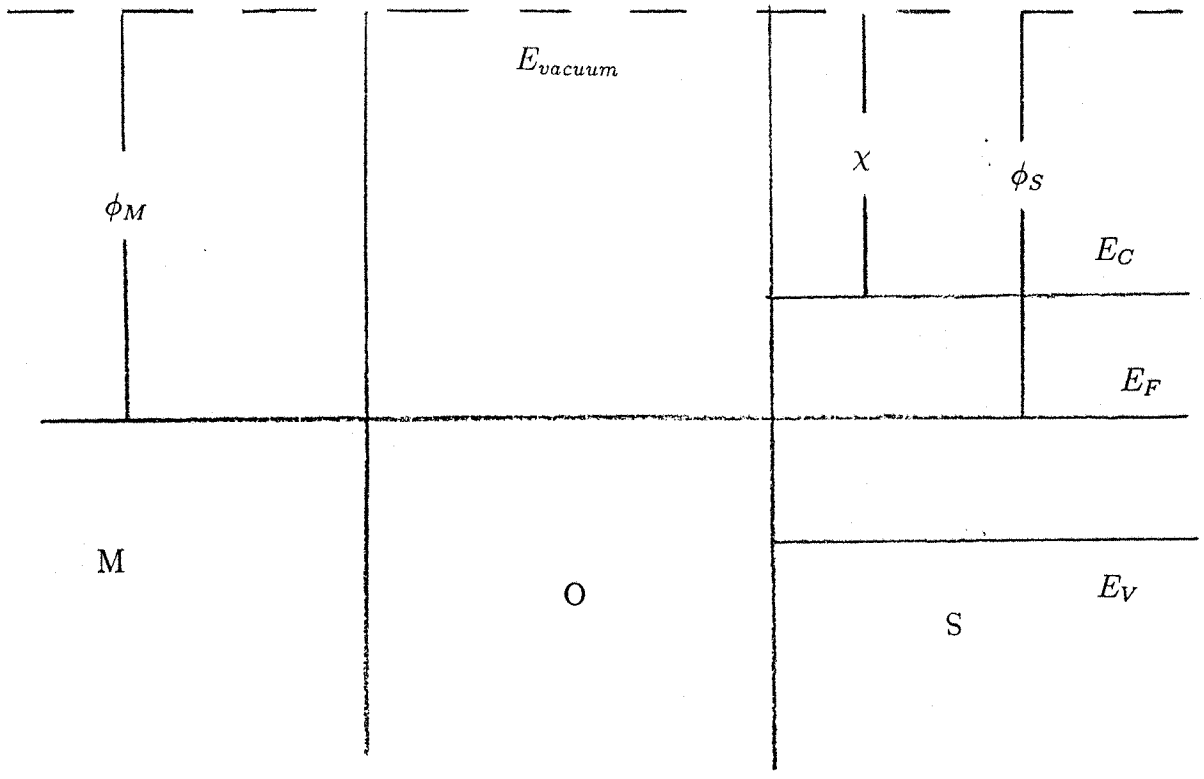

Figure 1.7: Individual energy band diagrams for the metal, insulator and semiconductor.

E_{vacuum}, and represents the minimum energy an electron must posses to completely free itself from the material. In a metal, the energy difference between the vacuum level, E_{vacuum}, and the Fermi energy, E_F, is known as the work function, ϕ_M. In the semiconductor the height of the surface energy barrier is specified in terms of the electron affinity, χ, the energy difference between the vacuum level, E_{vacuum}, and the conduction band edge, denoted E_C, at the surface. χ is used instead of $E_{vacuum} - E_F$, since the latter quantity is not a constant in semiconductors, but varies as a function of doping and band bending near the surface. Since the Fermi levels must line up in any structure in thermal equilibrium, and because $\phi_M = \phi_S = \chi + (E_C - E_F)$, in a perfect MOS capacitor, where ϕ_S denotes the work function of the semiconductor, the vacuum levels in the metal and semiconductor are in perfect alignment. Thus, no charges or electric fields are induced into the system. Even when there is an applied gate voltage the Fermi level in the metal or semiconductor remains constant over x, since it is assumed there is zero current flow under steady conditions.

Applying a negative voltage to the metal, a negative charge is effectively deposited there. In response, an equal but positive charge appears at the semiconductor surface, known as the accumulation layer, shown in figure 1.8 (a). Since the applied negative voltage depresses the electrostatic potential of the metal relative to the semiconductor, the electron energies are raised in the metal relative to the semiconductor. Therefore, the Fermi level in the metal lies above its equilibrium position by an amount qV, where q is the charge of a proton and V is the applied gate voltage. This causes a tilt in the oxide conduction band. This seems reasonable

since an electric field causes a gradient in E_i, E_C and E_V, from the equation,

$$E(x) = \frac{1}{q}\frac{dE_i}{dx},$$

where E_i is the Fermi energy of the intrinsic semiconductor, E_C energy of the conduction band edge and E_V the energy of the valence band edge. The reader is referred to Chapter 2 for a more detailed definition of these quantities. From elementary Fermi statistics, it can be shown that in equilibrium, holes and electrons are described by,

$$p = n_i \exp\left(\frac{E_i - E_F}{kT}\right),$$

and,

$$n = n_i \exp\left(\frac{E_F - E_i}{kT}\right),$$

respectively. Here k is Boltzmann's constant, T is the temperature in degrees Kelvin, E_F is the Fermi energy level and n_i is the intrinsic carrier concentration of the semiconductor. Again the reader is referred to Chapter 2 for more detailed explanations of these quantities. The bending up of the E_i energy band causes an increase in the concentration of holes, (from the above relation). Thus, as intuition would tell us, a negatively applied voltage causes holes to build up near the semiconductor surface. Applying a positive voltage, the potential of the metal relative to the semiconductor is raised, lowering the metal Fermi level by an amount qV. As a result the oxide conduction band and the semiconductor bands bend. From the hole concentration equation it can be seen that as E_i bends toward the semiconductor Fermi level the hole concentration drops near to its intrinsic level. Since the negatively charged dopant acceptor ions that are present cannot move, this area, depleted of holes, acquires a net negative charge, as shown in figure 1.8 (b).

Continuing to increase the voltage further, the bands bend more strongly. In fact, for sufficiently large bias E_i bends below the Fermi level. In this situation the electron concentration is greater than the hole concentration. The region near the semiconductor surface has the conduction properties of an n-type material. This region is known as the inversion layer. This inversion layer, separated from the p-type substrate by a depletion layer, is the key to MOS operation. The energy band diagram for inversion is shown in figure 1.8 (c).

Above is a qualitative description of the operation of the MOS capacitor. However, there are many assumptions made that are not true in a real device.

Firstly, the difference between the Fermi energy and the vacuum level is unlikely to be the same in the isolated metal and semiconductor components, (i.e. there is a work function difference). The ideal theory is easily modified to account for this,

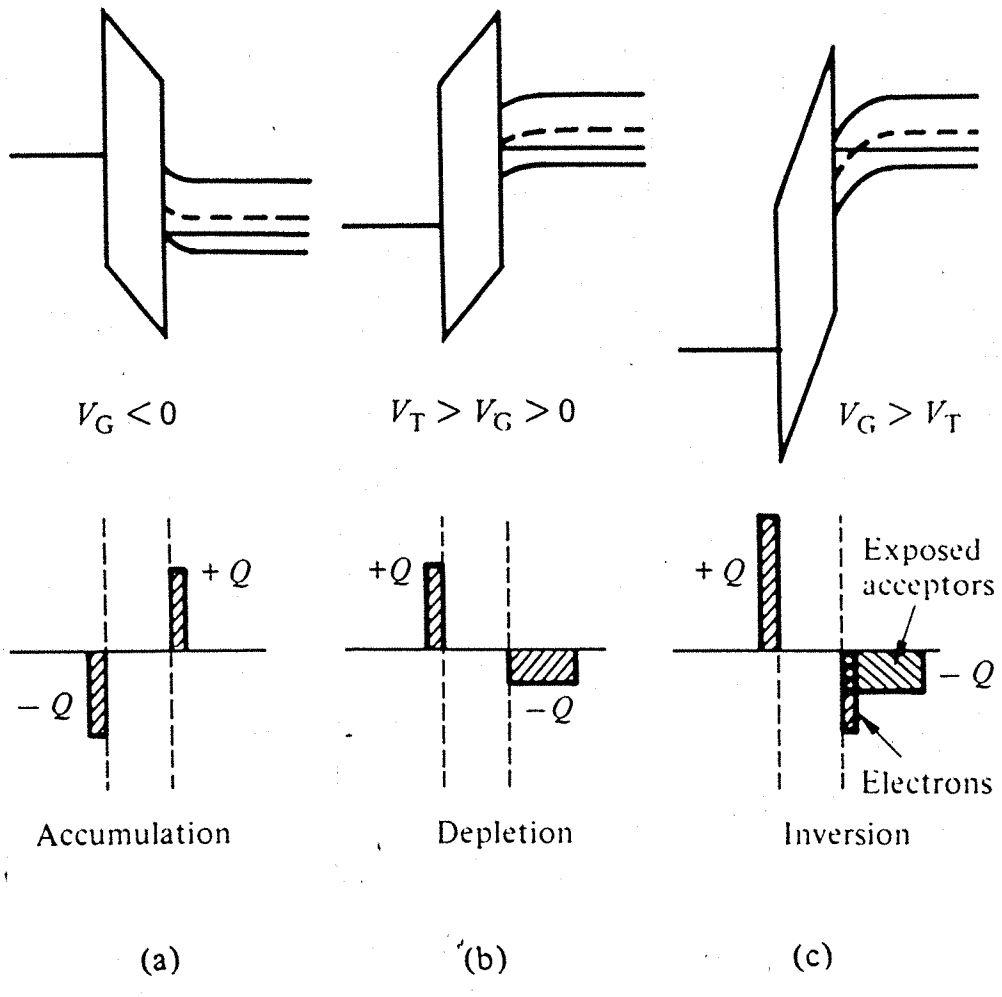

Figure 1.8: Energy band and block charge diagrams for a p-type device in, (a) accumulation, (b) depletion, and (c) inversion.

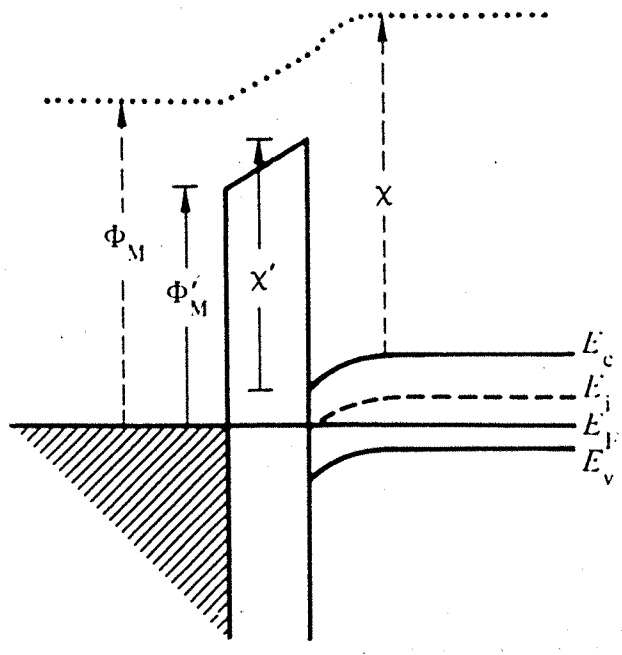

Figure 1.9: Equilibrium, ($V_G = 0$), energy band diagram typical of real MOS structures.

and it is found there is simply a built-in potential given by,

$$\phi_{MS} = \frac{1}{q}(\phi_M - \phi_S) \ .$$

Flat band, for the ideal device occurs at zero gate voltage. But as can be seen from the figure 1.9, a negative voltage $V_G = \phi_{MS}$ must be applied to the non-ideal device to achieve flat band conditions. Having a non-zero work function difference is a relatively minor non-ideality, since it only causes a voltage shift in the device characteristics, and is incapable of causing instabilities.

Oxide charges can, on the other hand, give rise to large voltage shifts and instabilities. There are various types of charge centres as outlined below.

1)Mobile Ions

When subjected to bias-temperature stressing, a common reliability testing procedure where a device is heated under bias to accelerate device degrading processes, the MOS device characteristics are shifted positively or negatively, depending on the sign of the bias. In extreme circumstances the instability can be observed at room temperature. It is now well established that the instability is caused by mobile ions inside the oxide layer. The voltage shift is found to be dependent on where the charge is located in the layer, and in fact the shift is largest when the ions are near to the oxide-semiconductor interface. Specifically, Na^+, Li^+ and K^+ ions are found to be the dominant cause, present in chemical reagents and glass apparatus. Care is taken to reduce the contamination, and new manufacturing

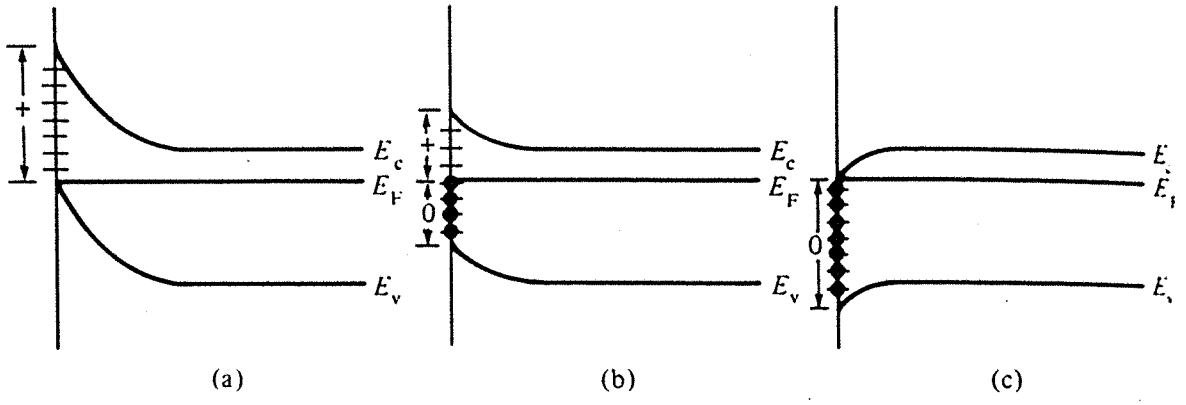

Figure 1.10: Filling of interface traps under, (a) inversion, (b) depletion, and (c) accumulation.

processes have been developed to minimise the effects further.

2)Fixed Charges

Another voltage shift is explained by the presence of charge located near to the oxide-semiconductor interface. This charge is reproducibly fabricated and fixed in position. It is found be to independent of oxide thickness, doping concentration, and the semiconductor type, (n or p). During the thermal formation of the Si-SiO_2 layer, the oxidising species diffuses through the oxide and reacts at the Si-SiO_2 layer to form more Si-SiO_2. Thus, the last oxide formed lies closest to the Si-SiO_2 interface and contains the fixed oxide charge. This fixed oxide charge is due to excess ionic silicon, which has broken away from the silicon lattice, and is waiting to react in the vicinity of the Si-SiO_2 interface, where the oxidation process is abruptly terminated. Annealing in an inert atmosphere apparently reduces the excess reaction components, and thereby lowers the fixed charge.

3)Interfacial Traps

Interfacial traps are allowed energy states in which electrons are localised in the vicinity of a material's surface. These traps introduce a continuous distribution of energy levels into the forbidden gap at the Si-SiO_2 interface. Interface levels do occur at energies greater than E_C or less than E_V, but such levels are obscured by the much larger density of conduction or valence band states. Figure 1.10 gives some understanding of the role of these states. In the following explanation the traps are assumed to be donorlike, (i.e. positively charged when empty, and neutral

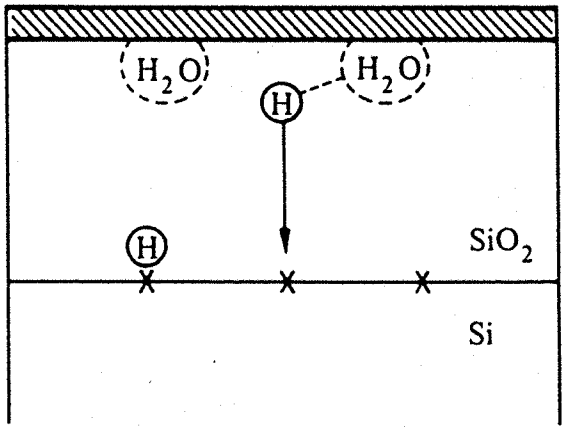

Figure 1.11: Annihilation of interface states during the post-metalisation annealing process.

when filled). To first order approximation, all energy levels above the Fermi level E_F are empty, and all those below are full. Thus, the movement of the Fermi level changes the amount of charge contained in these traps. Under accumulation most of the traps lie above E_F and are therefore empty. This then gives a maximum positive charge. Under inversion however, most of the states are below E_F, and hence full. Therefore, the charge contained is at a minimum value. The important thing to note is the traps charge and discharge as a function of bias, thereby affecting the charge distribution in the device, and hence the device characteristics.

Much experimental evidence supports the view that interfacial traps are caused by the existence of "dangling" bonds at the surface of the semiconductor. When the silicon lattice abruptly terminates along a given plane to form a surface, one of the four surface atom bonds is left dangling. The thermal formation of the SiO_2 layer ties up some but not all of the Si surface bonds. It is the remaining dangling bonds that become the interfacial traps.

Annealing of MOS devices is performed to minimise the interfacial trap concentration. This is accomplished in one of two ways.

1) Post-metalisation annealing - In this process, which requires a chemically active gate material such as Al or Cr, the metalised structure is simply placed in a nitrogen surrounding at $\approx 450°C$ for 5 to 10 minutes. During the formation of the MOS structure, minute amounts of water vapour become absorbed on the SiO_2 surface. At the postmetalisation annealing temperature the active gate material

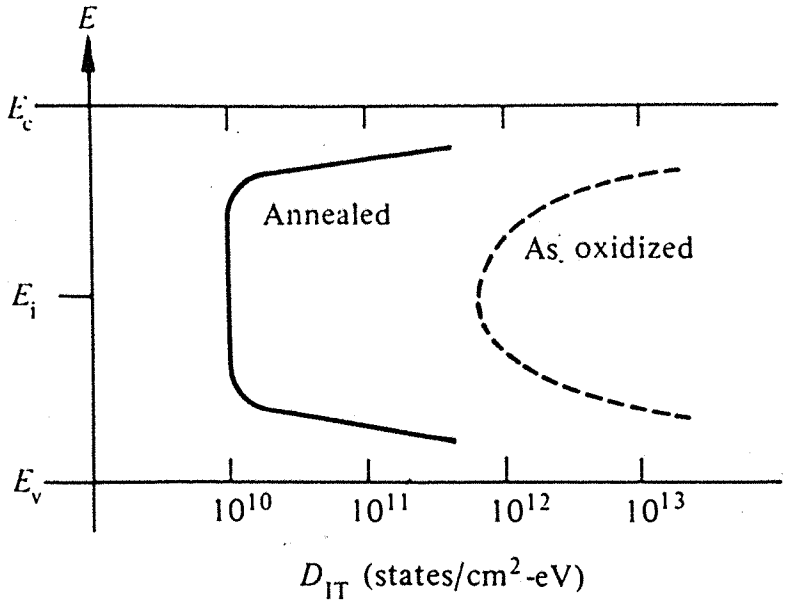

Figure 1.12: General form of the interfacial trap density observed before and after annealing.

reacts with the water vapour on the oxide surface to release a hydrogen species. As illustrated in figure 1.11 a hydrogen species then migrates through the SiO_2 layer to the Si-SiO_2 interface, where it attaches itself to a dangling bond, thereby making the bond electrically neutral.

2) The hydrogen-ambient process - This operates on a similar principle, except the hydrogen is supplied directly in the ambient environment and the structure need not be metalised.

Figure 1.12 shows the concentration of surface traps before and after annealing. As can be seen the interfacial trap density is more or less constant over the mid-gap region and increases rapidly as one approaches the band edges. The states near the two band edges are usually about equal in number and opposite in their charging character, (i.e. states near the conduction and valence bands are acceptorlike and donorlike in nature, respectively).

One of the more important applications of the MOS capacitor is its use in charge coupled devices (CCD's). These are dynamic devices that move charge along a predetermined path under the control of clock pulses.

The basis of the CCD is the dynamic storage and withdrawal of charge in a series of MOS capacitors. If a positive gate voltage is applied to a MOS capacitor for a sufficiently long time, electrons accumulate at the surface and the steady state inversion layer exists. The time required to fill this "potential well" is called the thermal relaxation time. For good materials the thermal relaxation time is much

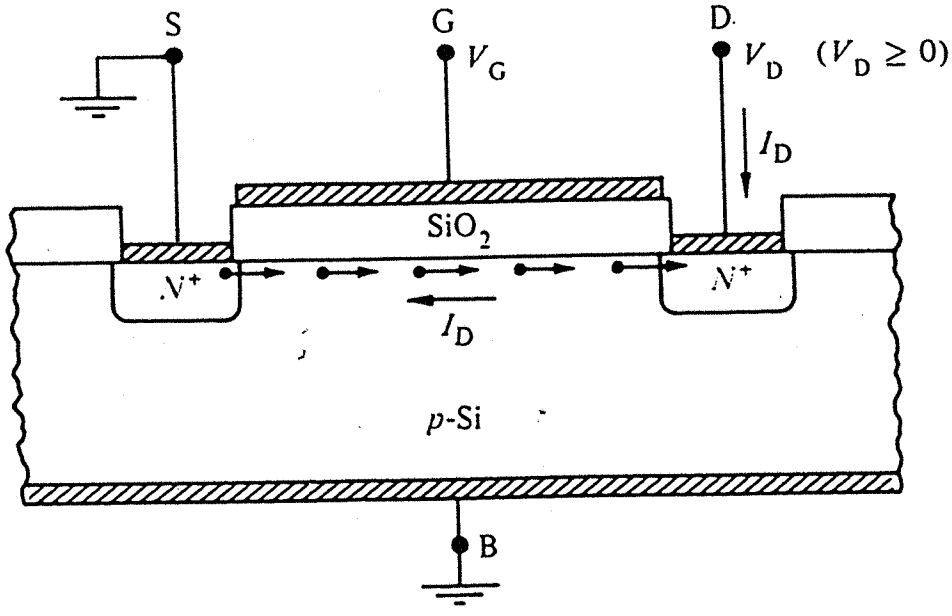

Figure 1.14: Cross-sectional view of the basic p-bulk (n-channel) MOSFET structure.

1.1.3 Metal Oxide Silicon Field Effect Transistors (MOSFET's).

Essentially, a MOSFET is no more than a MOS capacitor with two pn junctions placed immediately adjacent to the region of the semiconductor controlled by the MOS gate. The device can either have a p-type substrate and two n^+ islands or an n-type substrate with p^+ islands. I will consider the former case. An illustration of the device is shown in figure 1.14. As with the J-FET, the source is the end where the majority carriers enter the device, and the drain is the end where they leave. The voltage applied to the gate relative to ground is denoted V_G, and the voltage applied to the drain relative to ground is denoted V_D. The source and back of the device are grounded.

Consider an applied a gate voltage with no drain bias. When the applied V_G results in accumulation or depletion the region between the source and drain islands has either an excess or deficit of holes, but always very few electrons. Thus, under these conditions there is effectively an open circuit between the source and drain. But when V_G is applied so there is inversion, there exists an n-type conducting channel, as shown in figure 1.15 (a). V_T is defined as the depletion-inversion transition point voltage. Thus, if $V_G < V_T$, the device is in depletion or accumulation, and $V_G > V_T$ the device is in inversion. Now that there is an induced channel an applied drain voltage will result in a drain current, denoted I_D. For small positive voltages the channel is a simple resistor and the resulting current is proportional to the applied voltage. Note that the application of this drain voltage

means the pn junctions are in reversed bias, and therefore the associated leakage currents will contribute to the drain current. In most devices these currents are so small they can be ignored. Once V_D is increased above a few tenths of a volt the device enters a new phase of operation, where the voltage drop from the drain to the source starts to negate the inverting effect of the gate.

As illustrated in figure 1.15 (b) the depletion region widens going from the source to the drain end, and the number of carriers in the inversion layer decreases. The reduction in the number of carriers in the channel reduces the conductance, and hence means a decrease in the slope of the I_D-V_D characteristics. The greatest decrease in carriers occurs at the drain end. Eventually, a situation is reached, shown in figure 1.15 (c), when the region near the drain end completely disappears. This is referred to as pinch off and corresponds to the slope of the characteristic approaching zero. For drain voltages in excess of the pinch off voltage the channel widens from just a point to a depleted channel of length δL. The pinched off section absorbs most of the voltage drop in excess of V_{Dsat}, since this is a depletion region and is high in resistance. If the device is long in comparison to δL, then the shape of the conducting n channel, and the potential applied across it remain invariant and the current I_{Dsat} remain invariant.

The above results can be used to obtain a complete set of characteristics, illustrated in figure 1.16. For $V_G < V_T$ the gate voltage does not create a surface channel, and $I_D = 0$. Since the conductance of the channel increases with increasing V_G it follows that the slope on the $I_D - V_D$ characteristics increases with increasing V_G. Also, the greater V_G then the more inversion layer carriers there are present, so the larger the drain voltage to achieve pinch off. Thus, V_{Dsat} increases with increasing V_G.

In the above calculations, the channel length is assumed to be long, but as this channel length is reduced departures from long channel behaviour may occur. Short channel effects arise from 2-d potential distributions, and high electric fields in the channel region. As the channel length is reduced, the depletion layer widths of the source and drain junctions become comparable to the channel length. The potential distribution in the channel now depends on both the transverse field E_x, (controlled by the gate and bulk surface bias), and the longitudinal field E_y, (controlled by the drain bias). In other words, the potential becomes 2-d and the gradual-channel approximation, ($E_x \gg E_y$), is no longer valid. As the electric field increases, the channel mobility becomes field dependent, and eventually velocity saturation occurs. In addition, a non-uniform doping concentration can exist in the channel, leading to deviations from ideal behaviour. Modern MOSFET technologies use ion implantation extensively to improve device performance. This ion implantation causes a threshold voltage shift, which has to be taken into account.

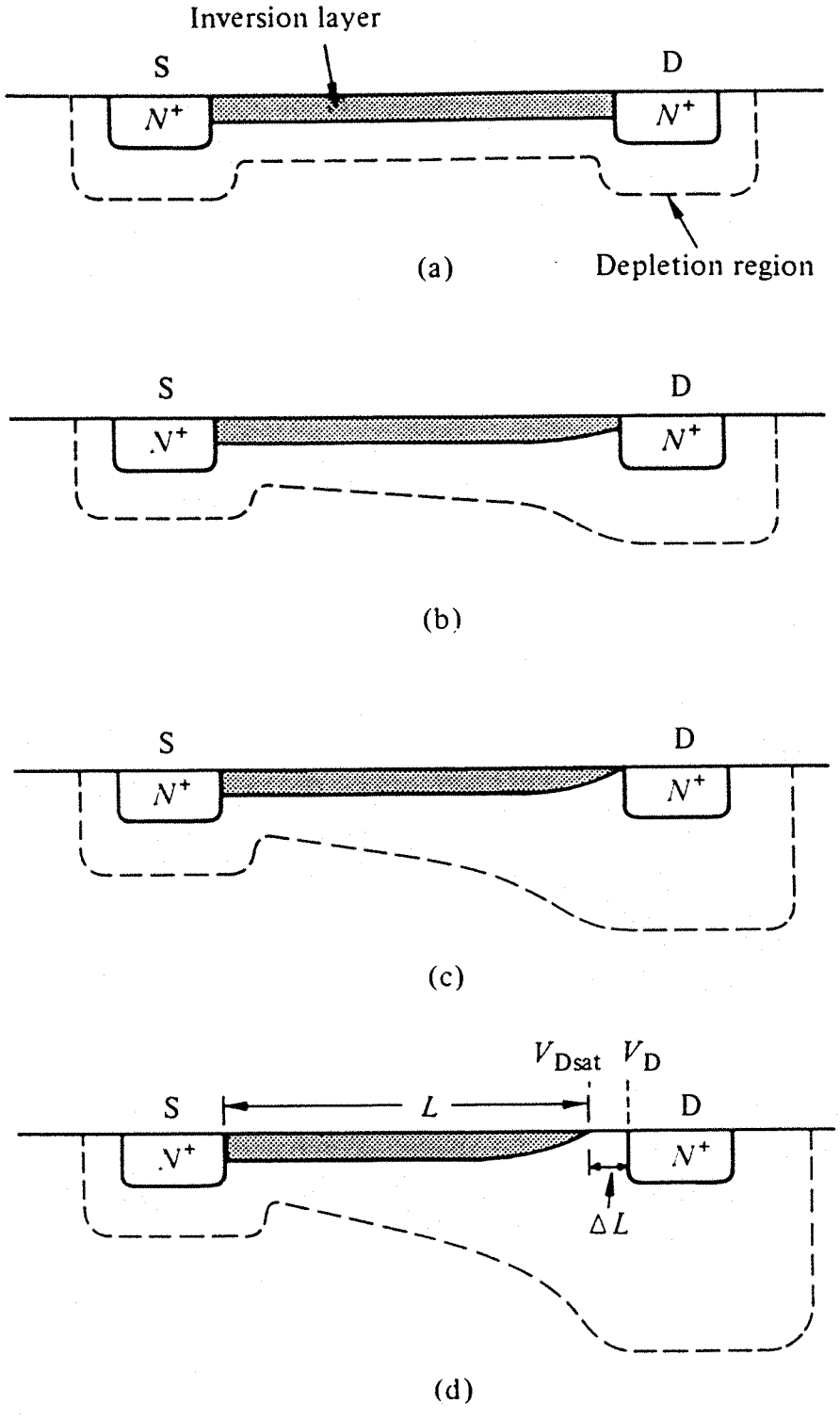

Figure 1.15: The different phases of MOSFET operation, (a) $V_D = 0$, (b) inversion layer narrowing under moderate V_D biasing, (c) pinch-off, and (d) post pinch-off.

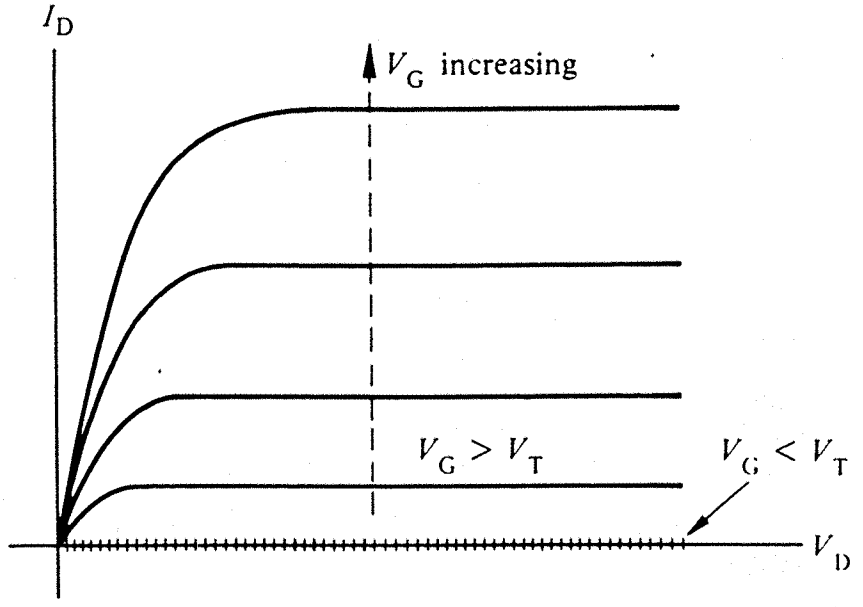

Figure 1.16: General form of the $I_D - V_D$ characteristics expected from a long channel MOSFET.

MOSFET's are the most important devices used in very large scale integrated circuits, such as microprocessors and semiconductor memories. They are also important power devices. Other applications are elaborated on in the previous section on J-FET's.

1.1.4 Thin Film Transistors (TFT's)

The active region of the device is a thin polycrystalline or amorphous film of semiconductor, laid down by evaporation or some epitaxial technique on an insulating substrate. The device itself, shown in figure 1.17 (a), is composed of very thin layers deposited on an insulating substrate, whereas the MOS transistor is formed by diffusion or deposition on a semiconductor substrate. The difference is of considerable importance, since the use of a semiconductor substrate forms a severe restriction in the design and fabrication of integrated circuits. The electrical isolation of the TFT and any other circuit elements deposited on the same substrate results in simplified fabricating procedures, and increased design flexibility. The understanding of these devices is less advanced than MOS transistors, and they suffer from a variety of instability problems.

The characteristics are similar to the MOSFET and are shown figure 1.17 (b).

The polycrystalline or amorphous semiconductor deposited contains a considerable number of traps close to the insulator-semiconductor interface. These

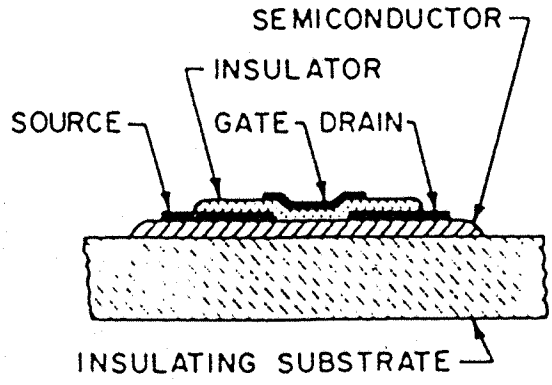

(a)

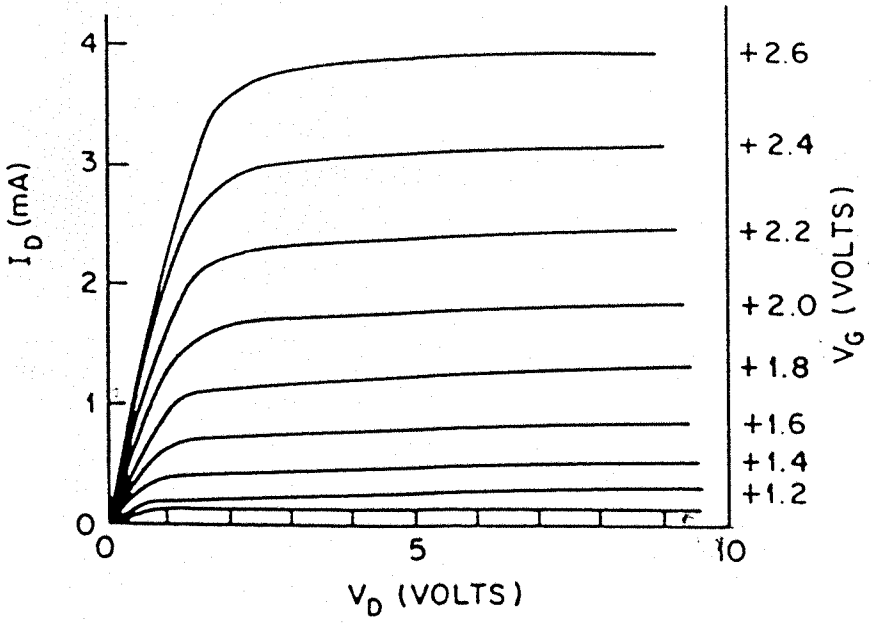

(b)

Figure 1.17: (a) Cross-sectional view of a typical TFT. (b) General form of the $I_D - V_D$ characteristics for a TFT.

traps appear to dominate the device threshold voltage, rather than the oxide charges as in the case of the MOS transistor. It operates by forming an accumulation layer rather than an inversion layer. Hence, the channel produced is the same conducting type as the semiconductor. The accumulation layer is formed by the metal gate charge attracting majority carriers into the semiconductor. If a sufficient number are attracted to more than fill up the traps present, the conductance from drain to source will be increased. On the other hand, if there is a high density of surface states present which trap more majority carriers in the surface region, the device behaves like a depletion MOS device.

Because the semiconductor layer is formed by deposition, more defects and crystalline imperfections occur in the layer than in the corresponding single crystal semiconductor, resulting in more complicated transport processes. In a-Si:H there exists a continuous distribution of localised states in the band gap, which causes even larger deviations from ideal behaviour. To improve device performance, reproducibility and reliability, the bulk and interface trap densities are reduced. The high density of traps present on the surface and in the bulk of the device are the cause of instability. One of the most important is the threshold voltage shift, that occurs after a prolonged gate voltage of an a-Si:H TFT. This is caused by charge trapping in the gate insulator, and the creation of metastable states in the a-Si:H layer.

T.F.T's are becoming widely used in a range of input and output circuitry in displays, image scanners, and printers. A-Si:H has made a major impact on these applications because of the relative ease with which the material can be manufactured over large areas. Systems where visual images for human interfaces need to be generated, sensed, and transmitted require the use of large area devices. The application of TFT's to liquid crystal displays is the first example of this new technology. A-Si:H has already made a major impact in TFT and sensor technology because of the existence of a manufacturing capability in a-Si solar cells, where large area films with well defined electronic properties are fabricated on glass. In a complex high density LCD display there is a requirement for an active element to switch each pixel in the display. Various TFT's and diodes are used for this purpose, however, the most widely used system is the a-Si:H TFT active matrix LCD display.

1.1.5 P-type insulator N-type Diodes (PIN Diodes)

The device, illustrated in figure 1.18 (a), basically consists of a p-n junction with a doping profile tailored so an intrinsic layer, the 'i' region, is sandwiched between a p and n layer. However, the idealised i region is approximated by either a high resistivity p layer, (π layer), or a high resistivity n layer, (ν layer). The variation of

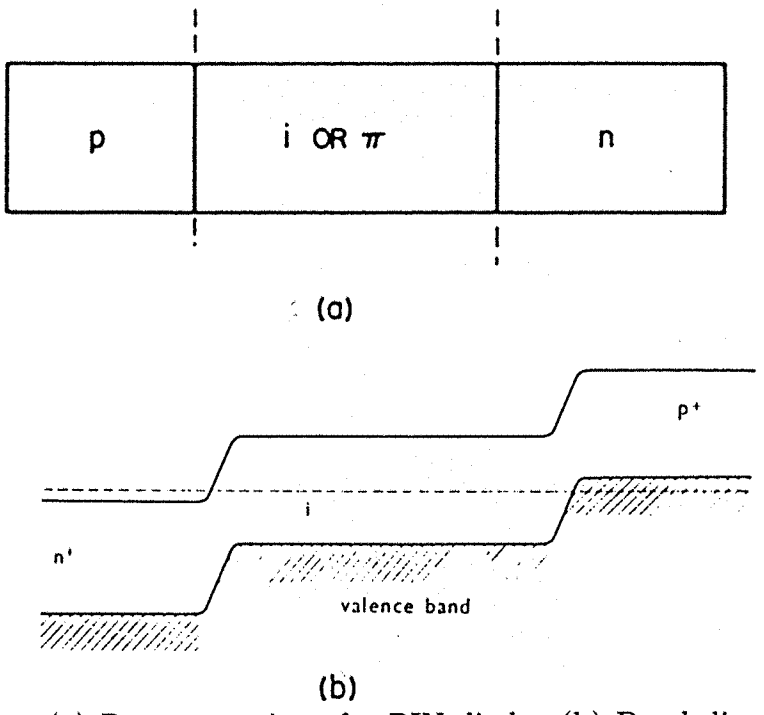

Figure 1.18: (a) Representation of a PIN diode. (b) Band diagram of a PIN diode under equilibrium.

the conduction and valence band energy levels at equilibrium are illustrated in figure 1.18 (b). As can be seen, the Fermi levels line up, and the built-in voltages at the two i-region edges prevent any net flow of charge. The drift of electrons, (or holes), in one direction, is exactly balanced by the diffusion of electrons, (or holes), in the other.

On reverse bias, figure 1.19 (a), the depletion region extends right across the intrinsic region into the edge of the p and n contacts. Since there are no impurities in the i-region, there is no charge from the ionised impurities, and the field is constant. The field only falls to zero near the highly doped contacts. By making the width of the i layer long, the breakdown field E_b can be reached only at large voltages, $V_b = E_b \times d$. Thus, the PIN diode makes a good high voltage rectifier.

The PIN diode does not behave in quite the same manner on forward bias as the conventional pn junction. When a forward bias is applied to the device, the drift-diffusion balance is upset, as seen in figure 1.19 (b). The applied electric field opposes this built-in field, and hence the drift of the carriers is reduced. Thus, the diffusion of carriers from their respective regions will flood the i-region. However, any holes close to the n region, and any electrons close to the p region are pushed back into the i region. Thus, injected carriers are confined mainly to the i-region by these fields at the i-region edges. The distribution is more or less uniform, with equal numbers of holes and electrons. With a recombination time τ_r,

$$I = \frac{dQ_s}{dt} + \frac{Q_s}{\tau_r},$$

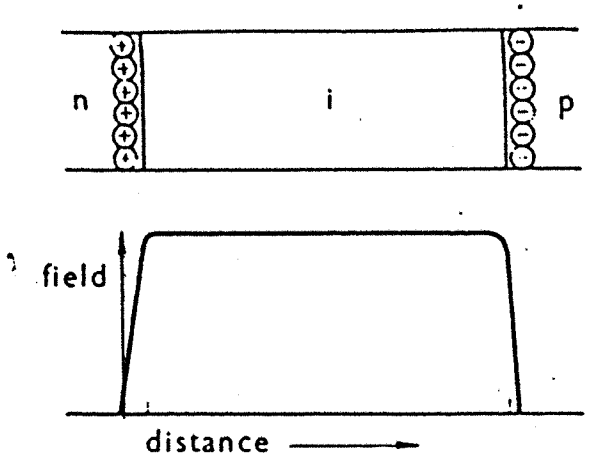

(a)

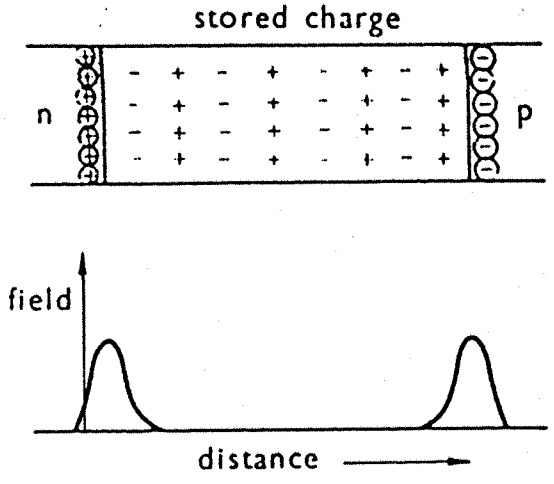

(b)

Figure 1.19: Diagram representing field and charge on, (a) reverse bias, and (b) forward bias.

where Q_s - the amount of stored charge. In steady state,

$$I\tau_r = Q_s \ .$$

The voltage applied across the terminals is such to give,

$$I \approx I_s \exp \frac{eV}{\nu kT} \qquad\qquad \nu \approx 2 \ ,$$

where I_s is the reverse bias saturation current, e is the electronic charge of an electron, V is the voltage applied across the device and ν is the emission coefficient of the device. Thus, if τ_r is large enough, the diode has a low voltage and a high charge, and consequently look like a high capacitance on forward bias. However, on reverse bias, once the charge carriers have been removed from the depletion region, the diode looks like a low capacitance. This behaviour is very useful for non-linear applications where signals of different frequencies have to be mixed together.

Like all pn junctions, the forward bias state cannot be immediately reversed until the storage charge is removed. However, unlike the pn junction, the stored minority charge is not buried in the p and n regions where the electric field cannot penetrate. It is stored in the i-region, where on reverse bias the electric fields can remove the carriers with a velocity of up to $10^5 \mathrm{ms}^{-1}$, (for Si). Thus, when the diode is biased from a forward to a reverse state, the final stages of the removal of charge can be very rapid, and the voltage will snap to a high reverse voltage. Such diodes are known as step recovery or snap diodes.

The PIN diode has found wide applications in microwave circuits. It can be used as a microwave switch, with essentially constant depletion layer capacitance and high power handling capability. In addition, the PIN diode is used as a variable attenuator by controlling the device resistance, which varies approximately linearly with the forward current.

1.2 A Review Of The Relevant Research Publications

Many papers have been written on amorphous semiconductors and it is the purpose of this section to give a review of some of these publications. The topics of research germane to my studies are the recombination statistics of carriers, the understanding of the distribution of defect states in the forbidden gap, and the various physical characteristics that amorphous devices possess. Of particular importance to the defect densities is the defect pool model. This model is used to understand and predict the types of defect distributions that occur in amorphous

silicon devices under given chemical conditions. A summarised review of the papers written on the defect pool model is given here, but a more detailed account is presented in Chapter 2.

Thin film transistors feature heavily in the research of amorphous devices, since they are very important in the new technology, and a comprehensive guide to the physics and performance issues of these devices is given in [7]. It explains the problems that these devices posses and many of the characteristics, which largely seem to be determined by the band gap defect distribution. In addition, a paper by [8] gives an account of the physics and applications of amorphous thin film transistors and image sensors.

One of the earliest and perhaps most important papers written on the statistics of recombination of semiconductor devices is by W.Shockely and W.T.Read, [9]. It describes the basics of recombination of holes and electrons via a single trap in the band gap and explains some non-equilibrium steady-state processes in crystalline semiconductors. The mechanisms explained here form the basis for the modelling of amorphous semiconductor devices. The concept of a single trap in the band gap is extended to a continuous arbitrary distribution of traps and the basic crystalline semiconductor device equations are transformed into a system describing amorphous semiconductor devices. Joze Furlan, [10], then develops an analytical approach to these amorphous device equations. A set of approximate equations, describing excess carrier non-equilibrium in an amorphous semiconductor, are obtained by integrating only over regions bounded by electron and hole trap quasi-Fermi levels in both acceptor-like and donor- like states. A paper by J.G.Simmons and G.W.Taylor, [11], applies Shockely-Read-Hall statistics to an arbitrary distribution of traps under non-equilibrium steady-state conditions. A form identical to the occupancy function f in the single trap case results. They proceed to analyze some of the more important properties of this statistic. In addition, there are discussions of charge neutrality, net rate of recombination and free carrier lifetimes. Finally, an expression for the photocurrent in an amorphous semiconductor is obtained. A subsequent paper by J.G.Simmons and G.W.Taylor, [12], applies the theory to steady-state photoconductivity in amorphous semiconductors. A further paper by J.G.Simmons and G.W.Taylor, [13], investigates the energy dependence of the statistic, f, and there is a categorisation of traps into shallow traps, recombination centers, and dead states.

Computer simulations by J.G.Shaw, M.Hack, and P.G.LeComber, [14], have been developed to describe the transient behaviour of amorphous silicon diodes and thin film transistors. The full set of amorphous device equations are solved, fully accounting for the traps in the band gap. These traps are assumed to obey Shockely-Read-Hall kinetics. Good agreement between experimental data and numerical simulations are shown. F.R. Shapiro, [15], has developed a general

purpose simulator for transient experiments in semiconductors and insulators based on microscopic transport of carriers including an arbitrary distribution of localised states in the band gap. This simulator directly solves the complete set of microscopic differential equations governing the transient experiments on semiconductors and insulators when localised states are important. Results of simulations of time-of-flight experiments with an exponential band tail of localised states, believed to be present in a-Si:H, are presented. Similar approaches have also been used in papers by [16] and [17].

C.Van Berkel, J.R. Hughes and M.J. Powell, [18], investigate the switching characteristics of amorphous silicon thin film transistors. They suggest that these transient effects are controlled by trapping and 'thermalisation') from the deep states in amorphous silicon. The free carrier concentration is assumed to be independent of time. An earlier paper by J.M. Marshall and C. Main, [19], investigates the transient photoconductivity of amorphous semiconductors and explains this in terms of thermalisation of excess charge with localised states distributed over a range of energies. However, their research only considers discrete sets of traps. Both papers give a good insight into the types of problems that exist in amorphous devices in terms of carrier recombination processes. However, like many papers, they highlight the need for more analytical research into the basic amorphous semiconductor device equations as applied to continuous distributions of traps. The influence of traps on the characteristics of thin film transistors has be analyzed by M.G Hack, A.G Lewis and J.G Shaw, [20], vindicating the view that traps strongly determine the threshold and sub-threshold voltages of these devices.

Much work has been carried out investigating the instability mechanisms present in amorphous silicon thin film transistors. Two papers by M.J.Powell, C.van Berkel, and J.R.Hughes, [22], and [23], have measured the voltage threshold shift that occur in a series of silicon-silicon nitride thin film transistors after prolonged gate voltages. These instabilities are resolved into two distinct mechanisms. Firstly, there is an increase in the density of metastable states, taking place in the hydrogenated amorphous silicon layer. Secondly, there is charge trapping, occurring the amorphous silicon nitride layer, usually used as the gate dielectric. Other papers written on this subject include [24], and [25]. Research progressed onto investigations into the creation of these metastable states; [26], and [28], give good insight into the chemical processes responsible for defect formation in a-Si:H, and suggest that the defect states are in chemical equilibrium with weak-bond valence band tail states. [26] gives a good explanation of the concept of the defect pool model, which is used to predict and understand the formation of these metastable states. Other papers written on the subject include [29], and [38].

There are several important papers, [31], [32], and [33] that approach the problem of device modelling in a more mathematical way, employing asymptotic

techniques. These publications give a good insight into the methods used to model the basic semiconductor equations and M.J. Ward, F.M. Odeh and D.S. Cohen, [32], give a very good account of the general concepts on the asymptotic methods as applied to the metal oxide semiconductor field effect transistor.

Chapter 2

Derivation Of The Model Equations

In this chapter, I derive and discuss the model equations describing the behaviour of amorphous semiconductor devices, the boundary conditions applied, and the physical parameters present that are used to form the non-dimensional system. However, it seems appropriate to first introduce to the reader the basic concepts of semiconductor physics.

2.1 Basics Of Crystalline Semiconductor Physics

2.1.1 Band Theory Of Solids

The references [2], [34], and [3] are used to provide the necessary information contained in the following section. These texts are also useful background reading on the general subject of crystalline semiconductor devices.

An important consequence of quantum mechanics, applied to the description of electrons in a solid, is that the allowed energy levels of electrons are grouped into bands. The bands are separated by regions which contain energies that the electron in the solid cannot possess. These regions are called forbidden gaps. The electrons in the outer most shells of the atoms, referred to as valence electrons and shown in figure 2.1 (a), occupy the lowest possible energy states. The band of these states is called the valence band. Electrons that posses enough energy, can be promoted from the valence band into the conduction band, where they are free to move through the lattice structure and participate in electrical conduction. Solids can

then be be put into three classes - metals, insulators, and semiconductors - distinguished by the size of the forbidden gap.

The corresponding band diagram for conductors is shown in figure 2.1 (b). The two bands mentioned earlier overlap and there is in effect no forbidden gap. As a consequence, lattice vibrations provide enough energy for many valence electrons to be promoted into the conduction band. The solid possesses a "sea" of electrons, capable of conducting electricity.

Turning to the example of an insulator, the valence electrons form strong bonds between neighbouring atoms, which are difficult to release. Therefore, very few electrons are available to participate in the conduction process. In terms of the band diagram, shown in figure 2.1 (c), there is a large forbidden gap. In a perfect insulator, all levels in the valence band are occupied by electrons, and all levels in the conduction band are empty. For this reason, a perfect insulator will not conduct electricity.

The intermediate case between the two classes above, is the semiconductor. The bonds between neighbouring atoms are only moderately strong, and the electrons participating in the bonding structure can be released by thermal vibrations of the lattice. When an electron is released, it is promoted into the conduction band, free to move, and able to participate in the conduction process. However, the release of the electron results in a deficit of charge at this incomplete bonding site. This deficit is referred to as a hole. A valence band electron can then jump from a neighbouring atom, into the position of the hole, also leaving behind a charge deficit. The movement of this lower energy valence electron can be thought of as the movement of a positively charged particle, or hole, in the opposite direction. Under the application of an electric field, these holes are able to move and participate in the conduction of electricity. In terms of the band diagram, shown in figure 2.1 (d), the forbidden gap of a semiconductor is not as large as that of an insulator. Because of this, some of the electrons will acquire enough energy to jump from the valence band into the conduction band, leaving behind holes. From now on, I will refer to the movement of high energy conduction band electrons as the movement of electrons, and the movement of low energy valence band electrons as the movement of holes in the opposite direction.

2.1.2 Intrinsic and Extrinsic Semiconductors

In pure semiconductors at absolute zero all the valence band energy levels are occupied by electrons, and all the conduction band energy levels are empty. As the temperature is increased the valence band electrons can gain energy from thermal lattice vibrations, promoting them into the conduction band. The description of the

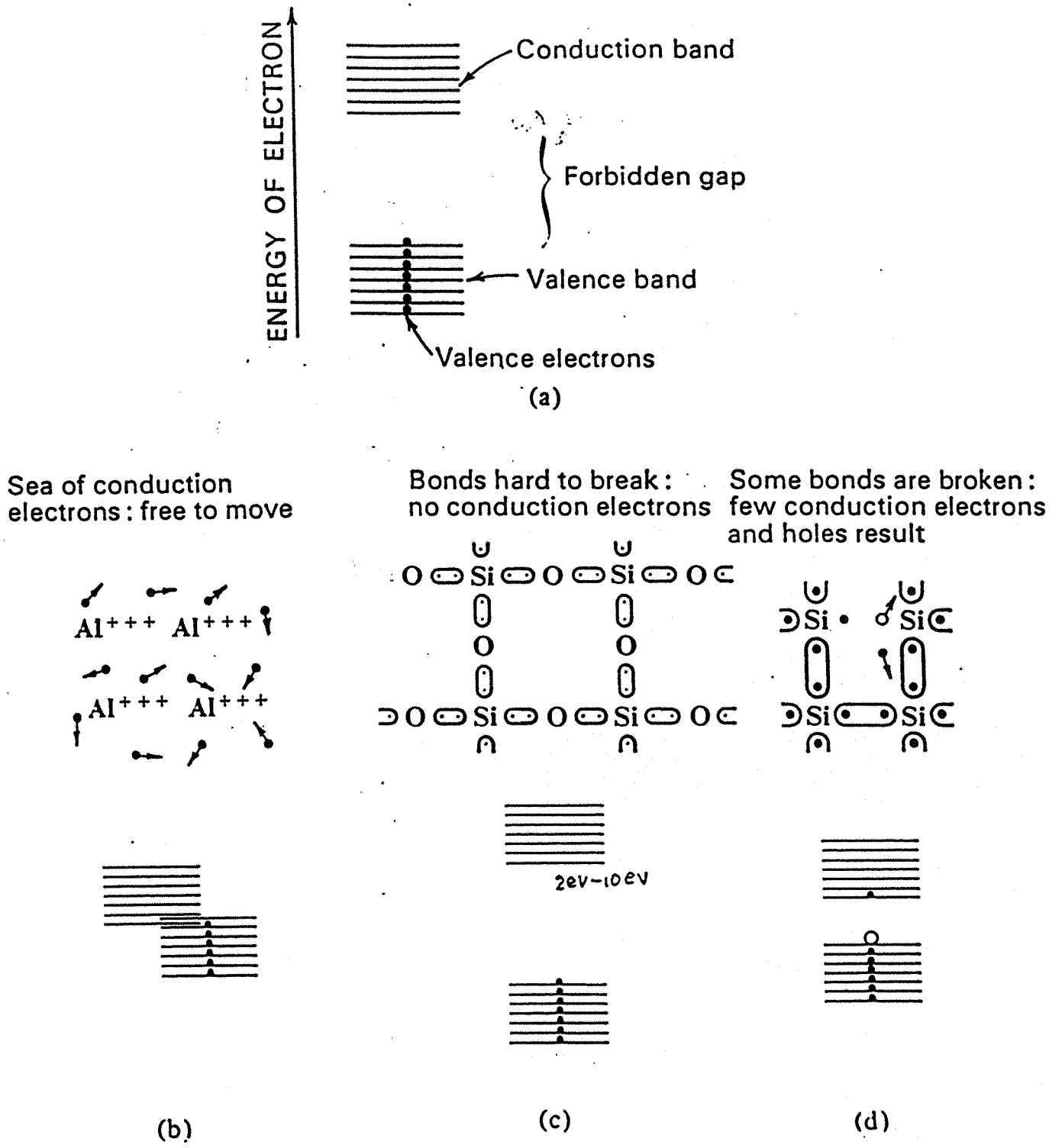

Figure 2.1: Illustrations of, (a) the valence and conduction bands in a solid, (b) a conductor, (c) an insulator, and (d) a semiconductor.

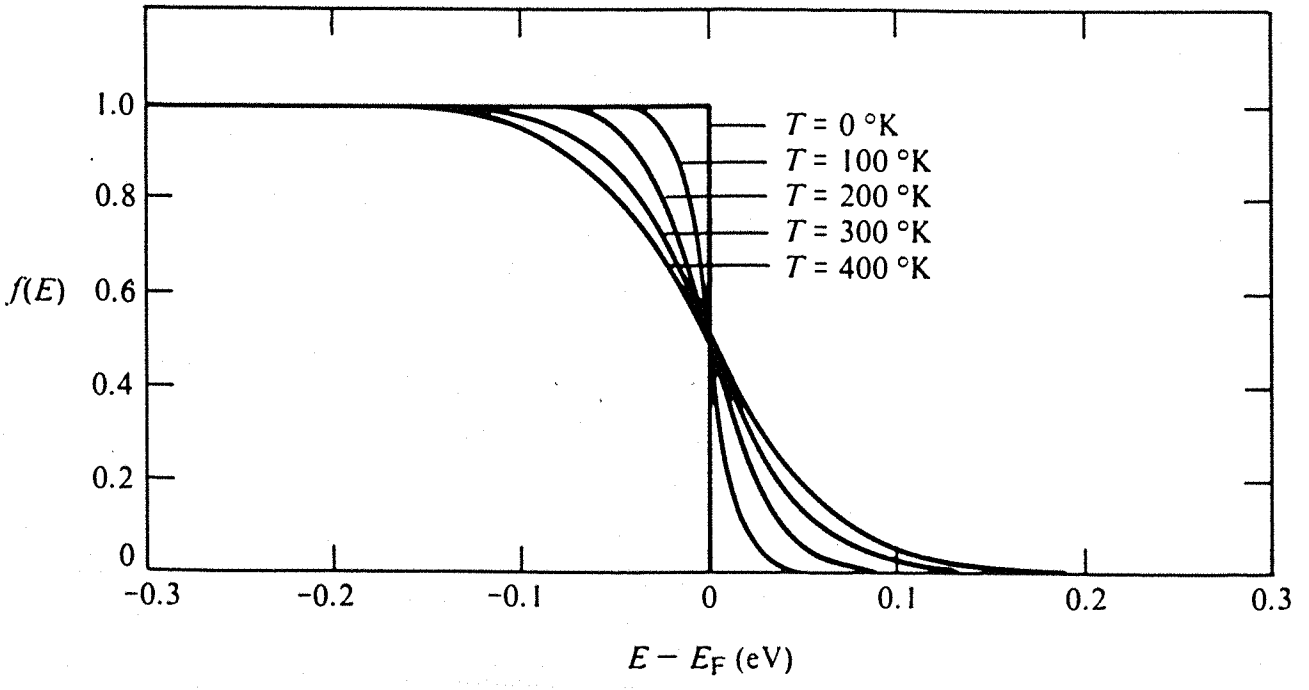

Figure 2.2: Value of the Fermi function versus energy with the system temperature as a parameter.

occupation of states by electrons is given in terms of $f(E)$ and specifies how many of the existing states at energy E will be filled with an electron. In equilibrium f takes on a particular form termed the Fermi function. The details of its derivation require some statistical reasoning that will not be entered into here. However, the final form for this Fermi function is

$$f(E) = \frac{1}{1 + e^{\frac{(E-E_F)}{kT}}},$$

where k is Boltzmann's constant, T is the temperature in degrees Kelvin and E_F is the Fermi energy of the electrons in the solid. E_F is the maximum energy the electrons have at zero degrees Kelvin. At higher temperatures the probability of occupation has exactly the value $\frac{1}{2}$ at the Fermi level. In general f can take on many different forms and it must be understood that the above form is only valid in equilibrium.

In figure 2.2 is a graph of the function for various temperatures. Notice, at $T = 0$ all the valence band states are occupied, but all the conduction band states are empty.

Since the creation of a conduction band electron simultaneously creates a hole, the concentration of electrons, n, equals the concentration of holes, p. These concentrations are called the intrinsic carrier concentrations n_i, and the semiconductor is referred to as intrinsic.

Next consider an impurity added to the semiconductor in concentrations much

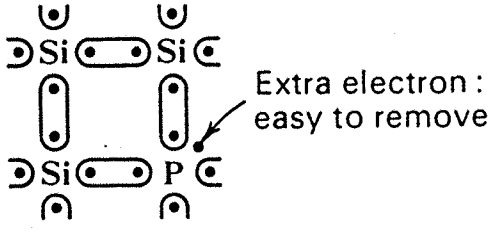

Figure 2.3: Visualisation of a donor ion, (phosphorus), incorporated into the silicon lattice.

larger than n_i. In particular, first consider the case when an impurity atom which has five valence electrons, such as phosphorus, is added to silicon, which has four. The extra electron cannot be incorporated into the regular arrangement of the silicon lattice, but is out of place, as shown in figure 2.3. It is easier to free, or ionise the extra electron, and the lattice vibrational energy of silicon at room temperature is large enough to ionise nearly all of these electrons, (complete ionisation). Under these conditions, the concentration of free electrons, to highest order, is equal to the concentration of the impurity atom. Figure 2.4 is a diagram to explain the above in terms of band-energy. The dopant ions introduce an extra energy level into the forbidden gap below the conduction band. The electrons in this energy level need only a small amount of energy to be ionised into the conduction band.

Similarly, an impurity atom with three valence electrons, such as boron, can be added to the silicon lattice, as shown in figure 2.5. This impurity atom has a hole associated with the bonding. It can be removed relatively easily since only a small amount of energy is needed for a valence electron to jump to this level. The valence electrons thus leave behind holes in the valence band. Because the amount of energy required for this to happen is small, nearly all of the holes associated with the impurity atoms are occupied by electrons. The concentration of holes is then equal, to highest order, to the concentration of impurity atoms, (complete ionisation).

Figure 2.6 illustrates the resulting band energy diagram due to the introduction of impurity atoms, (boron). An extra energy level is introduced into the forbidden gap, and valence electrons readily fill these states. Materials that have impurity

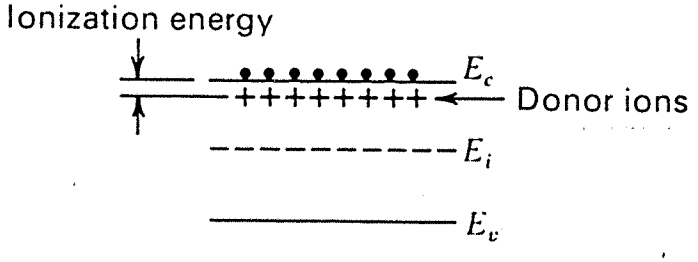

Figure 2.4: Energy-band diagram representing donor ions.

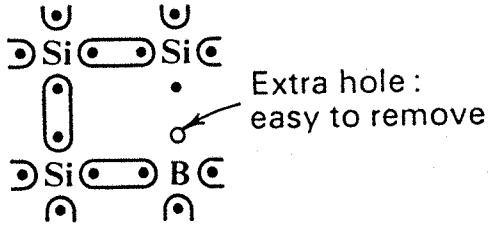

Figure 2.5: Visualisation of an acceptor ion, (boron), incorporated into the silicon lattice.

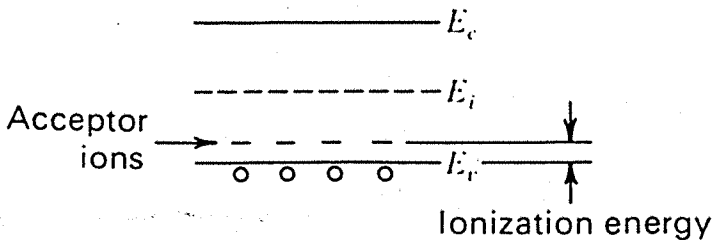

Figure 2.6: Energy-band diagram representing acceptor ions.

atoms added in the above manner are referred to as extrinsic semiconductors.

2.1.3 Equilibrium Distribution Of Carriers

The distribution of carriers is obtained by simply multiplying the appropriate density of states by the appropriate occupancy function. If $g_c(E)\,dE$ represents the number of conduction band states /cm^3 in the E to $E + dE$ energy range then $g_c(E)\,f(E)$ yields the distribution of electrons in the conduction band. Similarly, if $g_v(E)\,dE$ represents the number of valence band states /cm^3 and lying in the range E to $E + dE$ then $g_v(E)\,[1 - f(E)]\,dE$ yields the distribution of holes in the valence band. The general form for the carrier distributions is that the concentrations are zero at the band edges, reach a peak close to E_C or E_V, and then decay very rapidly to zero as one moves upward into the conduction band or downward into the valence band. When the Fermi level is positioned in the upper half of the band gap, the electron population greatly outweighs the hole population. Conversely, when the Fermi level is in the lower half of the band gap the hole population greatly outweighs the electron population. When the Fermi level is near the midgap the number of holes is equal to the number of electrons. All of this is summarised in figure 2.7.

The concentration of electrons with energies between E and E+dE is $g_c(E)\,f(E)\,dE$ and the concentration of holes with energies between E and E+dE is $g_v(E)\,[1 - f(E)]\,dE$. The total carrier concentrations are obtained by simply

integrating the appropriate distribution function over the energy band, thus,

$$n = \int_{E_c}^{E_{top}} g_c(E) f(E) dE .$$

$$p = \int_{E_{bottom}}^{E_v} g_v(E) [1 - f(E)] dE .$$

If the Fermi level lies more than $3kT$ away from either band gap then the Fermi functions can be approximated by,

$$f(E) \approx \exp\left[-\frac{(E - E_F)}{kT}\right] .$$

for conduction band energies, and,

$$1 - f(E) \approx \exp\left[\frac{(E - E_F)}{kT}\right] .$$

for valence band energies. A semiconductors whose Fermi level satisfies the above is referred to as non-degenerate. The occupancy functions are replaced by the above expressions, and the following approximations for the carrier concentrations are obtained,

$$n \approx N_C e^{\frac{(E_F - E_C)}{kT}} \qquad E_C - E_F \geq 3kT ,$$

$$p \approx N_V e^{\frac{(E_V - E_F)}{kT}} \qquad E_F - E_V \geq 3kT ,$$

where,

N_C – the effective density of conduction band states .

N_V – the effective density of valence band states .

The carrier concentrations obey Maxwell-Boltzmann statistics. If the Fermi level violates the above inequalities the semiconductor is said to be degenerate, and the carrier concentration approximations break down.

In an intrinsic non-degenerate semiconductor,

$$n_i = N_C e^{\frac{(E_i - E_C)}{kT}} .$$

$$n_i = N_V e^{\frac{(E_V - E_i)}{kT}} .$$

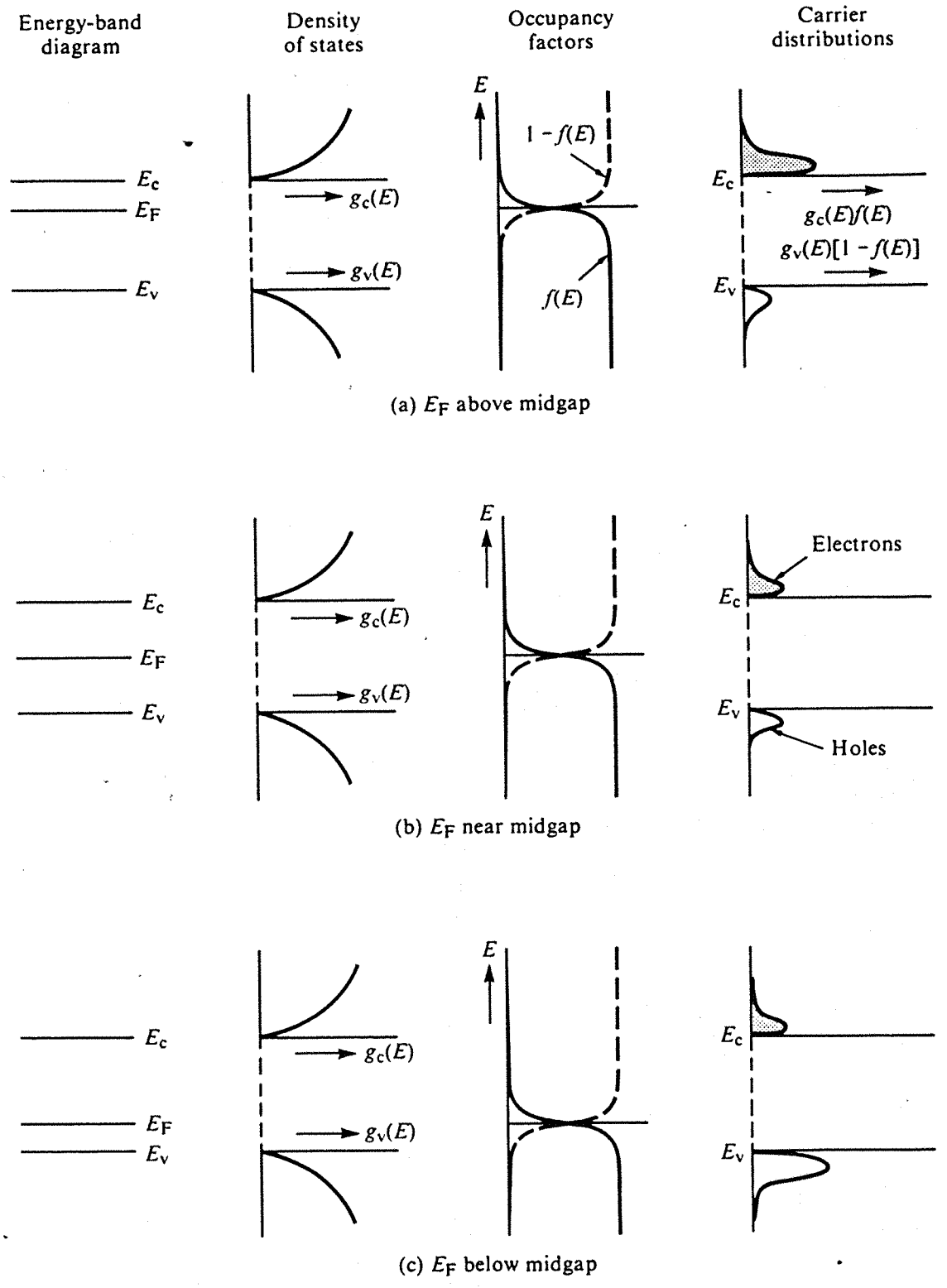

(a) E_F above midgap

(b) E_F near midgap

(c) E_F below midgap

Figure 2.7: Carrier distributions in the respective bands when the Fermi level is positioned, (a) above the midgap, (b) near the midgap, and (c) below midgap. Also shown are sketches of the energy-band diagram, density of states, and the occupancy factors.

The above equations can be used to express N_C and N_V in terms of n_i, E_i, E_C and E_V. Hence, the equilibrium extrinsic non-degenerate semiconductor carrier concentrations can be written in terms of the intrinsic carrier concentration,

$$n = n_i e^{\frac{(E_F - E_i)}{kT}} .$$

$$p = n_i e^{\frac{(E_i - E_F)}{kT}} .$$

As can be seen from the above expressions the product np gives,

$$np = {n_i}^2 ,$$

which is always satisfied when the semiconductor is in thermal equilibrium.

All semiconductors mentioned henceforth will be assumed to be non-degenerate.

2.2 The Basic Semiconductor Device Equations

In the following section the reader is referred to [5]. This text gives a good account of the origins of the crystalline semiconductor device equations. It has also been used to construct the summary below.

The full set of equations used to model amorphous semiconductors are derived from the basic semiconductor equations. However, due to the nature of amorphous silicon, extra terms will appear, which will be discussed later in the chapter. The basic equations can be classified into three groups: Maxwell's equations, continuity equations and carrier transport equations.

2.2.1 Maxwell's Equations

These equations describe the propagation of electromagnetic fields in an arbitrary medium. The differential form is listed below.

$$\nabla \wedge \vec{E} = -\frac{\partial \vec{B}}{\partial t} . \tag{2.1}$$

$$\nabla \wedge \vec{H} = \vec{J} + \frac{\partial \vec{D}}{\partial t} , \tag{2.2}$$

$$\nabla \cdot \vec{D} = \rho \,. \tag{2.3}$$

$$\nabla \cdot \vec{B} = 0 \,. \tag{2.4}$$

Here $\vec{E}$ and $\vec{D}$ are the electric field and displacement vector respectively, $\vec{H}$ and $\vec{B}$ are the magnetic field and induction vector respectively, ρ is the electric charge density, and $\vec{J}$ denotes the current density vector. Faraday's law of induction, (2.1), tells us that a time varying magnetic field produces an electric field. The Ampere-Maxwell law, (2.2), states that both electric currents and changing electric fields produce magnetic fields. The following two equations are the electric and magnetic flux laws. Gauss' law, (2.3), is an equivalent statement to the inverse square law. Equation (2.4) states that there are no magnetic charges.

2.2.2 Poisson's Equation

Poisson's equation is derived from equation (2.3). Firstly, the electric displacement vector is replaced by the electric field using,

$$\vec{D} = \epsilon \vec{E} \,,$$

where ϵ is the permittivity of the medium. The above is valid for all materials where ϵ is time-independent, and where polarisation effects due to mechanical forces are negligible. It is assumed the permittivity is homogeneous in the device, and that the device is isotropic. Hence, the permittivity can be treated as a scalar quantity. To simplify the above equations, the magnetic induction vector $\vec{B}$ is assumed independent of time. Therefore, from equation (2.1),

$$\nabla \wedge \vec{E} = 0 \,,$$

i.e. the vector field $\left(\vec{E}\right)$ is irrotational. From differential calculus, a sufficiently smooth irrotational vector field in a simply connected region can be expressed as a gradient field. Therefore, the electric field can be expressed as,

$$\vec{E} = -\nabla \psi \,,$$

for some scalar potential ψ. Substituting this expression for $\vec{E}$ into equation (2.3), it can be shown,

$$\nabla^2 \psi = -\frac{\rho}{\epsilon} \,.$$

The electric space charge density ρ can be further specified as the product of the elementary charge, q, times the sum of the positively charged hole concentration, p, the negatively charged electron concentration, n, and a quantity denoted by C.

$$\rho = q\,(p - n + C) \,. \tag{2.5}$$

The constituents that make up C depend on the assumptions made about the semiconductor material. Here the device equations for a perfect crystalline semiconductor are being derived and therefore C only contains terms accounting for the charge stored in the dopant energy level. However, in real crystalline semiconductors, imperfections can occur in the lattice creating discrete "trap" states in the forbidden gap. These states also contain charge. Thus, extra entries in the quantity C appear, in such cases to take account of these "defects".

The occupancy of an energy level in equilibrium is given by the Fermi function,

$$F(E) = \frac{1}{1 + \exp(E - E_F)/kT} .$$

Since, typically, the donor energy level is much greater than the Fermi level,

$$\exp(E - E_F)/kT \gg 1 \qquad \Rightarrow \qquad F(E) \approx 0 ,$$

whereas typically, the acceptor energy level is much less than the Fermi level,

$$\exp(E - E_F)/kT \approx 0 \qquad \Rightarrow \qquad F(E) \approx 1 .$$

In most models the above approximations are used. That is to say, the donor and acceptor energy levels are assumed to be far enough away from the Fermi level to be "fully ionised". The important point to make here is the donor states, when fully ionised, posses a charge of magnitude

$$qN_{D+} ,$$

where N_{D+} denotes the concentration of donor atoms, and the acceptor states, when fully ionised, posses a charge of magnitude,

$$-qN_{A-} ,$$

where N_{A+} denotes the concentration of acceptor atoms.

Finally, ρ is replaced by $q(n - p + N_{A-} - N_{D+})$ to give,

$$\nabla^2\psi = q(n - p + N_{A-} - N_{D+}) .$$

The problem of assuming full ionisation as opposed to partial ionisation of the acceptor dopant energy level in a p-type crystalline M.O.S capacitor is discussed later in the chapter, and its resolution constitutes part of my research.

In the case of a trap in the band gap, it too can be either an acceptor type or donor type defect. However, the trap may occur nearer to the Fermi level, invalidating the above approximations for the Fermi function. The full expression

for the occupancy function $F(E)$ is then used. Therefore, in equilibrium, the charge contained in an acceptor type trap is given by,

$$-qF_a(E_A) \ ,$$

where E_A is the energy of the acceptor defect, and the charge contained in a donor type trap is given by,

$$qF_d(E_D) \ ,$$

where E_D is the energy of the donor defect. It must be noted that the function f, describing the probability of a state being occupied by an electron will, in general, be different from F, the Fermi function, which describes the probability of occupation of a state by an electron under equilibrium conditions.

In amorphous semiconductors there exists a continuous distribution of "localised" defect states. This differs from the crystalline material in two ways. Firstly, the states are localised. That is, the defects that occur in the material are isolated in space from each other, and charge jumping from one defect state to another is very unlikely. Discrete traps occurring in crystalline semiconductors exist throughout every point of the material, and communication between traps is possible. Secondly, a continuous distribution of states in the forbidden gap, as opposed to discrete states, exists. Thus, in amorphous materials C will contain integral expressions to account for these continuous trap distributions.

2.2.3 Continuity Equations

The continuity equations can be derived from Maxwell's equations (2.2) and (2.3) by application of the divergence operator. Since $\mathrm{div}\left(\mathrm{curl}\left(\vec{H}\right)\right) = 0$, for a sufficiently smooth vector field $\vec{H}$ then,

$$\nabla.\vec{J} + \frac{\partial \rho}{\partial t} = 0 \ . \tag{2.6}$$

This means that if a fixed volume in the crystal is considered, the change in the density of any carrier balances the carrier flux out of the volume. Next, the total conduction current density $\vec{J}$, is split into an electron current, $\vec{J}_n$, caused by the flow of electrons, and a hole current, $\vec{J}_p$, caused by the flow holes, giving,

$$\vec{J} = \vec{J}_n + \vec{J}_p \ . \tag{2.7}$$

Assuming the doping profile is time-invariant,

$$\frac{\partial C}{\partial t} = 0 \ ,$$

and substituting equations (2.5) and (2.6) into equation (2.7) then,

$$\nabla.\left(\vec{J}_n + \vec{J}_p\right) - q\frac{\partial}{\partial t}(n-p) = 0\ .$$

The above equation can be split into an electron continuity equation, and a hole continuity equation by defining a new quantity R,

$$\nabla.\vec{J}_n - q\frac{\partial n}{\partial t} = qR\ .$$

$$\nabla.\vec{J}_p + q\frac{\partial p}{\partial t} = -qR\ .$$

The quantity R can be physically interpreted as the difference between the rate at which electron-hole pairs recombine and the rate at which they are generated. There are various recombination / generation processes, the more important of which are discussed in the next section.

2.2.4 Carrier Transport Equations

It is assumed that,

i) the sources of current flow are from drift and diffusion, (e.g magnetic field phenomena, such as the Hall effect, are not included).

ii) the electron and hole current densities are found by linearly superimposing the current flows caused by drift and diffusion. Thus,

$$\vec{J}_n = \vec{J}_n^{\,diff} + \vec{J}_n^{\,drift}\ . \tag{2.8}$$

$$\vec{J}_p = \vec{J}_p^{\,diff} + \vec{J}_p^{\,drift}\ . \tag{2.9}$$

In a semiconductor material carriers are continually gaining kinetic energy from thermal vibrations of the lattice, and losing energy from collisions with other particles and the lattice itself. The macroscopic effect is a random thermal motion of the particles, resulting in no net movement of charge. However, when an electric field $\vec{E}$ is applied to the semiconductor device, the charged particles gain extra kinetic energy and a net additional motion in the appropriate direction results, (along the field if it is positive and opposite to the field if it is negative). However, as in the equilibrium case, the particles are still colliding with each other and with the lattice, losing all their kinetic energy as a result. They again acquire kinetic energy from the field and the process is repeated. As a result, the carriers not only

posses this random thermal motion, but in addition posses net motion from the applied electric field. This net movement or "drift" of charge, superimposed onto the random thermal motions of the carriers, results in a current. Since current is the rate of movement of charge, the drift current density will be proportional to the product of the concentration of the carrier type, and its drift velocity, giving for the electron and hole drift current densities,

$$\vec{J}_n^{\,drift} = -qn\vec{v_n} , \tag{2.10}$$

$$\vec{J}_p^{\,drift} = qp\vec{v_p} , \tag{2.11}$$

where $\vec{v_n}$ and $\vec{v_p}$ denote the average drift velocities for electrons and holes respectively.

At moderate field strengths, the drift velocities are proportional to the applied electric field, giving,

$$\vec{v_n} = -\mu_n \vec{E} , \tag{2.12}$$

$$\vec{v_p} = \mu_p \vec{E} , \tag{2.13}$$

where μ_n and μ_p are the electron and hole mobilities respectively.

Using equations (2.10)-(2.13), the drift current densities are given by,

$$\vec{J}_n^{\,drift} = q\mu_n n\vec{E} , \tag{2.14}$$

$$\vec{J}_p^{\,drift} = q\mu_p p\vec{E} . \tag{2.15}$$

The diffusion current densities are caused by diffusion of electrons and holes from regions of high concentration, to regions of low concentration. The direction of diffusion of a charged particle is in the direction of steepest descent of the corresponding particle concentration. The diffusion flux densities are proportional to the gradients of the corresponding particle concentration. Thus, the diffusion current densities are obtained by multiplying the diffusion fluxes, with the charge per particle, q for holes and -q for electrons. Hence,

$$\vec{J}_n^{\,diff} = qD_n \nabla n , \tag{2.16}$$

$$\vec{J}_p^{\,diff} = -qD_p \nabla p , \tag{2.17}$$

where D_n and D_p are the diffusion co-efficients.

Substituting equations (2.14) and (2.15) for the drift current densities, and equations (2.16) and (2.17) for the diffusion current densities, into equations (2.8) and (2.9) the current relations become,

$$\vec{J_n} = qD_n\nabla n + q\mu_n n\vec{E} \tag{2.18}$$

$$\vec{J_p} = -qD_p\nabla p + q\mu_p p\vec{E} \tag{2.19}$$

The diffusion coefficients D_n and D_p, are related to the mobilities μ_n and μ_p by Einstein's relations,

$$D_n = U_T\mu_n \ ,$$

$$D_p = U_T\mu_p \ ,$$

where U_T is the thermal voltage, given by,

$$U_T = \frac{kT}{q} \ ,$$

where k denote's Boltzmann's constant and T is the absolute temperature.

2.2.5 The Basic Semiconductor Device Equations

Below, is a list of the equations derived at the beginning of this section, along with the assumptions made to obtain them.

$$\epsilon\nabla^2\psi = q\left(n - p - C\right) \ , \qquad \text{Poisson's equation.}$$

$$qR = \nabla.\vec{J_n} - q\frac{\partial n}{\partial t} \ , \qquad \text{electron continuity.}$$

$$-qR = \nabla.\vec{J_p} - q\frac{\partial p}{\partial t} \ , \qquad \text{hole continuity.}$$

$$\vec{J_n} = q\mu_n\left(U_T\nabla n - n\nabla\psi\right) \ , \qquad \text{electron current.}$$

$$\vec{J_p} = -q\mu_p\left(U_T\nabla p + p\nabla\psi\right) \ , \qquad \text{hole current.}$$

i) The only sources of current flow are drift of carriers caused by the electric field, and diffusion of carriers, due to the spatial variation of the carrier concentrations.

ii) Einstein's relations hold.

iii) The magnetic induction vector $\vec{B}$, is independent of time.

2.3 Recombination Processes

It was mentioned earlier that there are various recombination and generation processes. The quantity R, appearing in the charge continuity equations, can be described by a combination of different phenomena. It is the purpose of this section to outline the more important of these and the reader is referred to [2].

i) Band-to-Band Recombination.

As illustrated in figure 2.8 (a) this merely involves the direct annihilation of a conduction band electron and a valence band hole, the electron falling from an allowed conduction band state, into a vacant valence band state. This process is typically radiative, with the excess energy released during the process going into the production of a photon.

ii) Recombination / Generation (R-G) Centres.

Certain impurity atoms can introduce allowed energy levels into the mid-gap region of a semiconductor. Crystal defects can also give rise to deep level states. As shown in the figure 2.8 (b), the R-G centre is involved in the state to state transition of a single carrier. A carrier is first captured at the R-G site, and then makes an annihilating transition to the opposite carrier band. R-G centre recombination is characteristically non-radiative. Thermal energy is released during the process.

iii) Recombination via Shallow Levels.

Like R-G centres, donor and acceptor sites also function as intermediaries in the recombination process, (see figure 2.8 (c)). If an electron is captured at a donor site, however, it has a high probability of being re-emitted into the conduction band before completing the remaining steps of the recombination process. A similar statement can be made for holes captured at the acceptor sites. For this reason, donor and acceptor sites are extremely inefficient R-G centres, and the probability of recombination occurring via shallow levels is usually quite low. The largest energy step in shallow-level recombination is typically radiative.

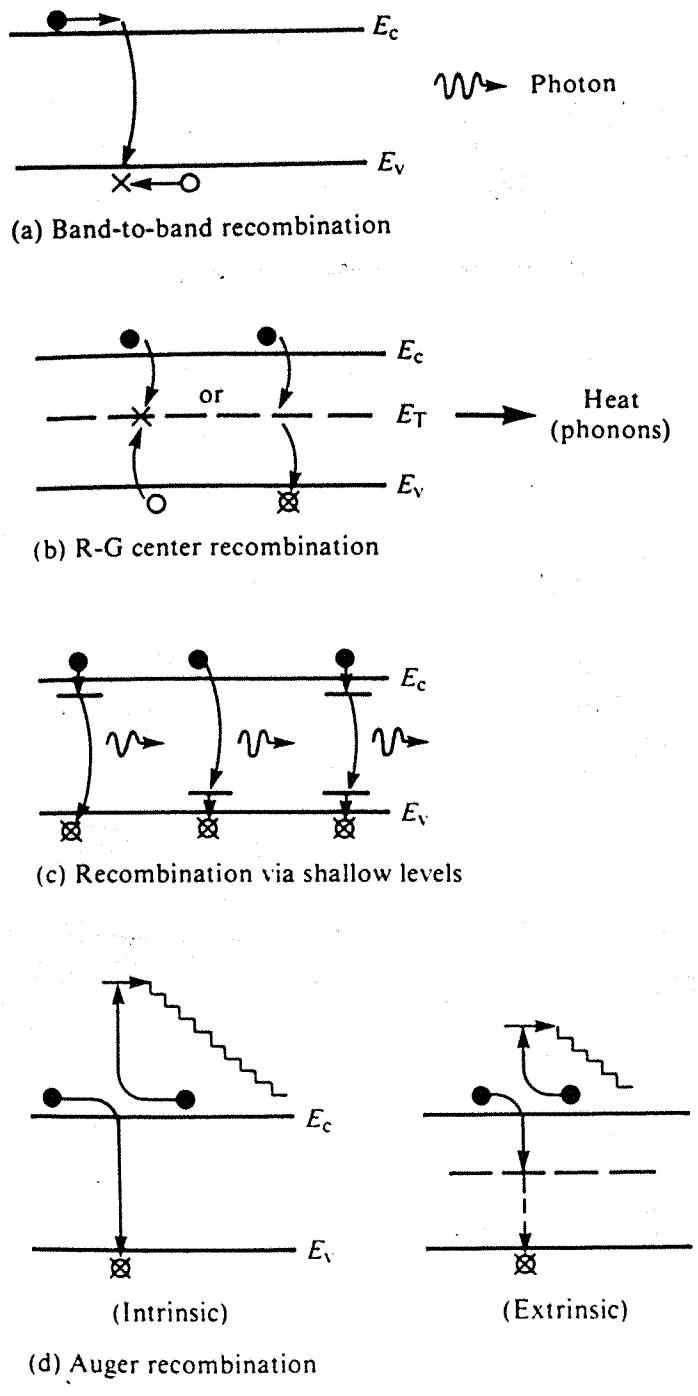

Figure 2.8: Energy-band diagrams of recombination processes for, (a) band to band recombination, (b) R-G centre recombination, (c) recombination via shallow levels, and (d) Auger recombination.

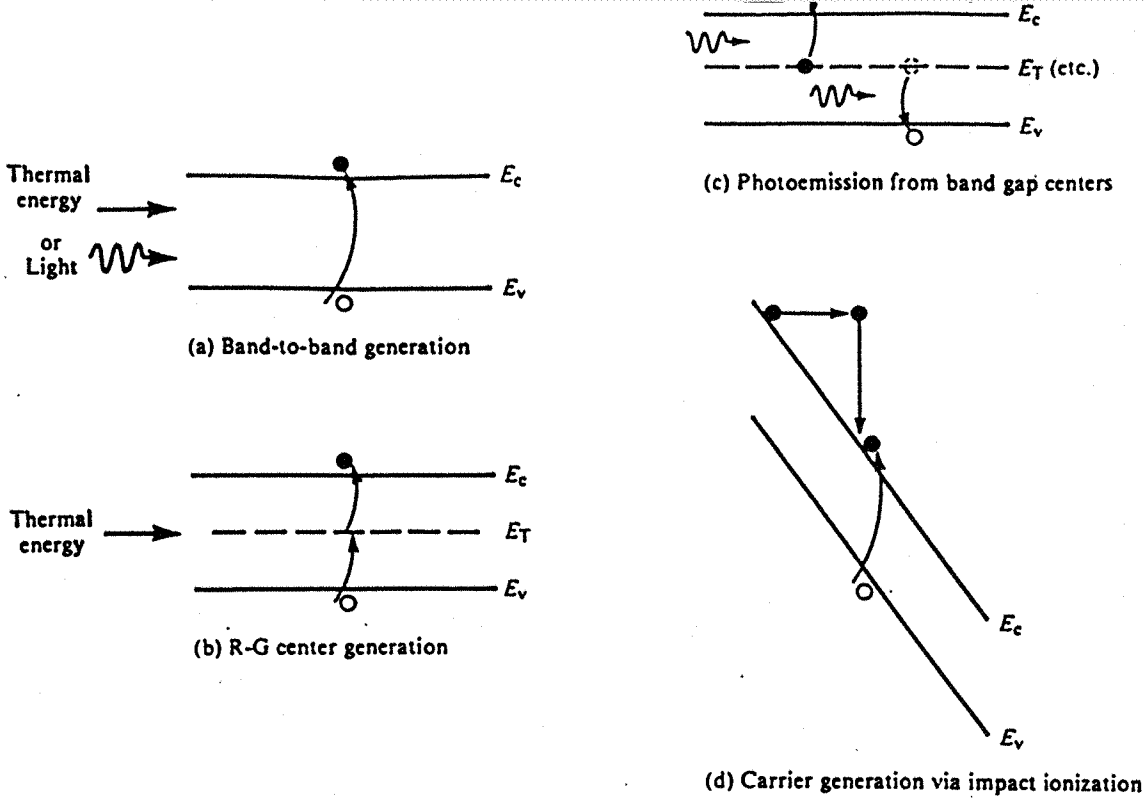

Figure 2.9: Energy-band diagrams for, (a) band to band generation, (b) R-G centre generation, and (c) carrier generation via impact ionisation.

iv) Auger Recombination.

In an Auger process, band-to-band recombination or trapping at a band gap centre occurs simultaneously with the collision between two like carriers. The energy released by the recombination or trapping subprocess, is transferred during the collision to the surviving carrier. Subsequently, this highly energetic carrier "thermalises"-loses energy in the small steps through collisions with the semiconductor lattice. The "staircases" in figure 2.8 (d), represent the envisioned step-wise lose of energy. Because the number of carrier collisions increases with carrier concentration, Auger recombination likewise increases with carrier concentration, becoming very important at high carrier concentrations.

2.3.1 Generation Processes

Any of the above recombination processes can be reversed to generate carriers, as depicted in figure 2.9. In band-to-band generation either thermal energy or light can provide the energy required, and thermally assisted generation of carriers is obtained with R-G centres acting as intermediaries. Impact ionisation is the reverse of Auger recombination. An electron-hole pair is produced as a result of the energy released, when a highly energetic carrier collides with the lattice. The generation of carriers through impact ionisations occurs in the high E-field regions of devices, and is responsible for the avalanche breakdown in pn junctions.

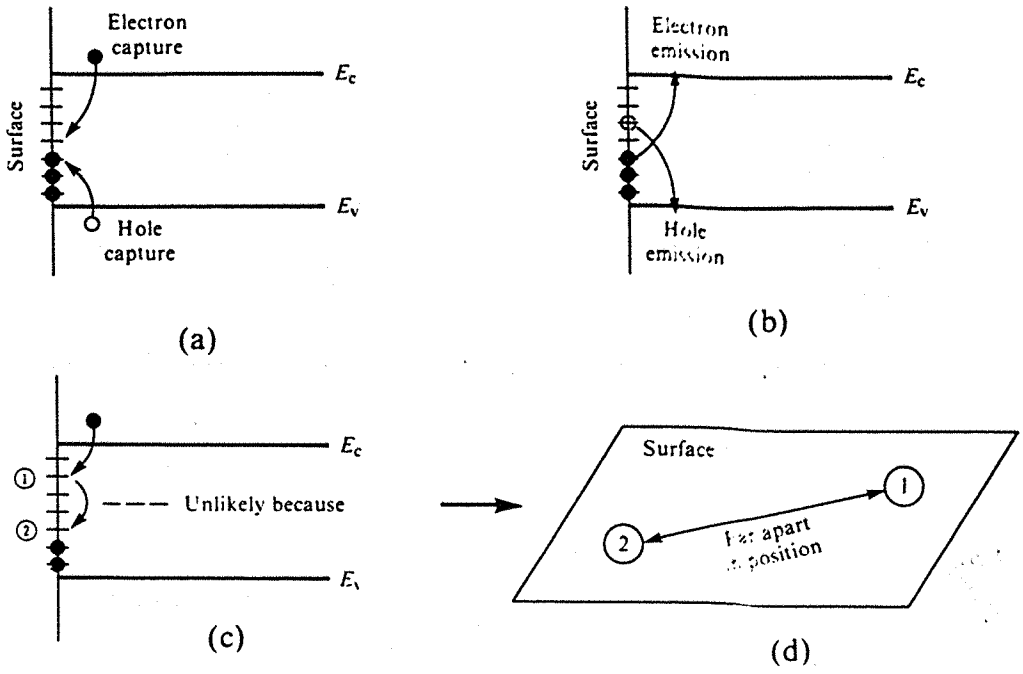

Figure 2.10: (a) Electron and hole capture leading to carrier recombination. (b) Electron and hole emission leading to carrier generation. (c) Visualisation of an inter-center surface transition. (d) A pictorial explanation of why such transitions are highly unlikely.

2.3.2 Surface Recombination-Generation

In many devices under certain conditions, surface recombination-generation can be as important as, or more important than, the bulk recombination-generation considered in the above section. Bulk R-G takes place at centres distributed throughout the volume of a semiconductor. Surface R-G refers to the creation/annihilation of carriers in the near vicinity of a semiconductor surface, via the interaction with interfacial traps. Interfacial traps are functionally equivalent to R-G centres localised at the surface of a material. Unlike bulk R-G centres in crystalline silicon, interfacial traps are typically found to be continuously distributed in energy throughout the band gap. As pictured in figure 2.10 (a) and (b), the fundamental processes which occur in the bulk also occur at the surface. Electrons and holes can be captured and emitted from surface centres. One might expect additional transitions to occur between surface centres at different energies. However, as illustrated in figure 2.10 (c) and (d), these states are localised in space on the surface plane. Whereas a single level usually dominates bulk R-G, the surface-centre interaction routinely involves centres distributed in energy throughout the band gap.

2.3.3 Recombination and Generation Through Centres

In this section, I will be discussing the effect that centres have on the recombination and generation of carriers. Emission and capture rate equations will be derived, and then used to calculate the steady state occupation function f. This function will then be used in later analysis of the M.O.S. capacitor. Specifically, the steady state problem of a constant gate voltage applied to the device. Partial, as opposed to complete ionisation of the dopant energy level will be investigated. Since this problem is steady state, the above occupation function can be used to calculate the number of traps that have been ionised. However, I will first discuss the essential mechanisms of these traps in the band gap.

The processes taking place in the recombination-generation centres has been studied by Hall, Read and Shockley, [9] . Figure 2.11 is an illustration of their findings.

Centres are "stepping stones" in the transition of electrons and holes from their respective bands. The probability of a transition depends on the size of the step. These centres can make such transitions more probable and hence influence the life-time of a carrier in a semiconductor. The rates of the various processes are now considered.

a) Capture of an electron from the conduction band by a centre. This process is proportional to the concentration of free electrons in the conduction band, and the concentration of centres which are not occupied by electrons, (only one electron can occupy a given centre). If the concentration of centres in the semiconductor is N_t, then the concentration of unoccupied centres is $N_t\,(1-f)$, where f is the probability of occupation of a state by an electron. Since the capture of an electron is determined by there being both an electron and an available trap site, the rate of capture will be proportional to the product of their probabilities. Therefore, the rate of process (a) is,

$$r_a = v_{th}\sigma_n n N_t\,(1-f)\ ,$$

where,

v_{th}- thermal velocity ,

σ_n- capture cross section of the centre .

The concept of capture cross-section is discussed at the end of this section.

b) The emission of an electron from a centre into the conduction band. This process will be proportional to the concentration of centres which are occupied by an electron, i.e. $N_t f$. Thus,

$$r_b = e_n N_t f\ ,$$

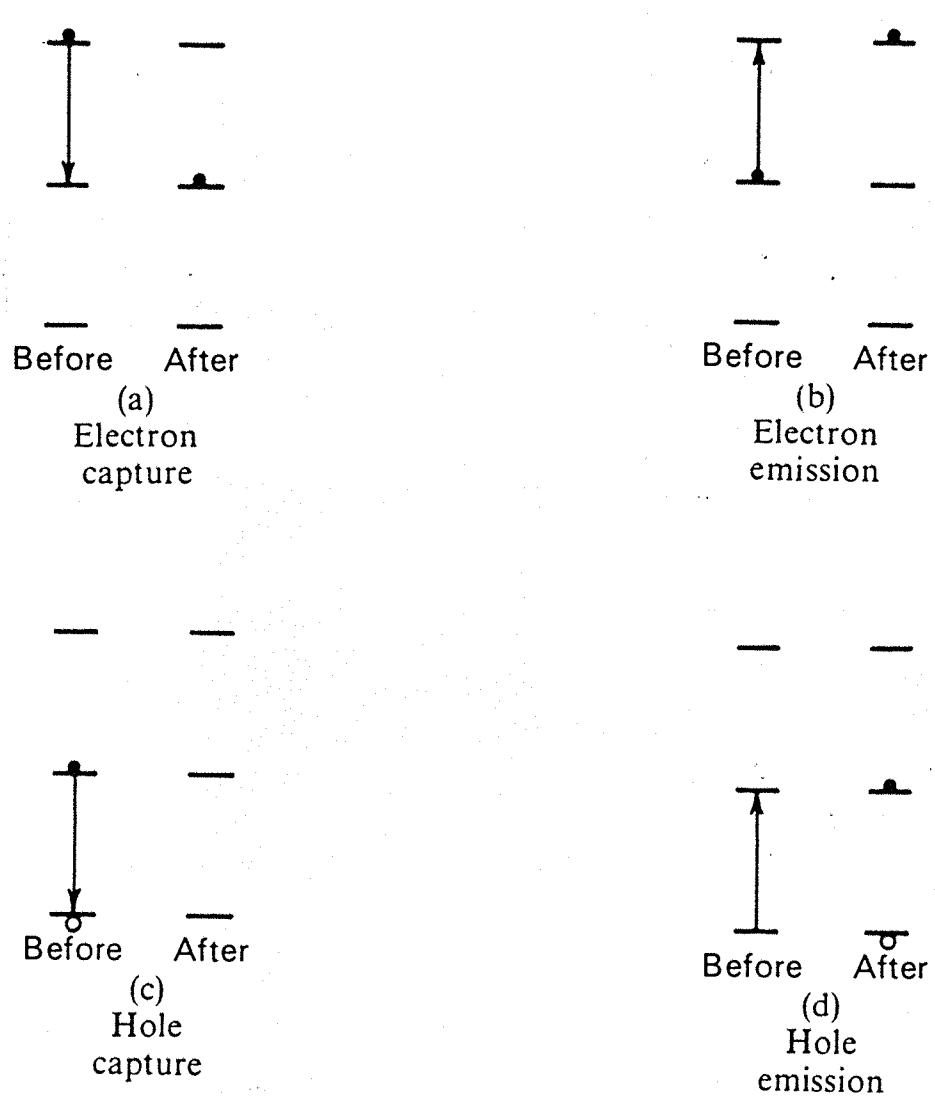

Figure 2.11: Energy-band diagrams for, (a) the capture of an electron from the conduction band by a centre, (b) an emission of an electron from a centre into the conduction band, (c) the capture of a hole from the valence band by a centre, and (d) an emission of a hole from a centre into the valence band.

e_n- emission probability of a jump from an occupied centre into the conduction band .

A similar approach is taken to find the rates of the processes for holes and it is found,

$$r_c = v_{th}\sigma_p p N_t f \ .$$
$$r_d = e_p N_t (1-f) \ .$$

The above equations describe the general recombination and generation processes of centres in semiconductor materials. The emission rates contain unknown constants, e_n, and e_p. These terms are calculated for the specific case of equilibrium. Then, when considering non-equilibrium conditions, the new emission rate constants will be assumed equal to their equilibrium counterparts.

In equilibrium, the rates of the processes describing the transition of electrons into and out of the conduction band, must be equal. Therefore, $r_a = r_b$. In addition, the electron concentration can be expressed in terms of the Fermi level,

$$n = N_c \exp\left(-\left(E_c - E_F\right)/kT\right) = n_i \exp\left(\left(E_F - E_i\right)/kT\right) \ .$$

Substituting the value of the electron concentration into $r_a = r_b$, it is found,

$$v_{th}\sigma_n n_i \exp\left(\left(E_F - E_i\right)/kT\right) N_t (1-f) = e_n N_t f \ .$$

Re-arranging,

$$e_n = v_t h \sigma_n n_i \exp\left(\left(E_F - E_i\right)/kT\right)\left(1 - \frac{1}{1+\exp\left(\left(E_t - E_F\right)/kT\right)}\right)$$
$$\times \ \left(1+\exp\left(\left(E_t - E_F\right)/kT\right)\right) \ .$$

Thus,

$$e_n = v_{th}\sigma_n n_i \exp\left(\left(E_t - E_i\right)/kT\right) \ .$$

Here it can be seen that e_n goes up exponentially as the centre energy level E_t approaches E_C.

e_p is found in a similar manner, by letting $r_c = r_d$, and noting $p = n_i \exp\left(\left(E_i - E_F\right)/kT\right)$,

$$e_p = v_{th}\sigma_p n_i \exp\left(\left(E_i - E_t\right)/kT\right) \ .$$

Considering steady state, with generation of carriers represented by G_L, the rate by which electrons enter the conduction band equals the rate by which they leave. Thus,

$$\frac{dn}{dt} = G_L - (r_a - r_b) = 0 \ .$$

Similarly, for holes,

$$\frac{dp}{dt} = G_L - (r_c - r_d) = 0 \; .$$

Eliminating G_L,

$$r_a - r_b = r_c - r_d \; .$$

Substituting in the appropriate expressions for these rates, the following algebraic equation for f is found,

$$v_{th}\sigma_n n N_t (1-f) - e_n N_t f = e_p N_t (1-f) - v_{th}\sigma_p p N_t f \; .$$

The equilibrium emission rates are used, and the equation is solved to give,

$$f = \frac{\sigma_n n + \sigma_p n_i \exp\left(\left(E_i - E_t\right)/kT\right)}{\sigma_n \left(n + n_i \exp\left(\left(E_t - E_i\right)/kT\right)\right) + \sigma_p \left(p + n_i \exp\left(\left(E_i - E_t\right)/kT\right)\right)} \; ,$$

or

$$f = \frac{\sigma_n n + \sigma_p N_v \exp\left(-\left(E_t - E_v\right)/kT\right)}{\sigma_n \left(n + N_c \exp\left(-\left(E_c - E_t\right)/kT\right)\right) + \sigma_p \left(p + N_v \exp\left(-\left(E_t - E_v\right)/kT\right)\right)} \; .$$

Capture Cross-Section

The capture of an electron or hole, is dependent on a quantity known as the capture-cross section of a centre. Above, the capture-cross section is simply introduced as a constant of proportionality. But here I give a more physical view of capture, and hence a deeper insight into the concept of capture-cross section. The visualisation of electron capture at an R-G centre is given in figure 2.12. The idealised view is that the centres are modelled as spheres randomly distributed about the semiconductor volume. An electron is considered to be captured if it penetrates the sphere surrounding an empty R-G centre. In a time t, (assumed to be small), an electron travels a distance $v_{th}t$, and passes through a volume of material equal to $Av_{th}t$, where A is the cross sectional area of the material normal to the electrons path. In this volume there is $N_t(1-f)$ empty R-G centres per cm^3, or a total number of $N_t(1-f)Av_{th}t$ empty centres. Since the centres are considered to be randomly distributed, the probability of an electron being captured in the volume can be determined by conceptually moving the centres to a single plane in the middle of the volume, and noting the fraction of the plane blocked by the R-G centres. If the area blocked by a single centre is σ_n, the total area blocked by empty centres is $N_t(1-f)A\sigma_n v_{th}t$. The fraction of the area giving rise to capture is $N_t(1-f)A\sigma_n v_{th}t/A$. The capture rate for a single electron is then $N_t(1-f)\sigma_n v_{th}$. Given n electrons per unit volume, the number of electrons/cm^3 captured per second is $nN_t(1-f)\sigma_n v_{th}$, or

$$\frac{\partial n}{\partial t} = -\sigma_n v_{th} N_t (1-f)\, n \; .$$

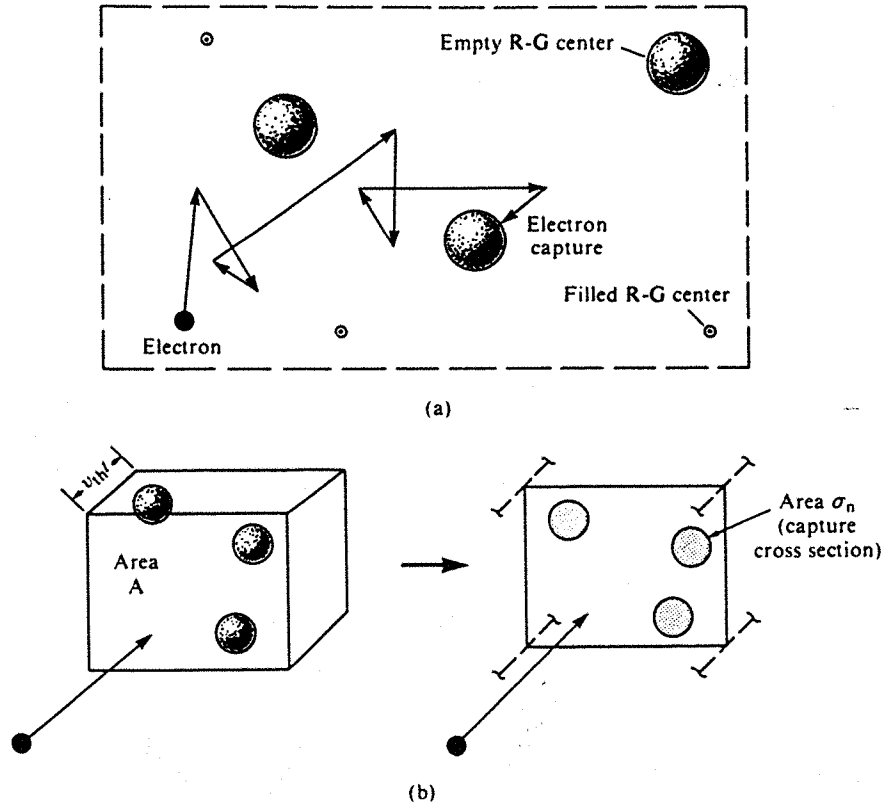

Figure 2.12: (a) Real space visualisation of electron capture at an R-G centre. (b) Construct employed in determining the capture rate. Left: volume through which an electron passes in a time t. Right: effective recombination plane.

2.4 The System Of Amorphous Equations

Above, a system of equations applicable to crystalline silicon was derived. However, due to the nature of amorphous silicon, further investigation into its structure is needed in order to derive equations that describe its behaviour more accurately. The important characteristic of amorphous silicon is the existence of a continuous distribution of localised traps in the band gap throughout the bulk as well as the surface. Depending on the nature of these traps, they can possess positive, negative or neutral charge. The significance of this can immediately be seen, for example, in Poisson's equation. In fact the recombination terms in the charge continuity equations depend on these traps also. The amount of charge stored in these traps, and the recombination of electrons and holes depend on their occupancy f. In the previous section, a more quantitative description of the recombination mechanisms in crystalline silicon was performed, where a single trap in the band gap occurred. The equations used to model amorphous silicon are taken from the basic semiconductor equations, but the discrete traps that occur in crystalline silicon, are extended to a continuous distribution of traps. The recombination processes for these traps are the same as for the single trap case, but integration over the whole band gap range is performed.

I will be considering two types of trap,

i) Donor traps - When a donor trap is occupied by an electron, it is neutral and when it is empty it has a positive charge.

ii) Acceptor traps - When an acceptor trap is occupied by an electron, it is negatively charged and when it is empty it is neutral.

To modify Poisson's equation the charge stored in these traps is considered. For acceptor traps of concentration N_{ta} at energy E the charge stored is,

$$-f_a N_{ta} \ ,$$

where f_a is the probability of an acceptor trap being occupied by an electron. As for donor traps of concentration N_{td},

$$N_{td}\left(1-f_d\right) \ ,$$

where f_d is the probability of a donor trap being occupied by an electron.

The above is for traps occurring at discrete energy levels. This is now modified and a continuous distribution of traps results. For donor and acceptor traps at energy levels between E and E+dE the charge stored is,

$$\left(N_{td}\left(1-f_d\right)-f_a N_{ta}\right) dE \ .$$

The donor and acceptor trap concentrations are, in general, dependent on the energy E. To find the total charge stored, integration over the whole band gap range, from the valence energy level to the conduction energy level, is carried out. Full ionisation of the dopant energy level is assumed from now onwards. The magnitude of the concentration of the dopant ions is denoted by N_{net}, (<0). This doping level can, in general, be dependent on x and the doping profile is therefore denoted by $N\left(x\right)$. Therefore, Poisson's equation is,

$$\nabla^2\psi = q\left(n-p+N_{net}N\left(x\right)+\int_{E_V}^{E_C} f_a N_{ta}-N_{td}\left(1-f_d\right)dE\right) \ .$$

The recombination term, R, in the continuity equations is now considered. From previous calculations, the recombination of electrons for a single trap is,

$$R=r_a-r_b \ . \qquad \text{i.e.} \qquad R=v_{th}\sigma_n n N_t\left(1-f\right)-v_{th}\sigma_n N_c \exp\left(-\left(E_C-E\right)/kT\right)N_t f \ .$$

The above equation applies to donor and acceptor traps, but the capture cross section, the concentration, and probability of occupation differ in value, and are therefore denoted with the appropriate subscripts. Note, a list of all variable

definitions is given in Appendix A and a table of parameter sizes is given in Appendix B. Summing the two expressions together, and integrating across the band gap,

$$\begin{aligned} -R &= v_{th}\int_{E_V}^{E_C}\left(\sigma_{na}N_C\exp\left(-\left(E_C-E\right)/kT\right)N_{ta}f_a-\sigma_{na}nN_{ta}\left(1-f_a\right)\right)dE \\ &+ v_{th}\int_{E_V}^{E_C}\left(\sigma_{nd}N_{td}N_C\exp\left(-\left(E_C-E\right)/kT\right)f_d-\sigma_{nd}nN_{td}\left(1-f_d\right)\right)dE\ . \end{aligned}$$

Similarly, for the hole recombination,

$$R=r_c-r_d\ ,\qquad \text{i.e}\qquad R=v_{th}\sigma_p pN_t f-v_{th}\sigma_p N_V\exp\left(-\left(E\right)/kT\right)N_t\left(1-f\right)\ .$$

Following the reasoning for electron recombination,

$$\begin{aligned} -R &= v_{th}\int_{E_V}^{E_C}\left(\sigma_{pa}N_V\exp\left(-\left(E-E_V\right)/kT\right)N_{ta}\left(1-f_a\right)-\sigma_{pa}pN_{ta}f_a\right)dE \\ &+ v_{th}\int_{E_V}^{E_C}\left(\sigma_{pd}N_{td}N_V\exp\left(-\left(E-E_V\right)/kT\right)\left(1-f_d\right)-\sigma_{pd}pN_{td}f_d\right)\ . \end{aligned}$$

Finally, the rate of change of occupancy of a trap for each species is calculated. In particular, the case for a single trap f, at an energy E is found to be,

$$\frac{\partial f}{\partial t}=\frac{r_a-r_b-r_c+r_d}{N_t}\ .$$

Note, the expression is divided by N_t since only a single trap is being considered. Putting in the values for the recombination rates computed earlier it is found,

$$\begin{aligned} \frac{\partial f}{\partial t} = &- v_{th}f\left[\sigma_n\left(n+N_C\exp\left(-\left(E_C-E\right)/kT\right)\right)\right. \\ &+ \left.\sigma_p\left(p+N_V\exp\left(-\left(E-E_V\right)/kT\right)\right)\right] \\ &+ v_{th}\left(\sigma_n n+\sigma_p N_V\exp-\left(\left(E-E_V\right)/kT\right)\right)\ . \end{aligned}$$

This equation for both types of species is used, denoting the capture cross sections etc. in the appropriate manner. Therefore,

$$\frac{\partial f_a}{\partial t} = - v_{th}f_a\left[\sigma_{na}\left(n+N_C\exp\left(-\left(E_C-E\right)/kT\right)\right)\right.$$

$$
\begin{aligned}
&+ \quad \sigma_{pa}\left(p + N_V \exp\left(-\left(E - E_V\right)/kT\right)\right)] \\
&+ \quad v_{th}\left(\sigma_{na} n + \sigma_{pa} N_V \exp\left(-\left(E - E_V\right)/kT\right)\right) . \\
\frac{\partial f_d}{\partial t} = &- \quad v_{th} f_d \left[\sigma_{nd}\left(n + N_C \exp\left(-\left(E_C - E\right)/kT\right)\right)\right. \\
&+ \quad \sigma_{da}\left(p + N_V \exp\left(-\left(E - E_V\right)/kT\right)\right)] \\
&+ \quad v_{th}\left(\sigma_{nd} n + \sigma_{pd} N_V \exp\left(-\left(E - E_V\right)/kT\right)\right) .
\end{aligned}
$$

2.4.1 The System of Amorphous Equations

The system of equations for amorphous silicon can now be written down.

Poisson's Equation,

$$
\nabla^2 \psi = q\left(n - p + N_{net} N\left(x\right) + \int_{E_V}^{E_C} f_a N_{ta} - N_{td}\left(1 - f_d\right) dE\right) .
$$

The continuity equation for electrons,

$$
\begin{aligned}
\frac{\partial n}{\partial t} - \frac{1}{q}\nabla.\vec{J}_n &= v_{th}\int_{E_V}^{E_C}\left(\sigma_{na} N_C \exp\left(-\left(E_C - E\right)/kT\right) N_{ta} f_a\right) dE \\
&- v_{th}\int_{E_V}^{E_C}\left(\sigma_{na} n N_{ta}\left(1 - f_a\right)\right) \\
&+ v_{th}\int_{E_V}^{E_V}\sigma_{nd} N_{td} N_C \exp\left(-\left(E_C - E\right)/kT\right) f_d dE \\
&- v_{th}\int_{E_V}^{E_C}\sigma_{nd} n N_{td}\left(1 - f_d\right) dE .
\end{aligned}
$$

The continuity equation for holes,

$$
\frac{\partial p}{\partial t} + \frac{1}{q}\nabla.\vec{J}_p = v_{th}\int_{E_V}^{E_C}\left(\sigma_{pa} N_V \exp\left(-\left(E - E_V\right)/kT\right) N_{ta}\left(1 - f_a\right) - \sigma_{pa} p N_{ta} f_a\right) dE
$$

$$+ \quad v_{th} \int_{E_V}^{E_C} \left(\sigma_{pd} N_{td} N_V \exp\left(-\left(E - E_V\right)/kT\right)\left(1 - f_d\right) - \sigma_{pd} p N_{td} f_d\right) dE \ .$$

The current relations,

$$\vec{J}_n = \mu_n \left(kT \frac{\partial n}{\partial x} - qn\nabla\psi \right) \ .$$

$$\vec{J}_p = -\mu_p \left(kT \frac{\partial p}{\partial x} + qp\nabla\psi \right) \ .$$

Finally, for the rate of change of the traps,

$$\begin{aligned} \frac{\partial f_a}{\partial t} = & - v_{th} f_a \left[\sigma_{na} \left(n + N_C \exp\left(-\left(E_C - E\right)/kT\right)\right)\right. \\ & + \left.\sigma_{pa} \left(p + N_V \exp\left(-\left(E\right)/kT\right)\right)\right] f_a \\ & + v_{th} \left(\sigma_{na} n + \sigma_{pa} N_V \exp\left(-\left(E - E_V\right)/kT\right)\right) \ . \end{aligned}$$

$$\begin{aligned} \frac{\partial f_d}{\partial t} = & - v_{th} f_d \left[\sigma_{nd} \left(n + N_C \exp\left(-\left(E_C - E\right)/kT\right)\right)\right. \\ & + \left.\sigma_{da} \left(p + N_V \exp\left(-\left(E - E_V\right)/kT\right)\right)\right] f_d \\ & + v_{th} \left(\sigma_{nd} n + \sigma_{pd} N_V \exp\left(-\left(E - E_V\right)/kT\right)\right) \ . \end{aligned}$$

2.4.2 The Non-Dimensionalised Form Of The System

Before starting to analyse the model it is appropriate to put it in a non-dimensional form using the following procedure from [21].

$$
\begin{aligned}
t &= \frac{1}{n_i v_{th} \sigma_{pa}} \bar{t} & x &= \sqrt{\frac{\epsilon kT}{q^2 n_i}} \bar{x} \\
n &= n_i \bar{n} & p &= n_i \bar{p} \\
\vec{J}_n &= \frac{\mu kT n_i}{L} \vec{\bar{J}}_n & \vec{J}_p &= \frac{\mu kT n_i}{L} \vec{\bar{J}}_p \\
\psi &= \frac{kT}{q} \bar{\psi} & E &= \tfrac{1}{2}\left(E_C - E_V\right)\left(1 + \bar{E}\right) + E_V \\
N_{ta} &= N_t \bar{N}_{ta} & N_{td} &= N_t \bar{N}_{td}
\end{aligned}
$$

With the above scalings, the non-dimensional set of equations for amorphous silicon are found.

$$
\nabla^2 \bar{\psi} = \left(\bar{n} - \bar{p} + \lambda N\left(\bar{x}\right) + \alpha \int_{-1}^{1} f_a \bar{N}_{ta} - \bar{N}_{td}\left(1 - f_d\right) d\bar{E} \right) .
$$

All subsequent analysis assumes uniform doping profiles as applied to a p-type semiconductor, implying $N\left(\bar{x}\right) = 1$. Hence,

$$
\nabla^2 \bar{\psi} = \left(\bar{n} - \bar{p} + \lambda + \alpha \int_{-1}^{1} f_a \bar{N}_{ta} - \bar{N}_{td}\left(1 - f_d\right) d\bar{E} \right) .
$$

$$
\begin{aligned}
\frac{\partial \bar{n}}{\partial \bar{t}} - \beta \nabla . \vec{J}_n &= \alpha \int_{-1}^{1} \left(\sigma_1 \exp\left(\bar{E}/\delta\right) \bar{N}_{ta} f_a - \sigma_1 \bar{n} \bar{N}_{ta}\left(1 - f_a\right) \right) d\bar{E} \\
&+ \alpha \int_{-1}^{1} \left(\sigma_2 \bar{N}_{td} \exp\left(\bar{E}/\delta\right) f_d - \sigma_2 \bar{n} \bar{N}_{td}\left(1 - f_d\right) \right) d\bar{E} .
\end{aligned}
$$

$$
\begin{aligned}
\frac{\partial \bar{p}}{\partial \bar{t}} + \beta \nabla . \vec{\bar{J}}_p &= \alpha \int_{-1}^{1} \left(\exp\left(-\bar{E}/\delta\right) \bar{N}_{ta}\left(1 - f_a\right) - \bar{p} \bar{N}_{ta} f_a \right) d\bar{E} \\
&+ \alpha \int_{-1}^{1} \left(\sigma_3 \bar{N}_{td} \exp\left(-\bar{E}/\delta\right)\left(1 - f_d\right) - \sigma_3 \bar{p} \bar{N}_{td} f_d \right) d\bar{E} .
\end{aligned}
$$

$$
\vec{\bar{J}}_n = \nabla \bar{n} - \bar{n} \nabla \bar{\psi} .
$$

$$\vec{\bar{J}}_p = -\mu\left(\nabla\bar{p} + \bar{p}\nabla\bar{\psi}\right) .$$

$$\begin{aligned}\frac{\partial f_a}{\partial \bar{t}} = & - f_a\left[\sigma_1\left(\bar{n} + \exp\left(\bar{E}/\delta\right)\right)\right. \\ & + \left.\left(\bar{p} + \exp\left(-\bar{E}/\delta\right)\right)\right] \\ & + \left(\sigma_1\bar{n} + \exp\left(-\bar{E}/\delta\right)\right) .\end{aligned}$$

$$\begin{aligned}\frac{\partial f_d}{\partial \bar{t}} = & - f_d\left[\sigma_2\left(\bar{n} + \exp\left(\bar{E}/\delta\right)\right)\right. \\ & + \left.\sigma_3\left(\bar{p} + \exp\left(-\bar{E}/\delta\right)\right)\right] \\ & + \left(\sigma_2\bar{n} + \exp\left(-\bar{E}/\delta\right)\right) .\end{aligned}$$

The parameters in the equations above are listed below.

$$\alpha = \frac{N_t E_g}{2n_i} \qquad \beta = \frac{\mu_n q}{\epsilon v_{th}\sigma_{pa}}$$

$$\frac{1}{\delta} = \frac{1}{2}\frac{E_g}{kT} \qquad \mu = \frac{\mu_p}{\mu_n}$$

$$\sigma_1 = \frac{\sigma_{na}}{\sigma_{pa}} \qquad \sigma_2 = \frac{\sigma_{nd}}{\sigma_{pa}}$$

$$\sigma_3 = \frac{\sigma_{pd}}{\sigma_{pa}} \qquad \lambda n_i = N_{net}$$

2.5 Defect Pool Model

In the succeeding section is an outline of the problems constituting my MPhil. But first, I feel it is appropriate to explain one of the more important concepts of amorphous semiconductors, namely the existence of a continuous distribution of localised states in the forbidden gap. Much research has been done in trying to understand the cause of these localised states, and how, if possible, to predict the

distribution, given certain constituents of the semiconductor. One successful method that is being used is the defect pool model. It has been discovered that dangling bonds, created by the breaking of weak silicon bonds, are the cause of these defect states. Since amorphous semiconductors are highly disordered materials, the weak silicon bonds are continually distributed in energy. Hence, the energy possessed by a defect depends on which weak silicon bond is broken. The continually distributed weak silicon bond energies imply the corresponding dangling bond energies are also continually distributed. The defect pool model approaches the problem by considering a chemical equilibrium between the weak silicon bonds and the dangling bonds. There are various choices for the specific reactions, and it is the purpose of this section to outline the basic types used. Firstly, however, I give a brief history of how these defect states were discovered, and why a weak bond-dangling bond chemical equilibrium is used to describe the defect distribution.

Two papers by Powell, Berkel and French, [22], and [23], reported on bias stress measurements on amorphous silicon T.F.T's. The first gives conclusive evidence that instability mechanisms occur when the device is subjected to a prolonged gate voltage, and that they are distinguishable. This bias produces a shift in the threshold voltage. The two mechanisms proposed to account for this behaviour are,

i) State creation, dominated at low positive bias.

ii) Charge trapping, dominated at high positive bias as well as negative bias.

The first paper does not indicate whether state creation occurs in the nitride gate insulator, or in the a-Si:H semiconductor. However, [23] investigates the mechanisms for various nitride compositions. There exists a strong dependence of charge trapping, as opposed to an independence of state creation, on the nitride composition. Therefore, state creation occurs in the a-Si:H semiconductor, and charge trapping occurs in the a-Si:H gate insulator. They also propose that the created states result from the breaking of weak Si-Si bonds. There are three types of dangling bond, classified by the charge they possess,

D_e states - negatively charged dangling bonds,

D_h states - positively charged dangling bonds,

D_0 states - neutral dangling bonds.

Virtually all the states in the lower part of the gap are D_e states, and all the states in the upper part are D_h states. Figure 2.13 illustrates the typical distribution of the states in a-Si:H, taken from [29].

Next, it has to be decided what causes these defects. The analysis of chemical

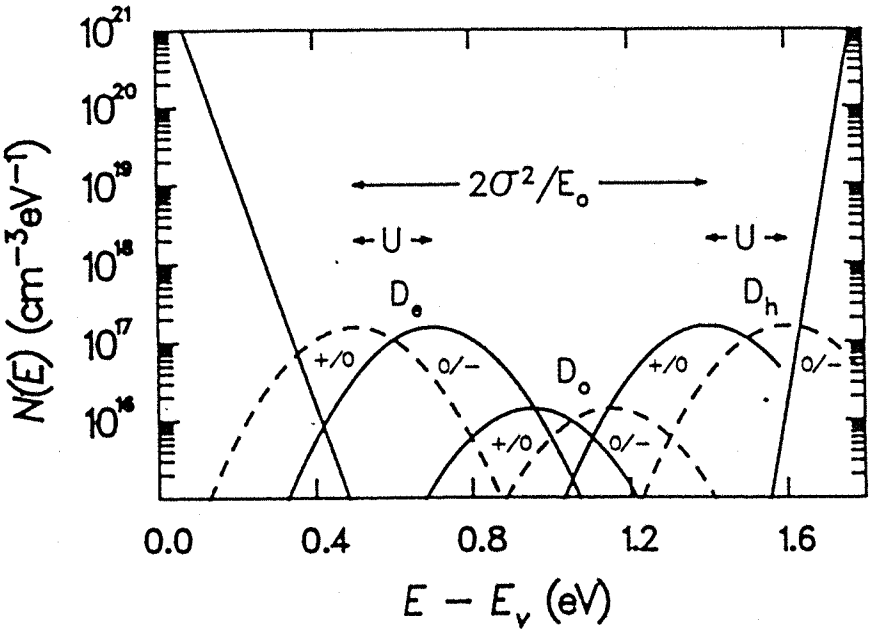

Figure 2.13: Density of states distribution in a-Si:H.

reactions in a-Si:H borrows heavily from the methods developed to analyze defect reactions in crystals. But the disordered nature of a-Si:H introduces a continuous distribution of reaction enthalpies. The kinetics of vacancy formation in C-Si depends on the motion of Si, but it is the dispersive diffusion of hydrogen that governs the kinetics in a-Si:H. When neutral defect concentrations were first discovered to vary reversibly with temperature, the effect was thought to be thermal. While these concentrations do depend on temperature, the long equilibrium times (up to 1 yr at 300K in n-type a-Si:H), make it clear some other type of equilibrium is going on. Therefore, chemical reactions mediated by molecules, not phonon exchange, are the key to interpreting the behaviour of defects in a-Si:H. A paper by R.A.Street and K.Winer, [28], discusses the different sorts of reactions that could be taking place. They adopt the same approach as an earlier paper by Z.Smith and S.Wagner, [35], but make three additional assumptions.

1) There is a non-equilibrium distribution of strained Si-Si bonds, which originates from the disorder of the a-Si:H network.

2) Defects are caused by the breaking of Si-Si bonds, which they are in thermal equilibrium with. The non-equilibrium distribution of Si-Si bonds implies there is a distribution of defect-formation energies, since the energy depends on which bond is broken.

3) The defect formation energy is equated to the difference in the one-electron energies of the defect gap state E_D, and the valence band tail state from which it is

derived. Therefore,

$$U = E_D - E_{VB} \ , \tag{2.20}$$

where,

E_D – the energy of the defect

E_{VB} – the energy of a weak Si-Si bond

The above assumptions form the weak-bond-dangling-bond conversion model, described by M.Stutzmann, [36].

Before looking at the reactions in more detail, a brief explanation of the chemical equilibrium between two molecules A and B, possessing energies E_A and E_B, respectively, is given. Chemical A reacts, and transforms into chemical B at a certain rate, determined by the reaction constant k_1. Similarly, chemical B reacts at a rate determined by k_2, transforming into chemical A. A point is reached when the amount of chemical A transforming into chemical B, is balanced by an equal amount of chemical A, forming from the transformation of B. The same reasoning applies to chemical B. Thus, the concentrations of chemicals A and B are constant and a dynamic equilibrium exists. This is represented by the following equation,

$$A \rightleftharpoons B \ .$$

In equilibrium, according to the law of mass action,

$$[B]_{\text{eq}} = [A]_{\text{eq}} e^{-\frac{\triangle E}{kT}} \ , \tag{2.21}$$

where $\triangle E = E_B - E_A$. When the system is perturbed, the transient concentrations can be solved. The rate at which A reacts, is equal to the product of the reaction constant k_1, and the amount of A present. The amount of A being created, is equal to the product of the amount of B present, and its corresponding reaction constant k_2. Thus, the rate of change of A satisfies,

$$\frac{dA}{dt} = k_2 B - k_1 A \ .$$

Similarly, for B,

$$\frac{dB}{dt} = k_1 A - k_2 B \ .$$

Note, adding the two equations above,

$$\frac{d(A+B)}{dt} = 0 \ , \qquad A + B = C \ , \qquad \text{where C is a constant} \ ,$$

vindicating the conservation of mass. Substituting B with C-A in the first differential equation,

$$\frac{dA}{dt} = k_2 (C - A) - k_1 A \ .$$

This can be easily solved to give,

$$A - A_{\text{eq}} = \left(A\,(0) - A_{\text{eq}}\right) \exp\left(-\left(k_1 + k_2\right) t\right) . \tag{2.22}$$

Similarly, for B,

$$B - B_{\text{eq}} = \left(B\,(0) - B_{\text{eq}}\right) \exp\left(-\left(k_1 + k_2\right) t\right) . \tag{2.23}$$

These relations are well established for defect reactions in crystals. But the disordered nature of a-Si:H introduces a distribution of reaction enthalpies $\triangle E$. The modification of equations (2.22) and (2.23) is treated by W.B Jackson, [38]. Here, only the study equation (2.21) is investigated.

Simply having the reaction,

$$\text{Si} \rightleftharpoons D_0 ,$$

gives,

$$[D_0]_{\text{eq}} = [\text{Si}]_{\text{eq}} \exp\left(-\frac{\triangle E}{kT}\right) .$$

But,

$$[\text{Si}]_{\text{eq}} \sim 5 \times 10^{22}\text{cm}^{-3} .$$

and

$$[D_0]_{\text{eq}} \sim 10^{16}\text{cm}^{-3} .$$

This requires $\triangle E \sim 0.7eV$, implying $[D_0]$ to be highly temperature dependent, which is not true. In fact $\triangle E$ has been measured to be 0.2 eV–0.3 eV by [39]. Therefore, an equilibrium between D_0 and a subset of Si must exist. Z.Smith and S.Wagner, [35], resolved this by invoking the weak-bond-dangling-bond model, originally proposed by M.Stutzmann, [36]. Since the weak bond concentration, [Si-Si], is $\sim 10^{19}\text{cm}^{-3}$, and this gives the correct defect density. Therefore, an equilibrium between the weak silicon bonds (Si-Si), and the dangling bonds (D_0) exists and is represented by,

$$\text{Si-Si} \rightleftharpoons D_0 .$$

Solving this gives,

$$[D_0]_{\text{eq}} = [\text{SiSi}]_{\text{eq}} \exp\left(-\frac{\triangle E}{kT}\right) .$$

However, the total number of Si-Si bonds is simply the sum of the equilibrium and broken bond concentrations,

$$[\text{SiSi}]_{\text{tot}} = [\text{SiSi}]_{\text{eq}} + [\text{SiSi}]_{\text{broken}} .$$

However,

$$[\text{SiSi}]_{\text{broken}} = [D_0]_{\text{eq}} , \qquad \Rightarrow \qquad [D_0]_{\text{eq}} = \left([\text{SiSi}]_{\text{tot}} - [D_0]_{\text{eq}}\right) \exp\left(-\frac{U}{kT}\right) .$$

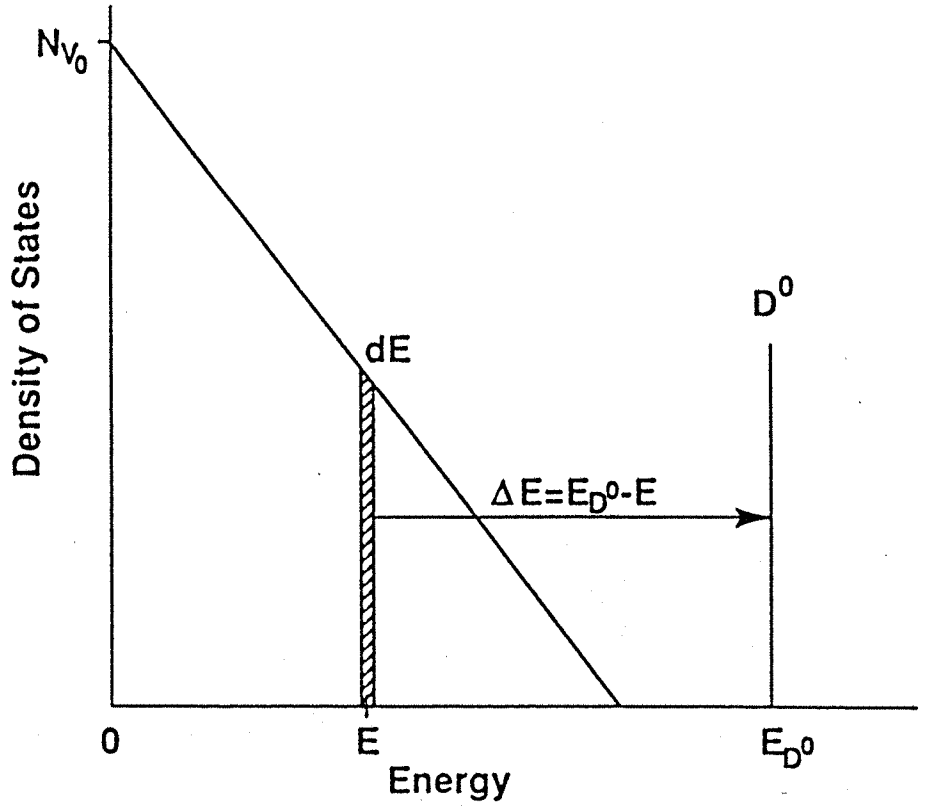

Figure 2.14: Density of states diagram to illustrate the distribution of reaction enthalpies in the weak-bond-dangling-bond model with a single defect D_0 in the gap at energy E_{D_0}.

Rearranging this equation,

$$[D_0]_{\text{eq}} = \frac{[\text{SiSi}]_{\text{tot}} e^{-\frac{U}{kT}}}{1 + e^{-\frac{U}{kT}}} .$$

The existence of a distribution of reaction enthalpies is made clear in figure 2.14, taken from [26], which depicts the valence-band tail, (weak Si-Si bonding states) described by $N_{V0} \exp(-E/E_0)$, and a single defect D_0 in the gap at energy E_{D_0}. It is essential to include in the calculations the distribution of formation energies, which originates from the variation of strain energies of the silicon bonds, (the contribution made by Smith and Wagner, [35]). According to the weak bond model, the distribution function is equated to the shape of the valence band tail, which is assumed to be of the form,

$$N_{V0}(E_{VB}) = N_{V0} \exp\left(-\frac{E_{VB}}{kT_v}\right) .$$

Each weak bond in the valence tail is assumed to be in chemical equilibrium with this single defect D_0. Therefore, integrating over all possible weak bond energies gives the defect concentration,

$$\begin{aligned} N_d &= \int_0^{\infty} \frac{N_{V0} E^{-\frac{E_{VB}}{kT_v}} e^{-\frac{U}{kT}}}{1 + e^{-\frac{U}{kT}}} dE_{VB} \\ &\approx \frac{N_{V0} kT T_v}{T_v - T} \left[\frac{T_v}{T} \exp(-E_D/kT_v) - \exp(-E_D/kT)\right] . \end{aligned}$$

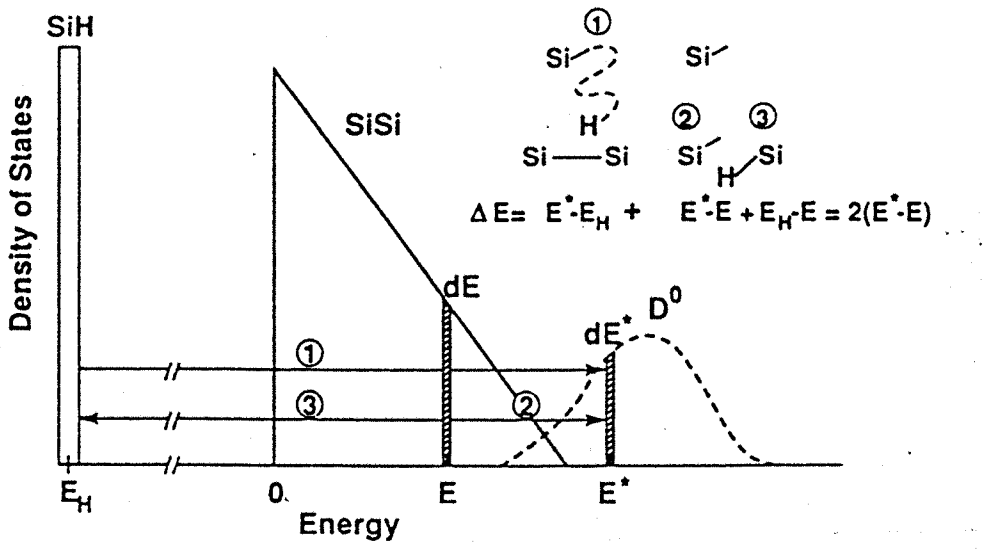

Figure 2.15: Density of states diagram to illustrate the distribution of reaction enthalpies in the weak-bond-dangling-bond model. The distribution involves both an exponential component due to the exponential valence band tail, and a Gaussian component due to the distribution of virtual defect states in the defect pool.

The above calculations are applicable to a single band gap defect. However, since there exists a continuous distribution of defect states, a chemical equilibrium between the valence band tail states and a distribution of potential, or pool, of defect sites needs to be considered. Mathematically speaking, this single defect is simply a δ-function. Therefore, to create a distribution of defects, a distribution of potential defect sites is considered. The true distribution is known to be nearly Gaussian. Therefore, this δ-function is replaced with a Gaussian pool of states of width σ, as illustrated in figure 2.15. Integrating across all possible defect state energies,

$$N_D = \frac{N_{V0} k T T_v}{T_v - T} \int_0^\infty \left[\frac{T_v}{T} e^{-\frac{E}{kT_v}} - e^{-\frac{E}{kT}} \right] \times \frac{e^{-\frac{(E-E_\mu)^2}{2\sigma^2}}}{(2\pi\sigma^2)^{\frac{1}{2}}} dE \ ,$$

where,

E_μ – most probable defect chemical potential ,

σ – Gaussian width .

This expression can be approximated,

$$\begin{aligned} N_D \ &\approx \ \frac{N_{V0} k T T_v}{T_v - T} \times \left(\frac{T}{T_v} \exp\left(-E_D/kT_v - \sigma^2/2(kT_v)^2 \right) \right) \\ &- \ \exp\left(-E_D/kT - \sigma^2/k^2 T_v^{\cdot} + \sigma^2/2(kT)^2 \right) , \end{aligned} \tag{2.24}$$

where,

$$E_D = E_\mu - \frac{\sigma^2}{kT_v} .$$

Equation (2.24), is identical to the discrete gap state (2.23), except the defect energy E_D is shifted from the average defect chemical potential E_μ, by the energy $\frac{\sigma^2}{kT_v}$, and the effective density of valence band tail states is reduced by a factor $\exp\left(-\frac{\sigma^2}{2(kT_v)^2}\right)$. The reason for this is straight forward. The formation enthalpy for defect states near the low-energy Gaussian tail is smaller than at the Gaussian peak. Consequently, many defect states "want" to form there. Yet, there are progressively fewer available sites as one moves down the sides of the Gaussian. The balance between the enthalpy reduction, for states formed in the lower energy tail of the "defect pool" distribution, and enthalpy increase due to increased distortion energy for states formed far from the defect pool maximum, results in the defect peak shift. In n-type and p-type a-Si:H, D_- and D_+ defects, respectively, dominate. In undoped a-Si:H, however, the dominant defect depends on the width of the Gaussian defect pool. For small values of, σ, (≈ 0.1 eV, D_0 defects dominate in intrinsic a-Si:H. For larger values of σ, (> 0.15 eV), charged D_- and D_+ defects dominate, when the appropriate electron occupation statistics are employed.

In reality, it is known that one broken weak silicon bond leads to two rather than one defect. The previous reaction does not account for this, and Smith and Wagner modified their analysis to take into account this extra defect, with the reaction,

$$\mathrm{SiSi} \rightleftharpoons 2D_0 .$$

However, for reasons not mentioned here, the two resulting dangling bonds must diffuse away from each other. This model, therefore, can only apply if the silicon defects are mobile. But there is no clear evidence mobile defects exist. However, such a mechanism is likely to determine the reaction kinetics. The kinetics of defect equilibration in a-Si:H has been measured and is consistent with a process whose rate is limited by the dispersive diffusion of hydrogen. The explicit introduction of H into the chemical reactions describing defect formation, resolves the problem of defect diffusion, and accounts for the kinetics of defect equilibration in a straightforward manner. The introduction of hydrogen into the reaction gives,

$$\text{Si-H} + (\text{weak bond}) \rightleftharpoons D_H + D_W ,$$

and is illustrated in figure 2.16. The defect labeled D_W refers to the one at the site of the weak bond, where it is immediately adjacent to the Si-H bond. This defect cannot be separated from the Si-H bond and the two must be considered a single entity. The isolated D_H defect is left by the removal of hydrogen from the Si-H bond. It is assumed that the two defects have the same energy. The application of the law of mass action to the above reaction is similar to the previous calculations on the earlier reaction.

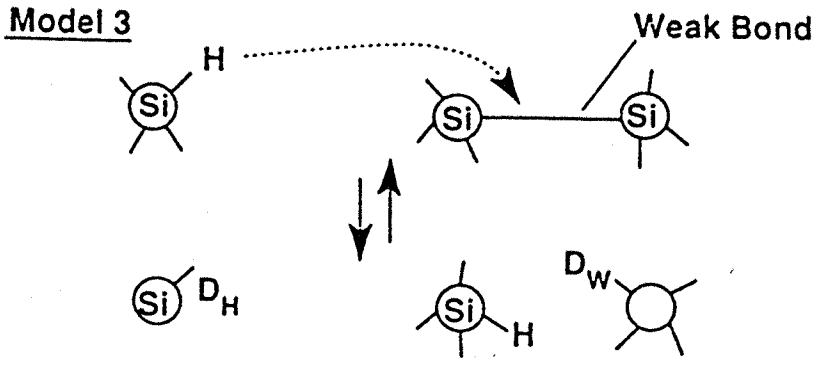

Figure 2.16: Schematic illustration of the defect reaction for the hydrogen diffusion model.

The basics of the defect pool model are to calculate defect distributions and concentrations. The distribution can be calculated as a function of temperature and Fermi energy. The results compare favourably with the available experimental data, suggesting the underlying basis of the theory to be correct.

The success of this chemical approach to understanding the behaviour of defects in a-Si:H can also be carried over into the description of optimal growth of a-Si:H, defined as those growth conditions that lead to the lowest equilibrium defect concentration. The key idea for this approach, is that the main role of the plasma is to supply the sources of the chemically reactive species, and the material properties of the a-Si:H are determined primarily by reactions that take place on or below the surface. The reliance on solid state chemical reactions, rather than plasma-gas processes, is radically different from most previous attempts to describe a-Si:H growth. Future work is to discover from this defect pool model, how to better control the material properties of a-Si:H.

2.6 An Introduction To The Three Problems Considered

Before entering into any detailed discussions on the problems considered a review of the current understanding of specific devices, such as the MOS capacitor and the

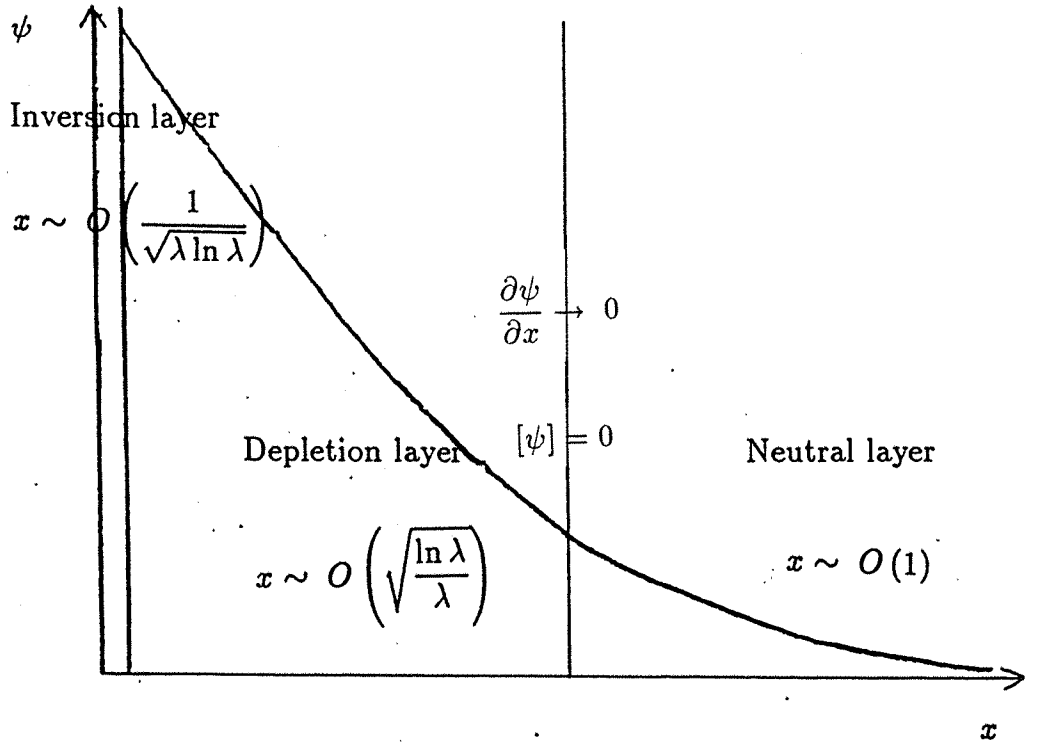

Figure 2.17: Diagram depicting the delta-depletion approximation.

p-n junction, is given.

A widely used approach for understanding the operation of devices makes use of the delta-depletion approximation. As an example of this approximation consider a p-type MOS capacitor in equilibrium subject to a steady positive gate voltage. The approximation considers the device to be divided into a depletion, neutral and inversion layer, see diagram 2.17. The neutral layer has zero space charge and hence there is a small uniform field. However, in the depletion region the application of this steady gate voltage repels holes into the neutral layer and attracts electrons towards the silicon-oxide interface. Since this region is now depleted of carriers the space charge is due solely to the fixed ionised dopant atoms. In order to patch the depletion and neutral layers two conditions are satisfied. Firstly, approaching the neutral layer from the depletion region the field is taken to be very small and secondly the electric potential is taken to be continuous. Finally, in a very thin layer at the oxide-silicon interface the electric field collects electrons and repels holes. If the applied gate voltage is large enough the concentration of electrons exceeds the bulk hole concentration and an inversion layer results. There are, however, inadequacies in this delta-depletion approximation. In particular, a discontinuity in the space-charge occurs at the depletion-neutral layer interface. In addition, there is a need to understand more deeply the mathematical structure of the inversion layer.

To shed light on the first of these inadequacies research undertaken by Please, [21], reveals a very thin 'transition' region, see diagram 2.18, between the depletion and neutral layers of a p-n junction. Here, the equations are non-dimensionalised in such a way that a large parameter λ results. This parameter, which is proportional

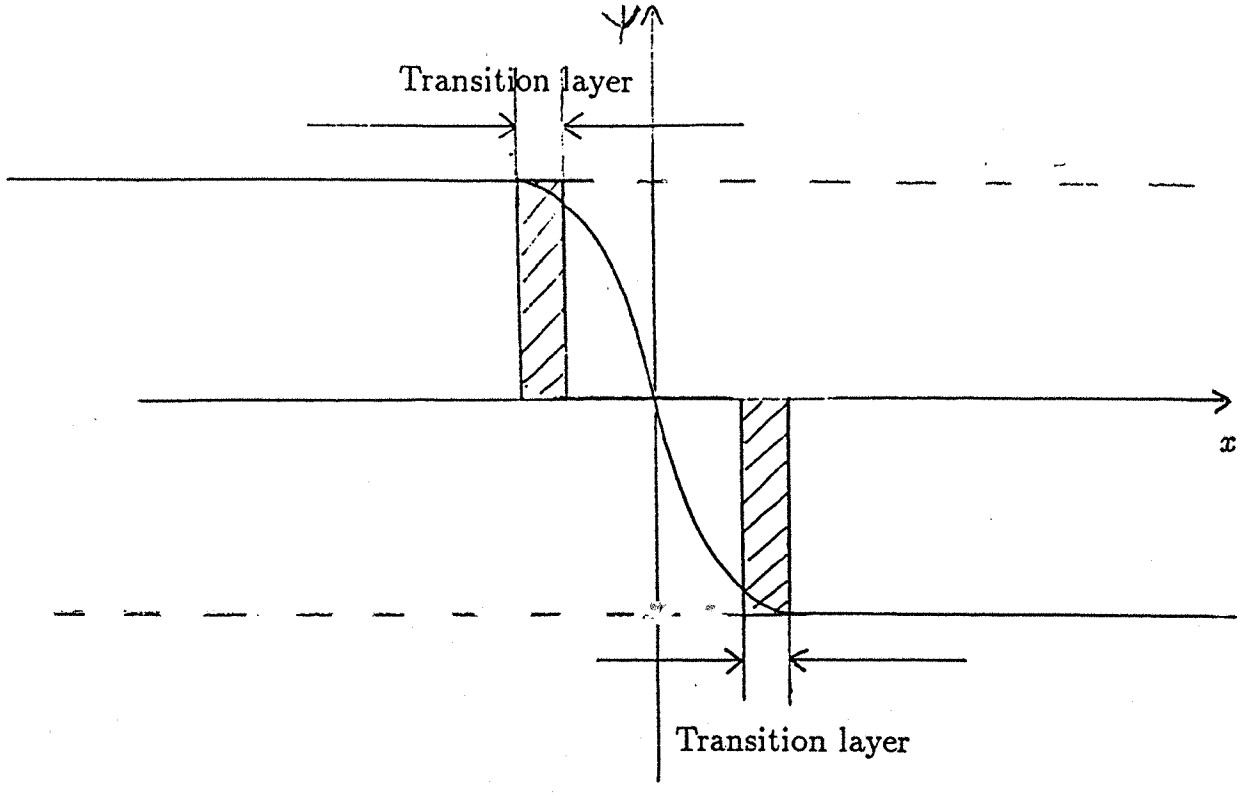

Figure 2.18: Diagram showing the voltage structure of a p-n junction.

to the doping level, is typically $0\,(10^{10})$. Asymptotic analysis in the limit $\lambda \to \infty$ was then carried out. It is found that in Chapter 3 the voltage across the MOS capacitor has a similar transition layer structure. In addition, this chapter investigates the structure of the inversion layer and a complete matched asymptotic solution for the electric potential is given.

Another common assumption made in modelling semiconductor devices is that the dopant atoms are completely ionised. In Chapter 4 this assumption is relaxed and a solution is sought for the problem of an MOS capacitor. Here the ionisation of the dopant atoms are considered by assuming that the dopant energy level is a single trap in the forbidden gap. The solution to this problem gives an initial insight into the behaviour of an amorphous MOS capacitor where a continuous distribution of traps exist in the band gap. However, this more difficult problem with a continuous distribution will not be considered.

There has been some analytical work into the transient behaviour of MOS capacitors. In [37] some asymptotic analysis of the transient behaviour of a p-n junction device is given and a brief review of the work is appropriate.

After an appropriate scaling of the semiconductor device equations [37] carries out a singular perturbation analysis. The resulting perturbation parameter is proportional to the minimal, (or extrinsic), Debeye length. It must be noted that this parameter is distinct from the parameter used in [21]. The Shockley-Read-Hall model for recombination is used and the hole and electron mobilities are assumed constant. It is found that two disparate time scales are present. The slow time scale

involves recombination of the carriers. The fast time scale corresponds to the conventional displacement current. In addition, some numerical solutions are given at the end of the paper.

In Chapter 5 the transient response of an amorphous MOS capacitor is investigated. It is anticipated at least two time scales are present. The fast time scale corresponds to the setting up of the deep-depletion phase. There is a slow time scale that corresponds to the return of the device to equilibrium, but this is not examined. The magnitude of the doping concentration is exploited and as in the previous chapters an asymptotic analysis in the limit $\lambda \rightarrow \infty$ is performed, as in [21]. Shockley-Read-Hall recombination is assumed and the electron and hole mobilities are considered field independent. In addition, the concentration of the continuous distribution of traps in the band gap are taken to be small enough not to influence the equations to highest order. The behaviour of these traps, however, is hoped to shed light on how they may influence the problem when occurring in larger concentrations.

The following three problems are concerned with the application of a steady positive voltage to the gate electrode of an amorphous silicon MOS capacitor. In the first two problems a steady solution is sought. However, as mentioned earlier, either complete or partial ionisation of the dopant acceptor energy level can be considered. The first problem is concerned with complete ionisation of the dopant ions, whereas the second is concerned with the more realistic scenario of partial ionisation. In connection to the first problem the reader may wish to refer to [21]. The parameter λ, denotes the concentration of dopant, which is typically $O\left(10^{10}\right)$. The magnitude of this parameter is exploited, and the problems are solved in the limit, $\lambda \rightarrow \infty$. Asymptotic analysis of the device equations is then carried out. In addition, to simplify the problems, small defect gap state concentrations are considered. In mathematical terms, I take the limit, $\alpha \rightarrow 0$, where, α denotes the defect gap state concentrations. The third and final problem is concerned with finding a transient solution to the device equations, when a constant positive voltage is applied to the MOS capacitor, initially in equilibrium. The complete ionisation of the dopant acceptor ions is assumed, and asymptotic analysis is performed under the same limits as above.

To simplify all the problems above, the analysis of the device only applies near the centre of the channel, as shown in the shaded strip in figure 2.19. Here edge effects are ignored and the voltage, carrier concentrations etc. only depend on the distance x. Leakage currents, due to continuous distributions of surface states at the oxide-semiconductor interface, do exist in real devices and the concentrations that occur are not negligible. However, for simplicity the three problems are analysed with the assumption of zero surface states. Finally, the applied voltage is assumed to be large enough so as to ensure the formation of an inversion layer.

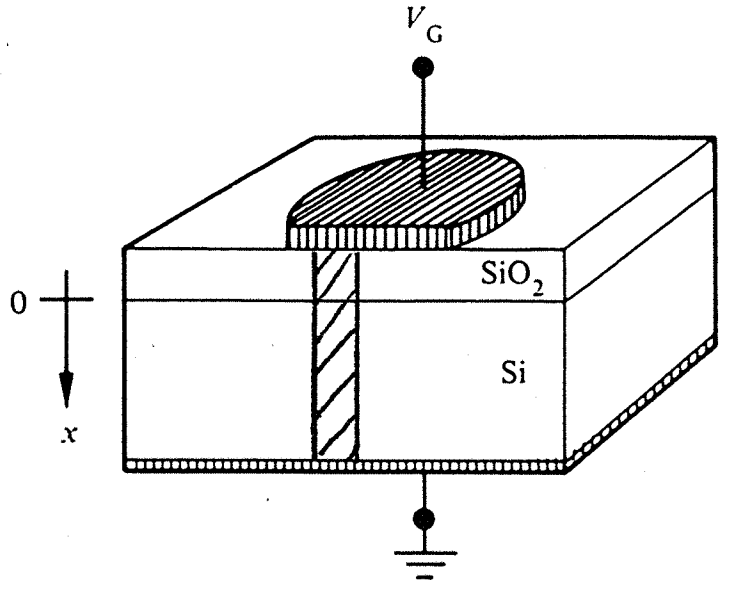

Figure 2.19: Diagram indicating the region of the MOS capacitor where the analysis is applicable.

Each of the previous mentioned problems is now discussed in greater detail.

2.6.1 The Steady Problem With Complete Ionisation Of The Dopant Ions

Chapter 3 is concerned with the problem of a steady voltage being applied to the gate electrodes of an MOS capacitor, and a steady solution is sought. One extremely useful property of the MOS capacitor is the absence of any current in steady state conditions. It is this property that simplifies the problem greatly, and enables the carrier concentrations to be described in terms of the voltage. In addition, very small defect gap state concentrations are assumed, and hence, to highest order, the device behaves as a crystalline MOS capacitor. These assumptions are made in the hope that the solution will give some insight into both the problem of partial ionisation of the dopant ions in the crystalline device, and the more complicated steady and transient problems of the amorphous device.

To set up the problem mathematically, the reader is referred to the non-dimensionalised system of amorphous equations at the end of section 2.4.

To highest order, in the limit $\alpha \rightarrow 0$, the continuity equations for electrons and

holes are,

$$\frac{\partial p}{\partial t} + \beta \frac{\partial J_p}{\partial x} = 0 .$$

$$\frac{\partial n}{\partial t} - \beta \frac{\partial J_n}{\partial x} = 0 .$$

However, a steady solution is being sought, therefore,

$$\frac{\partial n}{\partial t} = \frac{\partial p}{\partial t} = 0 .$$

Therefore, the continuity equations imply the electron and hole currents are constant under steady state conditions. In the limit $\alpha \rightarrow 0$, the leakage currents due to the interfacial traps at the oxide-semiconductor interface are, to highest order, zero. Thus,

$$J_n = 0 ,$$

$$J_p = 0 , \qquad \text{at} \qquad x = 0 .$$

Therefore, the currents are zero everywhere. Since there are no electron or hole currents,

$$0 = \frac{dn}{dx} - n\frac{d\psi}{dx} \tag{2.25}$$

$$0 = -\mu \left(\frac{dp}{dx} - p\frac{d\psi}{dx} \right) \tag{2.26}$$

These equations can easily be solved, and the electron and hole concentrations can be expressed in terms of the voltage ψ,

$$n = Ae^{\psi} .$$

$$p = Be^{-\psi} .$$

Under equilibrium, the product np=1 applies, and,

$$B = \frac{1}{A} .$$

Thus, in the limit $\alpha \rightarrow 0$, Poisson's equation to highest order is,

$$\frac{\partial^2 \psi}{\partial x^2} = Ae^{\psi} - \frac{1}{A}e^{-\psi} + \lambda .$$

The boundary conditions of the problem are now considered. The boundary conditions for the currents have already been mentioned and the remaining conditions are concerned with the voltage, ψ, and the electric field, $\vec{E}$. At the oxide-silicon interface, the voltage, ψ, is expected to be continuous, and is given the value $\psi(x=0)$. It also seems reasonable to assume continuity of the electric field. Since the oxide layer is assumed to be neutral, the electric field is linear. Continuity of this field across the oxide-silicon interface is therefore given by,

$$\frac{\partial \psi}{\partial x} = h\sqrt{\frac{\lambda}{\ln \lambda}}(\psi - v \ln \lambda) \ ,$$

where,

$v \ln \lambda$ – is the voltage applied to the gate electrode,

$\frac{1}{h}\sqrt{\frac{\ln \lambda}{\lambda}}$ – is the thickness of the oxide layer.

At the back of the device, $(x=a)$, it is assumed an ohmic contact exists between the silicon substrate and the rear contact. Thus,

$$\frac{\partial^2 \psi}{\partial x^2} = 0 \ , \qquad \text{and} \qquad np = 1$$

Finally, letting,

$$\psi = 0 \ ,$$

at x=a, fixes the arbitrary constant contained in the voltage potential. The boundary conditions for this problem are,

$$\frac{\partial \psi}{\partial x} = h\sqrt{\frac{\lambda}{\ln \lambda}}(\psi - v \ln \lambda) \ ,$$

at x=0, and,

$$\psi = 0 \ ,$$

$$\frac{\partial^2 \psi}{\partial x^2} = 0 \ ,$$

at x=a.

2.6.2 The Steady Problem With Partial Ionisation Of The Dopant Ions

The steady problem above assumes complete ionisation of the dopant ions. Here, this simplifyed description is removed, and a more realistic scenario, of partial

ionisation of the dopant atoms, is considered. In the section on recombination and generation of centres, a function f was derived, through the use of Shockley Read Hall statistics, to describe the occupancy of traps under steady state conditions. Here, a steady solution is being sought. Thus, f can be used to describe the occupancy of the dopant energy level.

Referring to the amorphous system of equations, in section 2.4, in steady state, the rate of change of the acceptor trap occupancy f_a is zero. This gives an algebraic equation for f_a, which is easily solved to obtain,

$$f_a = \frac{\sigma_1 \bar{n} + e^{-\bar{E}/\delta}}{\sigma_1 \bar{n} + \sigma_1 e^{\bar{E}/\delta} + e^{-\bar{E}/\delta} + \bar{p}} .$$

Since the semiconductor is assumed to be p-type the dopant ions are acceptor type in nature. Therefore, the occupancy of the dopant ions, f, is described by the function f_a. To simplify further, the problem with $\sigma_1 = 1$, is considered to give,

$$f = \frac{\bar{n} + \gamma}{\bar{n} + \frac{1}{\gamma} + \gamma + \bar{p}} ,$$

where $\gamma = e^{-\bar{E}/\delta}$. The assumption that $\sigma_1 = 1$ seems reasonable since the typical value is of the order of unity.

Under complete ionisation, the charge stored in the acceptor traps is simply λ. Here, however, the ionisation is only partial, and the amount of charge storage is given by $f\lambda$. Thus, Poisson's equation becomes,

$$\frac{\partial^2 \psi}{\partial x^2} = Ae^{\psi} - \frac{1}{A} e^{-\psi} + \lambda \left(\frac{n + \gamma}{n + \frac{1}{\gamma} + \gamma + p} \right) ,$$

where in the expression for f the bar notation has been dropped for clarity. This problem is identical to the previous in every respect, but for the partial ionisation of the dopant ions. The boundary conditions are the same, except at $x = 0$, where the thickness of the oxide layer is,

$$\frac{1}{\bar{h}} \sqrt{\frac{\frac{1}{2} \ln \lambda\gamma}{\lambda}} .$$

Thus,

$$\frac{\partial \psi}{\partial x} = \bar{h} \sqrt{\frac{\lambda}{\frac{1}{2} \ln \lambda\gamma}} \left(\psi - v \frac{1}{2} \ln \lambda\gamma \right) ,$$

at x=0, and,

$$\frac{\partial^2 \psi}{\partial x^2} = 0 ,$$
$$\psi = 0 ,$$

at x=a.

2.6.3 The Transient Problem With full Ionisation Of The Dopant Ions

Here, the transient effects of the capacitor, caused by the application of a steady voltage to the device initially in equilibrium, are considered. The main concern is the formation of a deep-depletion layer, and the succeeding development of the device into the steady state. For simplicity, a constant level of traps throughout the band gap is taken at a concentration far below the that of the dopant. The bulk traps taken are to be acceptor traps, to reduce the algebra. Again, the limit of large doping levels is taken,

$$\lambda \rightarrow \infty \, ,$$

and small bulk trap levels,

$$\alpha \rightarrow 0 \, .$$

It is assumed $\beta \, , \delta \gg 1$, but do not, as yet, specify their values relative to λ. In addition, to simplify matters, the problem assumes complete ionisation of the dopant ions.

The equations for this problem, to highest order, are,

$$\nabla^2 \psi = n - p + \lambda \, .$$

$$\frac{\partial n}{\partial \bar{t}} - \beta \frac{\partial J_n}{\partial x} = 0 \, .$$

$$\frac{\partial p}{\partial \bar{t}} + \beta \frac{\partial J_p}{\partial x} = 0 \, .$$

$$J_n = \frac{\partial n}{\partial x} - n \frac{\partial \psi}{\partial x} \, .$$

$$J_p = -\mu \left(\frac{\partial p}{\partial x} + p \frac{\partial \psi}{\partial x} \right) \, .$$

$$\begin{aligned} \frac{\partial f_a}{\partial \bar{t}} = & - f_a \left[\sigma_1 \left(\bar{n} + \exp\left(\bar{E}/\delta \right) \right) \right. \\ & + \left. \left(\bar{p} + \exp\left(-\bar{E}/\delta \right) \right) \right] \\ & + \left(\sigma_1 \bar{n} + \exp\left(-\bar{E}/\delta \right) \right) \, . \end{aligned}$$

Since initially, the device is in equilibrium, ($\psi = 0$), the carrier concentrations are simply,

$$n = A ,$$

$$p = \frac{1}{A} .$$

Initially, the device is equilibrium, which implies the rate of change of the acceptor traps is zero, i.e. $\frac{\partial f_a}{\partial t} = 0$. The above expression for $\frac{\partial f_a}{\partial t}$ therefore gives an algebraic equation for f_a. This is solved and,

$$f = \frac{1}{1 + \frac{1}{A} e^{\delta E}} ,$$

is the initial value for f_a. As discussed earlier, when the device is in equilibrium, charge neutrality holds and no currents flow. With all the above true in equilibrium, the initial conditions are,

$$J_n = 0 .$$

$$J_p = 0 .$$

$$n - p + \lambda = 0 .$$

$$\psi = 0 .$$

$$f_a = \frac{1}{\frac{1}{A} e^{\delta E} + 1} .$$

$$np = 1 .$$

The boundary conditions are similar to the first problem. However, since in this problem current flows, conditions on J_n and J_p must be imposed at $x = 0$. It is assumed that small surface trap concentrations at the oxide-semiconductor interface exist and to highest order no leakage currents are present. Therefore,

$$J_n = 0 , \qquad \text{and} \qquad J_p = 0 ,$$

at $x = 0$. Hence the boundary conditions for this problem are,

$$\frac{\partial \psi}{\partial x} = h \sqrt{\frac{\lambda}{\ln \lambda}} (\psi - v \ln \lambda) ,$$

$$J_n = 0 \ ,$$

$$J_p = 0 \ ,$$

at x=0, and,

$$np = 1 \ ,$$

$$\frac{\partial^2 \psi}{\partial x^2} = 0 \ ,$$

at x=a.

Chapter 3

The Steady Solution With Full Ionisation Of The Dopant Energy Level

In this chapter a steady solution for the M.O.S. capacitor, when its gate electrode is subject to a constant voltage, is sought. As discussed in the previous chapter, the one dimensional system of equations are considered, implying the solution is only valid near the middle of the device, where edge effects can be ignored.

The problem is then to solve,

$$\frac{\partial^2 \psi}{\partial x^2} = Ae^{\psi} - \frac{e^{-\psi}}{A} + \lambda \ , \tag{3.1}$$

with the following boundary conditions,

$$\frac{\partial \psi}{\partial x} = h\sqrt{\frac{\lambda}{\ln \lambda}}(\psi - v \ln \lambda) \ ,$$

at x=0, and,

$$\frac{\partial^2 \psi}{\partial x^2} = 0 \ ,$$
$$\psi = 0 \ ,$$

at x=a. Making use of the two boundary conditions at $x = a$, the arbitrary constant A can be found. Since, at $x = a$, equation (3.1) becomes,

$$0 = A - \frac{1}{A} + \lambda \ .$$

Thus, the solution for A is given by the roots of quadratic,

$$A^2 + \lambda A - 1 = 0 \, .$$

Using the fact $\lambda \gg 1$, and $A > 0$, the solution for A can be expanded in powers of λ to obtain,

$$A = \frac{1}{\lambda} + O\left(\frac{1}{\lambda^3}\right) \, .$$

In addition, $\frac{1}{A}$ is given by,

$$\frac{1}{A} = \lambda + O\left(\frac{1}{\lambda}\right) \, .$$

Substituting these equations into (3.1), gives,

$$\frac{\partial^2 \psi}{\partial x^2} = \left(\frac{1}{\lambda} + O\left(\frac{1}{\lambda^3}\right)\right) e^{\psi} - \left(\lambda + O\left(\frac{1}{\lambda}\right)\right) e^{-\psi} + \lambda \, . \tag{3.2}$$

To highest order, the $O\left(\frac{1}{\lambda^3}\right)$ electron concentration, and the $O\left(\frac{1}{\lambda}\right)$ hole concentration terms can be ignored. Therefore, equation (3.2) becomes,

$$\frac{\partial^2 \psi}{\partial x^2} = \frac{1}{\lambda} e^{\psi} - \lambda e^{-\psi} + \lambda \, . \tag{3.3}$$

In the following analysis four different regions of behaviour are found, illustrated in figure 3.1.

The scalings required are given below.

$x \sim O(1)$,	$\psi \sim O(1)$.	– Outer Solution
$x = x_0 + \frac{1}{\sqrt{\lambda}} \bar{x}$,	$\psi \sim O(1)$.	–Transition Layer
$x = \sqrt{\frac{u}{\lambda}} \hat{x}$,	$\psi = u \hat{\psi}$.	– Depletion Layer
$x = \frac{1}{\sqrt{\lambda u}} \breve{x}$,	$\psi = 2 \ln \lambda + \ln u + \breve{\psi}$.	– Inversion Layer

Where, u, ($\ll 2 \ln \lambda$) is a constant to be determined.

The remaining part of this chapter is concerned with the calculations necessary to find the leading order solutions, and the matching together of the four regions.

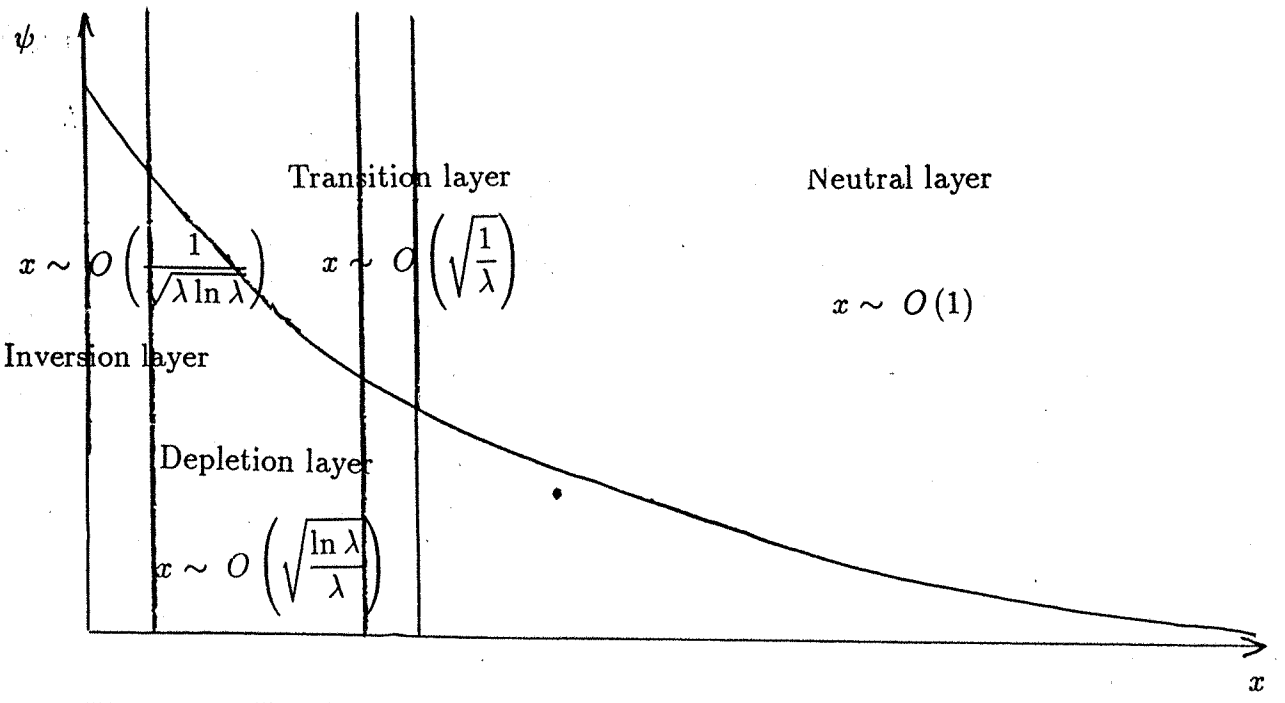

Figure 3.1: Sketch showing the different boundary layers of the steady solution with full ionisation of the dopant energy level.

3.1 The Outer Solution

In this region, far away from the oxide-semiconductor interface, the device is to highest order, neutral, and the hole concentration balances the dopant ion concentration.

Seeking ψ as a power series in $\frac{1}{\lambda}$,

$$\psi = \psi_0 + \frac{1}{\lambda}\psi_1 + O\left(\frac{1}{\lambda^2}\right) ,$$

and substituting into equation (3.3) gives,

$$\frac{\partial^2 \psi_0}{\partial x^2} + \frac{1}{\lambda}\frac{\partial^2 \psi_1}{\partial x^2} + \cdots = \frac{1}{\lambda}e^{\psi} - \lambda e^{-\psi} + \lambda .$$

But the exponential terms can be expanded to obtain,

$$\begin{aligned} \frac{\partial^2 \psi_0}{\partial x^2} + \frac{1}{\lambda} + \cdots &= \frac{1}{\lambda}e^{\psi_0}\left(1 + \frac{1}{\lambda}\psi_1 + \cdots\right) \\ &- \lambda e^{-\psi_0}\left(1 - \frac{1}{\lambda}\psi_1 + \cdots\right) + \lambda . \end{aligned}$$

Equating co-efficients of λ,

$$O(\lambda) , \qquad -\lambda e^{-\psi_0} + \lambda = 0 ,$$

$$\Rightarrow \qquad \psi_0 = 0 .$$

To highest order,

$$\psi = 0 \, .$$

3.2 Transition Layer

This is the very thin layer that separates the depleted region, where the hole concentration is small, from the neutral outer region, where the hole concentration is large. A concentration gradient therefore exists across the layer. Since a steady solution is being sought the net flow of holes is zero, implying the presence of an electric field to counter-balance the tendency of the holes to diffuse towards the interface. This is achieved by making the second order term, in Poisson's equation, balance the hole and dopant concentrations.

Expanding ψ in powers of $\frac{1}{\lambda}$,

$$\psi = \psi_0 + \frac{1}{\lambda}\psi_1 + \cdots \, ,$$

equation (3.3) becomes,

$$\lambda\left(\frac{\partial^2\psi_0}{\partial\bar{x}^2} + \frac{1}{\lambda}\frac{\partial^2\psi_1}{\partial\bar{x}^2} + \cdots\right) = \frac{1}{\lambda}e^{\psi_0}\left(1 + \frac{1}{\lambda} + \cdots\right) - \lambda e^{-\psi_0}$$
$$\left(1 - \frac{1}{\lambda}\psi_1 + \cdots\right) + \lambda \, .$$

To highest order,

$$\frac{\partial^2\psi_0}{\partial\bar{x}^2} = -e^{-\psi_0} + 1 \, . \tag{3.4}$$

However, equation (3.4) can be integrated to give,

$$\frac{1}{2}\left(\frac{\partial\psi_0}{\partial\bar{x}}\right)^2 = e^{-\psi_0} + \psi_0 + C \, , \tag{3.5}$$

where C is a constant of intergration.

Approaching the neutral region, $\bar{x} \to \infty$, and ψ_0, $\frac{\partial\psi_0}{\partial\bar{x}} \to \infty$. Substituting this into (3.5), gives $C = -1$. Equation (3.5) can be re-arranged to give,

$$\frac{\partial\psi_0}{\partial\bar{x}} = -\sqrt{2}\left(e^{-\psi_0} + \psi_0 - 1\right)^{\frac{1}{2}} \, . \tag{3.6}$$

It is known the gradient is negative, since only a positive gate voltage is being considered, therefore the negative root is chosen. Re-arranging equation (3.6)

results in the following integral equation,

$$\int_{\psi_0(\bar{x_1})}^{\psi_0} \left(\frac{1}{e^{-y} + y - 1} \right)^{\frac{1}{2}} dy = -\sqrt{2}\bar{x} + \sqrt{2}\bar{x_1} \; . \tag{3.7}$$

3.3 The Depletion layer

In this layer the concentrations of electrons and holes are small in comparison to the background acceptor ion concentration. This is simply because the large electric field present in this region repels any of the holes out towards the neutral layer, whereas the acceptor ions, 'stuck' in the lattice structure, are unable to move. Electrons are attracted beyond this region into the accumulation layer, and their concentration is also comparatively small.

Again, expanding ψ as a power series in $\frac{1}{\lambda}$, Poisson's equation becomes,

$$\begin{aligned} \lambda \left(\frac{\partial^2 \hat{\psi_0}}{\partial \hat{x}^2} + \frac{1}{\lambda} \frac{\partial^2 \hat{\psi_1}}{\partial \hat{x}^2} + .. \right) &= \frac{1}{\lambda} e^{u\hat{\psi_0}} \left(1 + \frac{v}{\lambda} \hat{\psi_1} + .. \right) \\ &- \lambda e^{-u\hat{\psi_0}} \left(1 - \frac{v}{\lambda} \hat{\psi_1} + .. \right) + \lambda \; . \end{aligned}$$

To highest order,

$$\frac{\partial^2 \hat{\psi_0}}{\partial \hat{x}^2} = 1 \; .$$

Therefore,

$$\hat{\psi_0} = \frac{1}{2} \hat{x}^2 + a\hat{x} + b \; . \tag{3.8}$$

The constants a and b are found through matching.

3.4 Strong Inversion

Here, the electron concentration, much larger than the hole and dopant concentrations, balances the second order term in Poisson's equation.

As with the other regions ψ is expanded in powers of $\frac{1}{\lambda}$. Equation (3.3) then becomes,

$$\begin{aligned} \lambda u \left(\frac{\partial^2 \breve{\psi_0}}{\partial \breve{x}^2} + \frac{1}{\lambda} \frac{\partial^2 \breve{\psi_1}}{\partial \breve{x}^2} + \cdots \right) &= \lambda u e^{\breve{\psi_0}} \left(1 + \frac{1}{\lambda} + \cdots \right) - \frac{u}{\lambda} e^{-\breve{\psi_0}} \\ &\left(1 - \frac{1}{\lambda} \breve{\psi_1} + \cdots \right) + \lambda \; . \end{aligned}$$

To highest order,

$$\frac{\partial^2 \breve{\psi}_0}{\partial \breve{x}^2} = e^{\breve{\psi}_0} .$$

This equation can be integrated to give,

$$\frac{1}{2}\frac{\partial \breve{\psi}_0}{\partial \breve{x}}^2 = e^{\breve{\psi}_0} + B ,$$

where B is a constant of integration. Re-arranging, the integral equation,

$$\int_{\breve{\psi}_0(\breve{x_1})}^{\breve{\psi}_0} \left(\frac{1}{e^y + B}\right)^{\frac{1}{2}} dy = -\sqrt{2}\breve{x} + \sqrt{2}\breve{x_1} ,$$

is obtained.

Letting $\breve{x_1} = 0$, then,

$$\int_{\breve{\psi}_0(0)}^{\breve{\psi}_0} \left(\frac{1}{e^y + B}\right)^{\frac{1}{2}} dy = -\sqrt{2}\breve{x} .$$

The value of $\breve{\psi}_0(0)$ can be found by the boundary condition at $x = 0$ and the constant B found by matching.

3.5 Matching The Solutions

The arbitrary constants found in the previous section are now determined using the method of matched asymptotic expansions. The procedure is to let each solution tend towards a neighbouring one. This is achieved by expressing a solution in terms of its neighbours variables and finding the highest order behaviour. The highest order behaviour of the solutions, in these overlap regions, are then equated. This method ensures a complete matched asymptotic solution is obtained for the voltage, ψ.

3.5.1 The Transition and Depletion Layers

In the transition region, the equation governing ψ is,

$$\int_{\psi_0(\bar{x_1})}^{\psi_0} \left(\frac{1}{e^{-y} + y - 1}\right)^{\frac{1}{2}} dy = -\sqrt{2}\bar{x} + \sqrt{2}\bar{x_1} .$$

The transition layer has already been matched into the outer region, and is now matched into the depletion layer. Writing the transition layer voltage, ψ, in terms of the depletion layer voltage, $\hat{\psi}$,

$$\psi = u\hat{\psi} \; .$$

In the limit $\lambda \rightarrow \infty$, matching the transition layer into the depletion region, is equivalent to letting $\psi \rightarrow \infty$. The above integral equation can be re-written,

$$\int_{\psi_0(\bar{x}_1)}^{\psi_0} \left(\frac{1}{\sqrt{(e^{-y}+y-1)}} \right) dy = \int_{\psi_0(\bar{x}_1)}^{\psi_0} \left(\frac{1}{\sqrt{(e^{-y}+y-1)}} - \frac{1}{\sqrt{y}} \right) dy + \int_{\psi_0(\bar{x}_1)}^{\psi_0} \frac{1}{\sqrt{y}} dy \; .$$

However,

$$\begin{aligned} \int_{\psi_0(\bar{x}_1)}^{\psi_0} \left(\frac{1}{\sqrt{(e^{-y}+y-1)}} - \frac{1}{\sqrt{y}} \right) dy &= \int_{\psi_0(\bar{x}_1)}^{\infty} \left(\frac{1}{\sqrt{(e^{-y}+y-1)}} - \frac{1}{\sqrt{y}} \right) dy \\ &- \int_{\psi_0}^{\infty} \left(\frac{1}{\sqrt{(e^{-y}+y-1)}} - \frac{1}{\sqrt{y}} \right) dy \; . \end{aligned}$$

It can be shown that,

$$\int_{\psi_0}^{\infty} \frac{1}{\sqrt{(e^{-y}+y-1)}} - \frac{1}{\sqrt{y}} dy \sim O\left(\frac{1}{\sqrt{\psi_0}} \right) \; ,$$

and,

$$\int_{\psi_0(\bar{x}_1)}^{\infty} \frac{1}{\sqrt{(e^{-y}+y-1)}} - \frac{1}{\sqrt{y}} dy = \alpha \; ,$$

where α is an order one constant. Thus, as $\psi_0 \rightarrow \infty$, to highest order,

$$\int_{\psi_0(\bar{x}_1)}^{\psi_0} \frac{1}{\sqrt{(e^{-y}+y-1)}} dy = 2\sqrt{\psi_0} \; .$$

Therefore, approaching the depletion layer, the relationship between ψ_0 and $\bar{x}$ is, to highest order,

$$-\sqrt{2}\bar{x} = 2\sqrt{\psi_0} \; .$$

Re-arranging this equation gives ψ as a function of $\bar{x}$,

$$\psi_0 = \frac{1}{2}\bar{x}^2 \; , \tag{3.9}$$

In the depletion layer the solution is,

$$\hat{\psi}_0 = \frac{1}{2}\hat{x}^2 + a\hat{x} + b \; .$$

Substituting the depletion layer variables for the transition layer variables,

$$\hat{x} = \sqrt{\frac{\lambda}{u}} x_0 + \frac{\bar{x}}{\sqrt{u}} , \qquad \hat{\psi_0} = \frac{\psi_0}{u} ,$$

the depletion layer solution becomes,

$$\begin{aligned} \frac{\psi_0}{u} &= \frac{1}{2}\left(\frac{\lambda}{u}{x_0}^2 + \frac{\bar{x}^2}{u} + 2\frac{\sqrt{\lambda}}{u} x_0 \bar{x}\right) \\ &+ a\left(\sqrt{\frac{\lambda}{u}} x_0 + \frac{\bar{x}}{\sqrt{u}}\right) + b . \end{aligned}$$

Hence,

$$\begin{aligned} \psi_0 &= \frac{1}{2}\bar{x}^2 + \bar{x}\left(\sqrt{\lambda} x_0 + a\sqrt{u}\right) \\ &+ u\left(\frac{1}{2}\frac{\lambda}{u}{x_0}^2 + a\sqrt{\frac{\lambda}{u}} x_0 + b\right) . \end{aligned} \tag{3.10}$$

In order that the depletion and transition layers match, the depletion layer solution, as it approaches the transition region, (equation (3.10)), must equal, to highest order, the transition layer solution as it approaches the depletion region, (equation (3.9)). Therefore, equating the co-efficients of $\bar{x}$ in equations (3.9) and (3.10), gives,

$$\sqrt{\lambda} x_0 + \sqrt{u} a = 0 .$$

Therefore,

$$\left(\sqrt{\frac{\lambda}{u}} x_0 + a\right) = 0 .$$

If x_0 is scaled,

$$x_0 = \sqrt{\frac{u}{\lambda}} \bar{x_0} ,$$

then,

$$\bar{x_0} = -a .$$

Equating co-efficients of $\bar{x}_0$ in equations (3.10) and (3.9) gives,

$$\left(\frac{1}{2}{\bar{x_0}}^2 + a\bar{x_0} + b\right) = 0 .$$

To completely determine the constants a b and $\bar{x_0}$ the depletion layer solution is matched into the inversion layer. However, as an aside, the analysis is continued, for the case when the applied gate voltage is small enough to only form a depletion

layer. The voltage at the oxide-semiconductor interface is $\psi_0(0)$, which gives $b = \hat{\psi}_0(0)$. Therefore, a and $\bar{x_0}$ can be calculated from the above quadratic and the relationship $\bar{x_0} = -a$, to give,

$$\frac{1}{2}\bar{x_0}^2 = \hat{\psi}_0(0) \ , \qquad \Rightarrow \qquad \bar{x_0} = \sqrt{2\hat{\psi}_0(0)} \ ,$$

Thus, the growth of the depletion layer is proportional to the square-root of interface voltage $\hat{\psi}_0(0)$.

3.5.2 The Depletion and Inversion Layers

The equation describing the inversion layer voltage, $\breve{\psi}$, is,

$$\int_{\breve{\psi}_0(0)}^{\breve{\psi}_0} \frac{1}{(e^y + B)^{\frac{1}{2}}} dy = -\sqrt{2}\breve{x} \ .$$

Expressing the inversion layer voltage, $\breve{\psi}$ in terms of the depletion layer voltage, $\hat{\psi}$, gives,

$$\breve{\psi} = -\left(2\ln\lambda + \ln u - u\hat{\psi}\right) \ .$$

Since $u \ll 2\ln\lambda$, then in the limit, $\lambda \to \infty$, approaching the depletion layer from the inversion region is equivalent to letting $\breve{\psi} \to -\infty$. Thus, as $\breve{\psi}_0 \to -\infty$, the highest order behaviour of the above integral is found. Splitting this integral into the following parts,

$$\int_{\breve{\psi}_0(0)}^{\breve{\psi}_0} \frac{1}{(e^y + B)^{\frac{1}{2}}} dy = \int_{\breve{\psi}_0(0)}^{\breve{\psi}_0} \frac{1}{(e^y + B)^{\frac{1}{2}}} - \frac{1}{B^{\frac{1}{2}}} dy + \int_{\breve{\psi}_0(0)}^{\breve{\psi}_0} \frac{1}{B^{\frac{1}{2}}} dy \ ,$$

and noting,

$$\begin{aligned} \int_{\breve{\psi}_0(0)}^{\breve{\psi}_0} \frac{1}{(e^y + B)^{\frac{1}{2}}} - \frac{1}{B^{\frac{1}{2}}} dy \ &= \ \int_{\breve{\psi}_0(0)}^{-\infty} \frac{1}{(e^y + B)^{\frac{1}{2}}} - \frac{1}{B^{\frac{1}{2}}} dy \ , \\ &- \ \int_{\breve{\psi}_0}^{-\infty} \frac{1}{(e^y + B)^{\frac{1}{2}}} - \frac{1}{B^{\frac{1}{2}}} dy \ , \end{aligned}$$

where,

$$\int_{\breve{\psi}_0(0)}^{-\infty} \frac{1}{(e^y + B)^{\frac{1}{2}}} - \frac{1}{B^{\frac{1}{2}}} dy \sim O(1) \ ,$$

and,

$$\int_{\breve{\psi}_0}^{-\infty} \frac{1}{(e^y + B)^{\frac{1}{2}}} - \frac{1}{B^{\frac{1}{2}}} dy \ll 1 \ .$$

The highest order behaviour of the integral is given by,

$$\int_{\breve{\psi}_0(0)}^{\breve{\psi}_0} \frac{1}{(e^y + B)^{\frac{1}{2}}} dy = \frac{\breve{\psi}_0}{\sqrt{B}} ,$$

giving,

$$\breve{\psi}_0 = -\sqrt{2}\sqrt{B}\breve{x}; . \tag{3.11}$$

The depletion layer solution is sent into the inversion layer, by expressing the depletion layer variables in terms of the inversion layer variables,

$$\hat{\psi}_0 = \frac{2\ln\lambda + \ln u + \breve{\psi}_0}{u} , \qquad \hat{x} = \frac{\breve{x}}{u} .$$

Thus, the depletion layer solution becomes,

$$2\frac{\ln\lambda}{u} + \frac{\ln v}{u} + \frac{\breve{\psi}_0}{u} = \frac{1}{2}\frac{\breve{x}^2}{u^2} + \frac{a}{u}\breve{x} + b ,$$

$$2\ln\lambda + \breve{\psi}_0 = O\left(\frac{1}{u}\right) + a\breve{x} + bu . \tag{3.12}$$

The terms in equations (3.11) and (3.12) are equated, and,

$$\text{co-efficients of } \breve{x} , \qquad a = -\sqrt{2B} .$$

$$\text{co-efficients of } \breve{x}_0 , \qquad bu - 2\ln\lambda = 0 .$$

Letting $u = \ln\lambda$ gives,

$$b - 2 = 0 .$$

Hence,

$$b = 2 ,$$

$$u = \ln\lambda ,$$

$$B = \frac{a^2}{2} .$$

The quadratic for $\bar{x_0}$ is then,

$$\frac{1}{2}\bar{x_0}^2 - \bar{x_0}^2 + 2 = 0 ,$$

giving,

$$x_0 = 2 ,$$

and therefore,

$$a = -2 \ , \qquad \text{and} \qquad B = 2 \ .$$

The final boundary condition,

$$\frac{\partial \psi}{\partial x} = h\sqrt{\frac{\lambda}{\ln \lambda}}\left(\psi - v \ln \lambda\right) \ , \qquad \text{at} \qquad x = 0 \ ,$$

is used to find $\breve{\psi}_0(0)$. Re-writing this boundary condition in terms of the inversion layer variables gives,

$$\sqrt{\lambda \ln \lambda}\frac{\partial \breve{\psi}_0}{\partial \breve{x}} = h\sqrt{\frac{\lambda}{\ln \lambda}}\left(2 \ln \lambda + \ln\left(\ln \lambda\right) + \breve{\psi} - v \ln \lambda\right) \ , \qquad \text{at} \qquad \breve{x} = 0 \ .$$

However, from the inversion layer section,

$$\frac{1}{2}\frac{\partial \breve{\psi}_0}{\partial \breve{x}}^2 = e^{\psi_0} + 2 \ .$$

Therefore, at $\breve{x} = 0$,

$$\frac{1}{2}\left(\frac{\partial \breve{\psi}_0(0)}{\partial \breve{x}}\right)^2 = e^{\psi_0(0)} + 2 \ .$$

Thus, $\breve{\psi}_0(0)$ is given by,

$$\sqrt{2\left(e^{\breve{\psi}_0(0)} + 2\right)} = h\left(2 - v + \frac{\ln \ln \lambda}{\ln(\lambda)} + \frac{\breve{\psi}_0(0)}{\ln \lambda}\right) \ .$$

Chapter 4

The Steady Problem With Partial Ionisation Of The Dopant Energy Level

4.1 Introduction

In this chapter the analysis of having a probability density function for the occupancy of electrons in the semi-conductor band gap is performed. The previous chapter assumed complete ionisation of the donor atoms, and the dopant charge density was simply λ. However, in this chapter only partial ionisation is considered, and the dopant charge density is λf. It is assumed that $\lambda \gg \gamma \gg 1$. If $\gamma \gg \lambda \gg 1$, then to highest order, the problem of the previous chapter, in which the dopant ions are fully ionised, results.

The problem is then,

$$\frac{\partial^2 \psi}{\partial x^2} = Ae^{\psi} - \frac{1}{A}e^{-\psi} + \lambda \left(\frac{Ae^{\psi} + \gamma}{Ae^{\psi} + \frac{1}{\gamma} + \gamma + \frac{1}{A}e^{-\psi}} \right) , \tag{4.1}$$

with the boundary conditions,

$$\frac{\partial \psi}{\partial x} = \bar{h} \sqrt{\frac{\lambda}{\frac{1}{2}\ln \lambda\gamma}} \left(\psi - v\frac{1}{2}\ln \lambda\gamma \right) ,$$

at x=0, and,

$$\frac{\partial^2 \psi}{\partial x^2} = 0 ,$$

$$\psi = 0 \, ,$$

at x=a. To find the highest order value of A and $\frac{1}{A}$ the boundary conditions at $x = a$ are imposed to equation (4.1), to give,

$$A - \frac{1}{A} + \lambda \left(\frac{A + \gamma}{A + \frac{1}{\gamma} + \gamma + \frac{1}{A}} \right) = 0 \, .$$

It can be seen by inspection that the final term in the above equation can be factorised to give,

$$A - \frac{1}{A} + \frac{\lambda A}{\left(A + \frac{1}{\gamma}\right)} = 0 \, .$$

A solution, where $A \ll 1$ is being sought, therefore, ignoring A, to highest order,

$$A = \frac{1}{\sqrt{\lambda\gamma}} + O\left(\frac{1}{\lambda}\right) \, ,$$

and,

$$\frac{1}{A} = \sqrt{\lambda\gamma} + O\left(\frac{1}{\lambda}\right) \, .$$

The values of A and $\frac{1}{A}$ can be put back into equation (4.1) to give, to highest order,

$$\frac{\partial^2 \psi}{\partial x^2} = \frac{1}{\sqrt{\lambda\gamma}} e^{\psi} - \sqrt{\lambda\gamma} e^{-\psi} + \lambda \left(\frac{\frac{1}{\sqrt{\lambda\gamma}} e^{\psi} + \gamma}{\frac{1}{\sqrt{\lambda\gamma}} e^{\psi} + \frac{1}{\gamma} + \gamma + \sqrt{(\lambda\gamma)} e^{-\psi}} \right) \, . \qquad (4.2)$$

The remainder of the chapter is concerned with the analysis of (4.2), subject to the afore mentioned boundary conditions, in the limit $\lambda \to \infty$. It is found that there are five basic layers, as shown in figure 4.1. The structure is similar to the solution of Chapter 3 with neutral, depletion and inversion layers. However, the thickness of the transition layer is such that it is greater than all but the outer, neutral, layer. This "spreading out" of the transition layer is due to the partial ionisation of the dopant atoms. An additional thin region exists where the dopant atoms undergo rapid ionisation and f changes from a near 0 value to a value close to 1. This is the ionisation layer. Approaching the oxide interface further the dopant atoms are, to highest order, fully ionised and the depletion and inversion layers, both similar in structure to the previous chapter, are encountered.

f can be classified into three regions of behaviour as outlined below.

(1) $\qquad f \sim \sqrt{\left(\frac{\gamma}{\lambda}\right)} e^{\psi} \qquad$ for $\quad \psi \sim O(1) \, .$

(2) $\qquad f \sim \frac{1}{1 + e^{-\hat{\psi}}} \qquad$ for $\quad \psi = \frac{1}{2} \ln \frac{\lambda}{\gamma} + \hat{\psi} \, .$

(3) $\qquad f \sim 1 \qquad$ for $\qquad \psi \geq \frac{1}{2} \ln (\lambda\gamma) \, .$

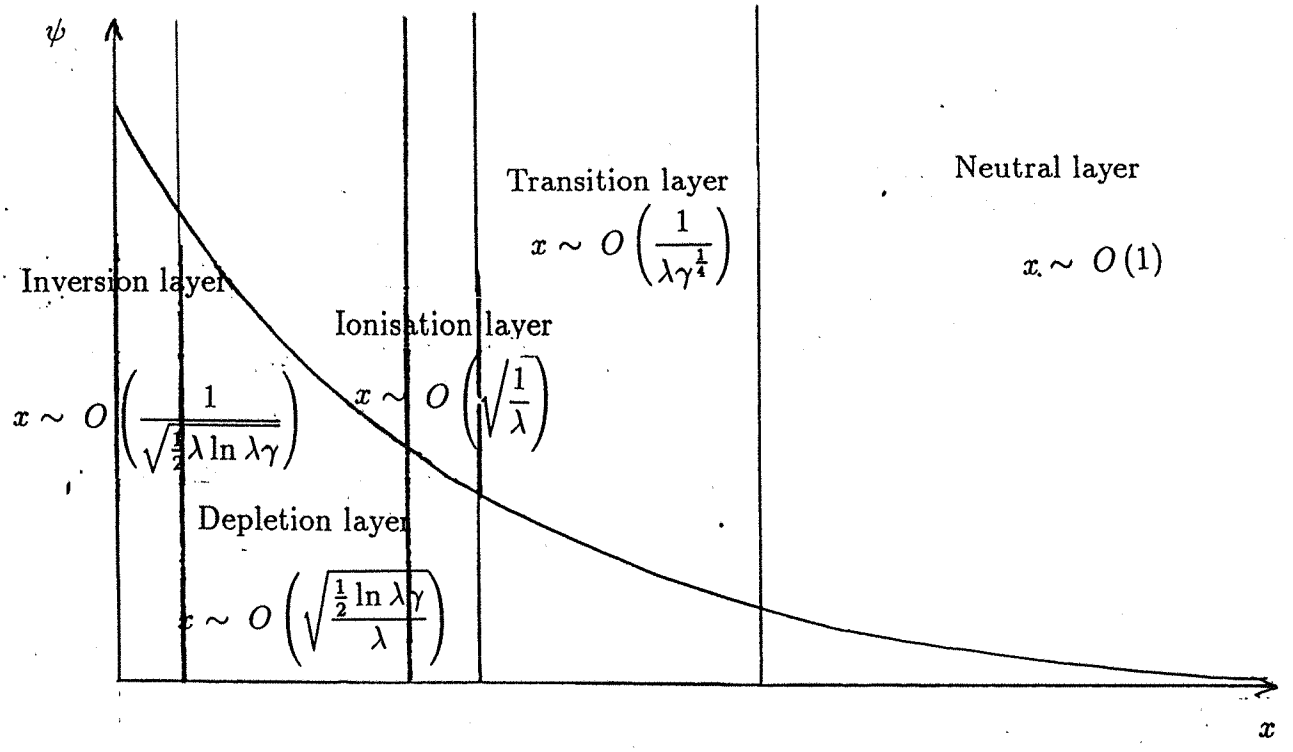

Figure 4.1: Sketch of the five layers of behaviour for the steady problem with partial ionisation of the dopant energy level.

Listed below are the scalings for the five different layers in this problem.

Outer Layer.

$$x \sim O(1)\ , \quad \psi \sim O(1)\ , \quad f \sim O\left(\sqrt{\left(\frac{\gamma}{\lambda}\right)}\right) e^{\psi}\ .$$

Transition Layer.

$$x = \left(\frac{1}{(\lambda\gamma)^{\frac{1}{4}}}\right)\bar{x}\ , \quad \psi \sim O(1)\ , \qquad f \sim O\left(\sqrt{\left(\frac{\gamma}{\lambda}\right)}\right) e^{\psi}\ .$$

Ionisation Layer.

$$f = \frac{1}{1+e^{-\hat{\psi}}}\ .$$

$$x = x_0 + \frac{1}{\sqrt{\lambda}}\hat{x}\ , \quad \psi = \frac{1}{2}\ln\frac{\lambda}{\gamma} + \hat{\psi}\ .$$

Depletion Layer.

$$x = \sqrt{\frac{\frac{1}{2}\ln\lambda\gamma}{\lambda}}\breve{x}\ , \quad \psi = \frac{1}{2}\ln(\lambda\gamma)\breve{\psi}\ , \qquad f = 1\ .$$

The Inversion Layer.

$$x = \frac{1}{\sqrt{\lambda\frac{1}{2}\ln\lambda\gamma}}\tilde{x}\ , \quad \psi = \ln\left(\lambda^{\frac{3}{2}}\gamma^{\frac{1}{2}}\frac{1}{2}\ln(\lambda\gamma)\right) + \tilde{\psi}\ , \qquad f = 1\ .$$

4.2 Outer Solution

Expressing ψ as a power series,

$$\psi = \psi_0 + \cdots$$

and substituting into equation (4.2),

$$\begin{aligned}\frac{\partial^2\psi}{\partial x^2} &= \frac{1}{\sqrt{(\gamma\lambda)}}e^{(\psi_0+\cdots)} - \sqrt{(\gamma\lambda)}e^{(-\psi_0+\cdots)} + \sqrt{(\lambda\gamma)}e^{(\psi_0+\cdots)} \\ &= \frac{1}{\sqrt{(\gamma\lambda)}}e^{\psi_0}(1+\cdots) - \sqrt{(\gamma\lambda)}e^{-\psi_0}(1+\cdots) + \sqrt{(\lambda\gamma)}e^{\psi_0}(1+\cdots)\ .\end{aligned}$$

To highest order,

$$-e^{-\psi_0} + e^{\psi_0} = 0 \quad \Rightarrow \psi_0 = 0\ .$$

4.3 Transition Layer

Here, as in the problem in the previous chapter, the second order term in Poisson's equation balances the hole and dopant concentrations. However, the thickness of this layer is much greater.

Letting,

$$\psi = \psi_0 + \cdots\ ,$$

equation (4.2) becomes,

$$\sqrt{\lambda\gamma}\frac{\partial^2\psi_0}{\partial\bar{x}^2} + \cdots = \frac{1}{\sqrt{(\gamma\lambda)}}e^{\psi_0+\cdots} - \sqrt{(\gamma\lambda)}e^{-\psi_0+\cdots} + \sqrt{(\lambda\gamma)}e^{\psi_0+\cdots}\ .$$

Expanding the exponential terms,

$$\sqrt{\lambda\gamma}\left(\frac{\partial^2\psi_0}{\partial\bar{x}^2}+\cdots\right) = \frac{1}{\sqrt{(\gamma\lambda)}}e^{\psi_0}(1+\cdots) - \sqrt{(\gamma\lambda)}e^{-\psi_0}(1+\cdots)+\sqrt{(\lambda\gamma)}e^{\psi_0}(1+\cdots)\ ,$$

to highest order,

$$\frac{\partial^2\psi_0}{\partial\bar{x}^2} = -e^{-\psi_0}+e^{\psi_0}\ .$$

This can be integrated, to give,

$$\frac{1}{2}\left(\frac{\partial\psi_0}{\partial\bar{x}}\right)^2 = e^{-\psi_0}+e^{\psi_0}+A\ , \tag{4.3}$$

where A is a constant of integration.

To match the solution into the neutral layer $\bar{x}\rightarrow\infty$. But, approaching the neutral layer, $\frac{\partial\psi}{\partial x}\ ,\psi\ \longrightarrow 0$. Putting these values into equation (4.3) it is found $A=-2$. Therefore,

$$\frac{1}{2}\frac{\partial\psi_0}{\partial\bar{x}}^2 = e^{-\psi_0}+e^{\psi_0}-2\ ,$$

which re-arranged gives,

$$\int_{\psi_0(\bar{x_1})}^{\psi_0}\frac{1}{\sqrt{(e^{-x}+e^{x}-2)}}dx = -\sqrt{2}\bar{x}+\sqrt{2}\bar{x_1}\ . \tag{4.4}$$

This integral equation can be solved, and an explicit solution for ψ_0 can be obtained.

Letting $s^2=e^y$, gives,

$$\begin{aligned}\int\frac{1}{\sqrt{(e^{-y}+e^{y}-2)}}dy &= \int\frac{2}{s}\frac{1}{\sqrt{\left(\frac{1}{s^2}+s^2-2\right)}}ds\\ &= \int\frac{2}{(s^2-1)}ds\\ &= \int\frac{1}{(s-1)}-\frac{1}{(s+1)}ds\\ &= \ln\left(\frac{s-1}{s+1}\right)+C\end{aligned}$$

Therefore,

$$\int_{\psi_0(\bar{x_1})}^{\psi_0}\frac{1}{\sqrt{(e^{-x}+e^{x}-2)}}dx = \ln\frac{e^{\frac{\psi_0}{2}}-1}{e^{\frac{\psi_0}{2}}+1}+A\ . \tag{4.5}$$

This equation is inverted to give ψ as a function of $\bar{x}$,

$$\psi_0 = \ln\left(\frac{e^{B-A}e^{-\sqrt{2}\bar{x}}+1}{1-e^{B-A}e^{-\sqrt{2}\bar{x}}}\right), \tag{4.6}$$

where $B = \sqrt{2}\bar{x}_1$.

4.4 The Ionisation Region

Letting,

$$\hat{\psi} = \hat{\psi}_0 + \cdots ,$$

equation (4.2) becomes, to highest order,

$$\lambda\frac{\partial^2\hat{\psi}}{\partial\hat{x}^2} = \frac{1}{\gamma}e^{\hat{\psi}} - \gamma e^{\hat{\psi}} + \frac{\lambda}{1+e^{-\hat{\psi}}} .$$

Since $\lambda \gg \gamma$, to highest order,

$$\frac{\partial^2\hat{\psi}_0}{\partial\hat{x}^2} = \frac{1}{e^{-\hat{\psi}_0}+1} .$$

Integrating gives,

$$\frac{1}{2}\left(\frac{\partial\hat{\psi}_0}{\partial\hat{x}}\right)^2 = \ln\left(e^{-\hat{\psi}_0}+1\right) + \hat{\psi}_0 + C .$$

This can be re-arranged to give the following integral equation,

$$\int_{\hat{\psi}_0(\hat{x}_1)}^{\hat{\psi}_0}\frac{1}{\sqrt{\ln\left(e^{-x}+1\right)+x+C}}dx = -\sqrt{2}\hat{x} + \sqrt{2}\hat{x}_1 .$$

4.5 The Depletion Region

Letting,

$$\breve{\psi} = \breve{\psi}_0 + \cdots ,$$

to highest order, equation (4.2) becomes,

$$\lambda\left(\frac{\partial^2\breve{\psi}_0}{\partial\breve{x}^2} + \cdots\right) = \frac{1}{\sqrt{(\gamma\lambda)}}e^{\frac{1}{2}\ln(\lambda\gamma)\left(\breve{\psi}_0+\cdots\right)} - \sqrt{(\gamma\lambda)}e^{-\frac{1}{2}\ln(\lambda\gamma)\left(\breve{\psi}_0\right)} + \lambda .$$

To highest order,

$$\frac{\partial^2 \breve{\psi}_0}{\partial \breve{x}^2} = 1 \ .$$

This gives the quadratic,

$$\breve{\psi}_0 = \frac{1}{2}\breve{x}^2 + a\breve{x} + b \ .$$

The constants a and b are found by matching the solution into the transition and accumulation layers.

4.6 Inversion

To highest order equation (4.2) is,

$$\frac{\partial^2 \tilde{\psi}_0}{\partial \tilde{x}^2} = e^{\tilde{\psi}_0} \ .$$

Integrating, and re-arranging gives,

$$\int_{\tilde{\psi}_0(0)}^{\tilde{\psi}_0} \frac{1}{\sqrt{\left(e^{\tilde{\psi}_0} + A\right)}} dy = -\sqrt{2}\tilde{x} \ .$$

4.7 Matching The Solutions

4.7.1 The Transition And Ionisation Layers

Here, the ionisation region, described by,

$$\int_{\hat{\psi}_0(\hat{x_1})}^{\hat{\psi}_0} \frac{1}{\sqrt{(\ln\left(e^{-x}+1\right) + x + C)}} dx = -\sqrt{2}\hat{x} + \sqrt{2}\hat{x_1} \ ,$$

is matched with the transition layer. Approaching the transition layer, from the ionisations region, is equivalent to letting $\hat{\psi}_0 \to -\infty$. The above integral equation can be re-written,

$$\begin{aligned} \int_{\hat{\psi}_0(\hat{x_1})}^{\hat{\psi}_0} \frac{1}{\sqrt{(\ln\left(e^{-x}+1\right) + x + C)}} dx &= \int_{\hat{\psi}_0(\hat{x_1})}^{\hat{\psi}_0} \frac{1}{\sqrt{\ln\left(e^{-x}+1\right) + x + C}} - \frac{1}{C^{\frac{1}{2}}} dx \\ &+ \int_{\hat{\psi}_0(\hat{x_1})}^{\hat{\psi}_0} \frac{1}{C^{\frac{1}{2}}} dx \ . \end{aligned}$$

However,

$$\int_{\hat{\psi}_0(\hat{x_1})}^{\hat{\psi_0}} \frac{1}{\sqrt{\ln\left(e^{-x}+1\right)+x+C}} - \frac{1}{C^{\frac{1}{2}}} dx = \int_{\hat{\psi}(\hat{x_1})}^{-\infty} \frac{1}{\sqrt{(\ln e^{-x}+1)+x+C}} - \frac{1}{C^{\frac{1}{2}}} dx - \int_{\hat{\psi}_0}^{-\infty} \frac{1}{\sqrt{\ln\left(e^{-x}+1\right)+x+C}} - \frac{1}{C^{\frac{1}{2}}} dx$$

where,

$$\int_{\hat{\psi}_0(\hat{x_1})}^{-\infty} \frac{1}{\sqrt{\ln\left(e^{-x}+1\right)+x+C}} - \frac{1}{C^{\frac{1}{2}}} dx \sim O\left(1\right) ,$$

and,

$$\int_{\hat{\psi}_0}^{-\infty} \frac{1}{\sqrt{\ln\left(e^{-x}+1\right)+x+C}} - \frac{1}{C^{\frac{1}{2}}} dx \sim O\left(1\right) .$$

Thus, approaching the transition layer gives, to highest order,

$$\int_{\psi_0(\hat{x_1})}^{\hat{\psi_0}} \frac{1}{\sqrt{(\ln e^{-x}+1+x+C)}} = \frac{\hat{\psi_0}}{C^{\frac{1}{2}}} .$$

To highest order, the voltage is linear, and does not match into the transition layer, unless C=0. Therefore, the solution in the ionisation layer is now described by,

$$\int_{\hat{\psi}_0(\hat{x_1})}^{\hat{\psi_0}} \frac{1}{\sqrt{\ln\left(e^{-x}+1\right)+x}} dx = -\sqrt{2}\hat{x} + \sqrt{2}\hat{x_1} .$$

Again, to approach the transition layer, $\hat{\psi}_0 \to -\infty$. In this limit the integral can be re-written,

$$\begin{aligned}\int_{\hat{\psi}_0(\hat{x_1})}^{\hat{\psi_0}} \frac{1}{\sqrt{(\ln e^{-x}+1+x)}} dx &= \int_{\hat{\psi}_0(\hat{x_1})}^{\hat{\psi_0}} \frac{1}{\sqrt{\ln\left(e^{-x}+1\right)+x}} - \frac{1}{e^{\frac{x}{2}}} dx + \int_{\hat{\psi}_0(\hat{x_1})}^{\hat{\psi_0}} \frac{1}{e^{\frac{x}{2}}} dx \\ &= \int_{\hat{\psi}_0(\hat{x_1})}^{-\infty} \frac{1}{\sqrt{\ln\left(e^{-x}+1\right)+x}} - \frac{1}{e^{\frac{x}{2}}} dx \\ &\quad - \int_{\hat{\psi}_0}^{-\infty} \frac{1}{\sqrt{(\ln\left(e^{-x}+1\right)+x)}} - \frac{1}{e^{\frac{x}{2}}} dx + \int_{\hat{\psi}_0(\hat{x_1})}^{\hat{\psi_0}} e^{-\frac{x}{2}} dx .\end{aligned}$$

Therefore, to highest order,

$$\int_{\hat{\psi}_0(\hat{x_1})}^{\hat{\psi_0}} \frac{1}{\sqrt{(\ln e^{-x}+1+x)}} dx = -2e^{-\frac{\hat{\psi_0}}{2}} .$$

Thus, the behaviour of the ionisation solution, as it approaches the transition layer, is

$$e^{-\frac{\psi_0}{2}} = \frac{1}{\sqrt{2}}\hat{x} \,. \tag{4.7}$$

The transition layer solution, described by (4.5), approaches the ionisation region by sending $\psi_0 \to \infty$. The resulting function is re-written in terms of the ionisation variables, and equated to equation (4.7). In this way the two layers are matched together. The solution in the transition layer is given by,

$$-\sqrt{2}\bar{x} + \sqrt{2}\bar{x}_1 = \ln\left(\frac{e^{\frac{\psi_0}{2}} - 1}{e^{\frac{\psi_0}{2}} + 1}\right) + A \,.$$

Approaching the ionisation layer, by letting $\psi_0 \to \infty$, gives,

$$\begin{aligned} \ln\left(e^{\frac{\psi_0}{2}} - 1\right) - \ln\left(e^{\frac{\psi_0}{2}} + 1\right) &= \ln e^{\frac{\psi_0}{2}} - \ln\left(1 - e^{-\frac{\psi_0}{2}}\right) - \ln e^{\frac{\psi_0}{2}} - \ln\left(1 + e^{-\frac{\psi_0}{2}}\right) \\ &= -2e^{-\frac{\psi_0}{2}} + \cdots \end{aligned}$$

Therefore, in the limit as $\psi_0 \to \infty$, the solution to highest order, is given by,

$$e^{-\frac{\psi_0}{2}} - \frac{A}{2} \sim \frac{1}{\sqrt{2}}\bar{x} - \frac{B}{2} \,, \tag{4.8}$$

where $\sqrt{2}\bar{x}_1 = B$, (an arbitrary constant). This solution is expressed in terms of the ionisation variables. Using the fact,

$$\bar{x} = (\lambda\gamma)^{\frac{1}{4}}\left(x_0 + \frac{1}{\sqrt{\lambda}}\hat{x}\right) \,,$$

and,

$$\psi_0 = \frac{1}{2}\ln\frac{\lambda}{\gamma} + \hat{\psi}_0 \,.$$

equation (4.8), gives, to highest order,

$$e^{-\frac{1}{4}\ln\frac{\lambda}{\gamma}} \quad e^{-\frac{\hat{\psi}_0}{2}} - \frac{A}{2} = \frac{1}{\sqrt{2}}\left(\frac{\gamma}{\lambda}\right)^{\frac{1}{4}}\hat{x} + (\gamma\lambda)^{\frac{1}{4}}x_0 - \frac{B}{2} \,.$$

On simplifying,

$$e^{-\frac{\hat{\psi}_0}{2}} = \frac{1}{\sqrt{2}}\hat{x} - \frac{1}{2}(B - A)\frac{1}{\sqrt{2}}x_0\sqrt{\lambda} \,.$$

This function is then equated to equation (4.7), implying,

$$\frac{1}{2}(A - B)\frac{1}{\sqrt{2}}x_0\sqrt{\lambda} = 0 \,.$$

In the following section it is found,

$$x_0 \sim \sqrt{\frac{\frac{1}{2}\ln(\lambda\gamma)}{\lambda}} .$$

Therefore, in the limit as $\lambda \to \infty$,

$$(B - A) = 0 ,$$

implying the solution in the transition layer to be,

$$\psi_0 = \ln\left(\frac{e^{-\sqrt{2}\bar{x}} + 1}{1 - e^{-\sqrt{2}\bar{x}}}\right) .$$

4.7.2 The Ionisation And Depletion Layers

Here, the ionisation layer solution, described by,

$$\int_{\hat{\psi}_0(\hat{x_1})}^{\hat{\psi}_0} \frac{1}{\sqrt{\ln(e^{-x}+1)+x}} dx = -\sqrt{2}\hat{x} + \sqrt{2}\hat{x_1} ,$$

is matched with the depletion layer solution,

$$\breve{\psi}_0 = \frac{1}{2}\breve{x}^2 + a\breve{x} + b .$$

Approaching the depletion region, from the ionisation layer, $\hat{\psi}_0$, and $x \to \infty$. In this limit, the ionisation layer solution can be re-written as,

$$\int_{\hat{\psi}_0(\hat{x_1})}^{\hat{\psi}_0} \frac{1}{\sqrt{\ln(e^{-x}+1)+x}} dx = \int_{\hat{\psi}_0(\hat{x_1})}^{\hat{\psi}_0} \frac{1}{\sqrt{\ln(e^{-x}+1)+x}} - \frac{1}{\sqrt{x}} dx + \int_{\hat{\psi}_0(\hat{x_1})}^{\hat{\psi}_0} \frac{1}{\sqrt{x}} dx .$$

However, it can be shown,

$$\begin{aligned} \int_{\hat{\psi}_0(\hat{x_1})}^{\hat{\psi}_0} \frac{1}{\sqrt{\ln(e^{-x}+1)+x}} - \frac{1}{\sqrt{x}} dx &= \int_{\hat{\psi}_0(\hat{x_1})}^{\infty} \frac{1}{\sqrt{\ln(e^{-x}+1)+x}} - \frac{1}{\sqrt{x}} dx \\ &- \int_{\hat{\psi}_0}^{\infty} \frac{1}{\sqrt{\ln(e^{-x}+1)+x}} - \frac{1}{\sqrt{x}} dx , \end{aligned}$$

where,

$$\int_{\hat{\psi}_0(\hat{x_1})}^{\infty} \frac{1}{\sqrt{\ln(e^{-x}+1)+x}} - \frac{1}{x^{\frac{1}{2}}} dx \sim O(1) ,$$

and,

$$\int_{\hat{\psi}_0}^{\infty} \frac{1}{\sqrt{\ln\left(e^{-x}+1\right)+x}} - \frac{1}{x^{\frac{1}{2}}} dx \sim O\left(1\right) .$$

Using the above results, gives, to highest order,

$$2\sqrt{\hat{\psi}_0} = -\sqrt{2}\hat{x} ,$$

for the solution of the ionisation layer, as it approaches the depletion region. Re-arranging,

$$\hat{\psi}_0 = \frac{1}{2}\hat{x}^2 . \tag{4.9}$$

In the depletion region,

$$\breve{\psi}_0 = \frac{1}{2}\breve{x}^2 + a\breve{x} + b . \tag{4.10}$$

Expressing the depletion layer variables in terms of the ionisation variables,

$$\breve{\psi}_0 = \frac{\hat{\psi}_0}{\frac{1}{2}\ln\lambda\gamma} + \frac{\frac{1}{2}\ln\frac{\lambda}{\gamma}}{\frac{1}{2}\ln\lambda\gamma} ,$$

$$\breve{x} = \sqrt{\frac{\lambda}{\frac{1}{2}\ln\lambda\gamma}}x_0 + \frac{\hat{x}}{\sqrt{\frac{1}{2}\ln\lambda\gamma}} ,$$

equation (4.10) becomes,

$$\frac{\frac{1}{2}\ln\frac{\lambda}{\gamma}}{\frac{1}{2}\ln\lambda\gamma} + \frac{\hat{\psi}_0}{\frac{1}{2}\ln\lambda\gamma} = \frac{1}{2}\frac{\hat{x}^2}{\frac{1}{2}\ln\lambda\gamma} + \hat{x}\left(2\frac{\sqrt{\lambda}}{\frac{1}{2}\ln\lambda\gamma}x_0 + \frac{a}{\sqrt{\frac{1}{2}\ln\lambda\gamma}}\right) + \frac{1}{2}\frac{\lambda}{\frac{1}{2}\ln\lambda\gamma}{x_0}^2 + a\sqrt{\frac{\lambda}{\frac{1}{2}\ln\lambda\gamma}}x_0 + b ,$$

Re-arranging,

$$\hat{\psi} = \frac{1}{2}\hat{x}^2 + \hat{x}\left(2\sqrt{\lambda}x_0 + a\sqrt{\frac{1}{2}\ln\lambda\gamma}\right) + \frac{1}{2}\lambda{x_0}^2 + a\sqrt{\lambda\frac{1}{2}\ln\lambda\gamma}\, x_0 + b\frac{1}{2}\ln\lambda\gamma - \frac{1}{2}\ln\frac{\lambda}{\gamma} .$$

Equating co-efficients of $\hat{x}$ in this expression to co-efficients of $\hat{x}$ in equation (4.9), gives,

$$\sqrt{\frac{1}{2}\ln\lambda\gamma}\left(2\sqrt{\frac{\lambda}{\frac{1}{2}\ln\lambda\gamma}}x_0 + a\right) = 0 ,$$

which implies, to highest order,

$$2\sqrt{\frac{\lambda}{\frac{1}{2}\ln\lambda\gamma}}x_0 + a = 0 .$$

Letting,

$$x_0 = \sqrt{\frac{\frac{1}{2}\ln\lambda\gamma}{\lambda}}\bar{x_0} \ ,$$

gives,

$$\bar{x_0} = -\frac{a}{2} \ .$$

In addition, co-efficients of $\hat{x}_0$ in the above expression are equated to co-efficients of $\hat{x}_0$ in equation (4.9), giving,

$$\frac{1}{2}\lambda {x_0}^2 + a\sqrt{\lambda\frac{1}{2}\ln\lambda\gamma}x_0 + b\frac{1}{2}\ln\lambda\gamma - \frac{1}{2}\ln\frac{\lambda}{\gamma} = 0 \ ,$$

which implies, to highest order,

$$\frac{1}{2}\left(\frac{\lambda}{\frac{1}{2}\ln\lambda\gamma}\right){x_0}^2 + a\sqrt{\frac{\lambda}{\frac{1}{2}\ln\lambda\gamma}}x_0 + b = 0 \ .$$

In terms of $\bar{x}$,

$$\frac{1}{2}\bar{x_0}^{\ 2} + a\bar{x_0} + b = 0 \ . \tag{4.11}$$

To solve this equation a and b need to be determined. This is achieved by matching the depletion layer into the inversion layer.

4.7.3 The Inversion And Depletion Layers

Here the inversion layer, described by,

$$\int_{\tilde{\psi}_0(0)}^{\tilde{\psi}_0} \frac{1}{(e^x + A)^{\frac{1}{2}}}dx = -\sqrt{2}\tilde{x} \ .$$

is matched with the depletion layer, described by,

$$\breve{\psi}_0 = \frac{1}{2}\breve{x}^2 + a\breve{x} + b \ .$$

Approaching the depletion region from the inversion layer, $\tilde{\psi}_0 \rightarrow -\infty$, and the inversion layer solution, to highest order, is given by,

$$\int_{\tilde{\psi}_0(0)}^{\tilde{\psi}_0} \frac{1}{(e^x + A)^{\frac{1}{2}}}dx = \frac{\tilde{\psi}_0}{\sqrt{A}} + O\left(1\right) = -\sqrt{2}\tilde{x} \ .$$

Therefore,

$$\tilde{\psi}_0 = -\sqrt{2A}\tilde{x} \ . \tag{4.12}$$

In the depletion layer, the solution is,

$$\breve{\psi}_0 = \frac{1}{2}\breve{x}^2 + a\breve{x} + b \, .$$

Expressing the depletion layer solution in terms of the inversion layer variables gives,

$$\frac{\ln\left((\lambda\gamma)^{\frac{1}{2}}\lambda \ln \lambda\gamma\right)}{\frac{1}{2}\ln\lambda\gamma} + \frac{\tilde{\psi}_0}{\frac{1}{2}\ln\lambda\gamma} = \frac{1}{2}\frac{\tilde{x}^2}{\left(\frac{1}{2}\ln\lambda\gamma\right)^2} + \frac{a}{\frac{1}{2}\ln\lambda\gamma}\tilde{x} + b \, .$$

Re-writing this gives, to highest order,

$$\tilde{\psi}_0 = a\tilde{x} + \frac{1}{2}b\ln\lambda\gamma - \ln\left((\lambda\gamma)^{\frac{1}{2}}\lambda\ln\lambda\gamma\right) \, .$$

Equating co-efficients of $\tilde{x}$ in this equation with the co-efficients in equation (4.12) implies,

$$-\sqrt{2A} = a \, .$$

In addition, co-efficients of $\tilde{x}_0$ in the above equation are equated with the co-efficients in equation (4.12), to give,

$$b = \frac{\ln\left((\lambda\gamma)^{\frac{1}{2}}\lambda\ln\lambda\gamma\right)}{\frac{1}{2}\ln\lambda\gamma} \, .$$

But,

$$\ln\left((\lambda\gamma)^{\frac{1}{2}}\lambda\ln\lambda\gamma\right) = \ln\left((\lambda\gamma)^{\frac{3}{2}}\frac{\ln\lambda\gamma}{\gamma}\right) = \frac{3}{2}\ln(\lambda\gamma) + \ln(\ln\lambda\gamma) - \ln\gamma \, ,$$

giving,

$$b = \frac{\frac{3}{2}\ln\lambda\gamma}{\frac{1}{2}\ln\lambda\gamma} + \frac{\ln(\ln\lambda\gamma)}{\frac{1}{2}\ln\lambda\gamma} - \frac{\ln\gamma}{\ln\lambda\gamma} \, .$$

Therefore, to highest order,

$$b = 3 \, .$$

In matching the depletion layer to the ionisation region it was found,

$$\frac{1}{2}\bar{x_0}^2 + a\bar{x_0} + b = 0 \, .$$

Since $b = 3$ and $a = -2x_0$, then,

$$\frac{1}{2}\bar{x_0}^2 - 2\bar{x_0}^2 + b = 0 \, , \qquad \Rightarrow \qquad \bar{x_0} = \sqrt{2} \, .$$

Thus, $A = 4$ and $a = -2\sqrt{2}$.

Transforming the final boundary condition,

$$\frac{\partial \psi}{\partial x} = \bar{h}\sqrt{\frac{\lambda}{\frac{1}{2}\ln \lambda\gamma}}\left(\psi - v\frac{1}{2}\ln \lambda\gamma\right) ,$$

at $x = 0$, into the inversion layer variables gives,

$$\frac{\partial \tilde{\psi}}{\partial \tilde{x}} = h\frac{1}{\frac{1}{2}\ln \lambda\gamma}\left(\ln\frac{1}{2}\left(\lambda^{\frac{3}{2}}\gamma^{\frac{1}{2}}\frac{1}{2}\ln \lambda\gamma\right) + \tilde{\psi} - v\frac{1}{2}\ln \lambda\gamma\right) .$$

From the inversion layer section,

$$\frac{1}{2}\left(\frac{\partial \tilde{\psi}(0)}{\partial \tilde{x}}\right)^2 = e^{\tilde{\psi}(0)} + A ,$$

giving,

$$\sqrt{\left(2e^{\tilde{\psi}(0)} + 4\right)} = h\left(\frac{\ln\frac{1}{2}\left(\lambda^{\frac{3}{2}}\gamma^{\frac{1}{2}}\frac{1}{2}\ln \lambda\gamma\right)}{\frac{1}{2}\ln \lambda\gamma} + \frac{\tilde{\psi}}{\frac{1}{2}\ln \lambda\gamma} - v\right) ,$$

which is used to find $\tilde{\psi}(0)$.

Chapter 5

The Transient Problem

As discussed in Chapter 3 the transient behaviour of an M.O.S capacitor, initially in equilibrium, subjected to a constant gate voltage is considered. The problem is to find the solution to,

$$\begin{aligned}
\frac{\partial^2 \psi}{\partial x^2} &= n - p + \lambda \,, \\
J_n &= \frac{\partial n}{\partial x} - n\frac{\partial \psi}{\partial x} \,, \\
-\frac{J_p}{\mu} &= \frac{\partial p}{\partial x} + p\frac{\partial \psi}{\partial x} \,, \\
\frac{\partial n}{\partial t} - \beta\frac{\partial J_n}{\partial x} &= 0 \,, \\
\frac{\partial p}{\partial t} + \beta\frac{\partial J_p}{\partial x} &= 0 \,, \\
\frac{\partial f}{\partial t} &= -\left[\sigma_2\left(n + e^{\gamma E}\right) + \sigma_3\left(p + e^{-\gamma E}\right) f\right] + \left(\sigma_2 n + \sigma_3 e^{-\gamma E}\right) \,,
\end{aligned}$$

subject to the conditions,

$$\begin{aligned}
J_n &= 0 \,, \\
J_p &= 0 \,, \\
np &= 1 \,,
\end{aligned}$$

$$
\begin{aligned}
n - p + \lambda &= 0 \,, \\
\psi &= 0 \,, \\
f &= \frac{1}{\lambda e^{\gamma E} + 1} \,, \\
f_s &= \frac{1}{\lambda e^{\gamma E_s} + 1} \,,
\end{aligned}
$$

at $t = 0$,

$$
\begin{aligned}
J_n &= 0 \,, \\
J_p &= 0 \,, \\
\frac{\partial \psi}{\partial x} &= h \sqrt{\frac{\lambda}{\ln \lambda}} (\psi - v \ln \lambda) \,,
\end{aligned}
$$

at $x = 0$, and,

$$
\begin{aligned}
\psi &= 0 \,, \\
np &= 1 \,, \\
\frac{\partial^2 \psi}{\partial x^2} &= 0 \,,
\end{aligned}
$$

at $x = a$. In the following analysis small bulk trap levels, $\alpha \to 0$, are considered and $\beta, \gamma \gg 1$.

5.1 Short Time Solution.

A time scale in which a depletion layer is forming is considered. The solution is found to have five boundary layers, and in figure 5.1 is an illustration of the regions. First, is the outer neutral layer far away from the oxide-semiconductor interface. Then, approaching the interface, is a minority diffusion region where the minority carriers diffuse towards the depletion layer. The transition layer, similar in structure to Chapter 3 and centered about $s(t)$, exists at the edge of the depletion layer and moves as the region widens. The depletion layer is similar in structure to the layers in the previous chapters and is depleted of charge. Finally, very close to the oxide

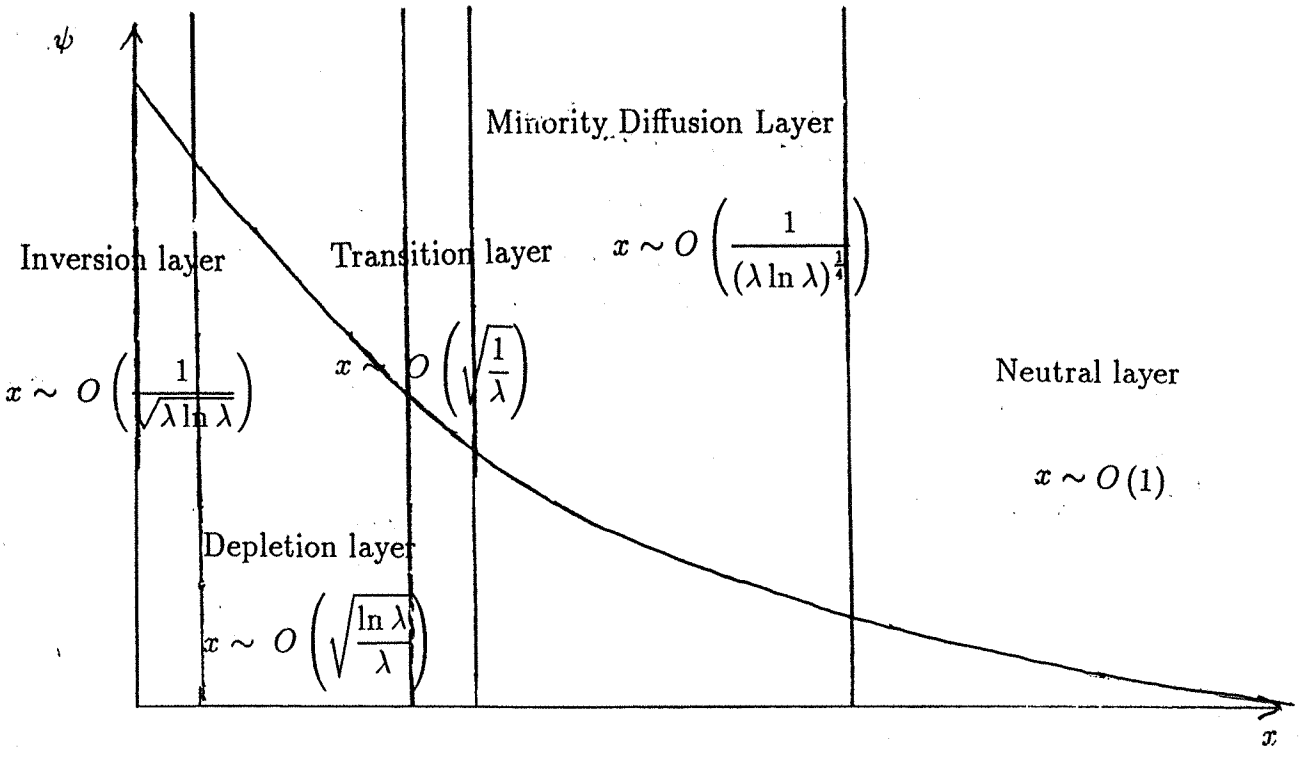

Figure 5.1: Sketch of the five layers found in the transient problem with full ionisation of the dopant energy level.

interface, is the inversion layer, where the minority carriers collect. However, on this time scale the carriers do not have enough time to collect and the concentration remains small.

To get an idea of the structure of the solution, and to find the necessary scalings for the time t etc. the simplified problem of a depletion layer and neutral region is considered. The problem is therefore,

$$\begin{aligned} \frac{\partial^2 \psi}{\partial x^2} &= \lambda \,, \\ -\frac{J_p}{\mu} &= p\frac{\partial \psi}{\partial x} \,, \\ \frac{\partial p}{\partial t} + \beta \frac{\partial J_p}{\partial x} &= 0 \,, \end{aligned}$$

in the depletion layer, and,

$$\begin{aligned} 0 &= -p + \lambda \,, \\ -\frac{J_p}{\mu} &= p\frac{\partial \psi}{\partial x} \,, \\ \frac{\partial p}{\partial t} + \beta \frac{\partial J_p}{\partial x} &= 0 \,, \end{aligned}$$

in the neutral layer, subject to,

$$p = \lambda \,,$$

$$np = 1 \ ,$$

$$J_p = 0 \ ,$$

$$\psi = 0 \ ,$$

at t=0.

$$\frac{\partial \psi}{\partial x} = h\sqrt{\frac{\lambda}{\ln \lambda}}\left(\psi - v \ln \lambda\right) \ ,$$

$$J_p = 0 \ ,$$

at x=0, and,

$$\psi = 0 \ ,$$

$$np = 1 \ ,$$

$$\frac{\partial \psi}{\partial x^2} = 0 \ ,$$

at x=a.

The following conditions across the transition layer are also imposed,

$$\text{(i)} \qquad \text{at } x = s(t) \qquad [\psi] = 0 \ ,$$

$$\text{(ii)} \qquad \text{as } x \rightarrow s(t)^{+} \qquad \mu\beta \frac{\partial \psi}{\partial x} = -\frac{ds}{dt} \ ,$$

$$\text{(iii)} \qquad \text{as } x \rightarrow s(t)^{-} \qquad \frac{\partial \psi}{\partial x} \rightarrow 0 \ .$$

Solving in the neutral region,

$$p = \lambda \ , \qquad \psi = \frac{(x)\,\psi\,(s\,(t))}{a} \ .$$

The depletion layer problem is then the moving boundary layer problem,

$$\frac{\partial^2 \psi}{\partial x^2} = \lambda \ ,$$

$$p = \lambda \ ,$$

with,

$$\frac{\partial \psi}{\partial x} = h\sqrt{\frac{\lambda}{\ln \lambda}}\left(\psi - v \ln \lambda\right) \ ,$$

at $x = 0$, and,

$$\frac{\partial \psi}{\partial x} = 0 \ ,$$

at $x = s(t)$, Using condition (ii), an equation for the movement of the transition layer is found,

$$\frac{ds}{dt} = \frac{\mu\beta\psi(s(t))}{a} .$$

Imposing the initial condition $s(0) = 0$, $s(t)$ is given by,

$$\sqrt{\frac{\lambda}{\ln\lambda}}s(t) = \frac{2vh\left(1 - \exp\left(-\sqrt{2v + h^{-2}}\frac{\mu\beta}{a}\sqrt{\lambda\ln\lambda}t\right)\right)}{\left(\left(\sqrt{2vh^2+1}+1\right) - \left(1 - \sqrt{2vh^2+1}\right)\exp\left(-\sqrt{2v + h^{-2}}\frac{\mu\beta}{a}\sqrt{\lambda\ln\lambda}t\right)\right)} .$$

The above calculation gives,

$$x = \sqrt{\frac{\ln\lambda}{\lambda}}\grave{x} ,$$

for the depletion layer scaling, and,

$$t = \frac{1}{\beta\sqrt{\lambda\ln\lambda}}\bar{t} .$$

for the time scaling.

5.2 The neutral layer

$$t = \tfrac{1}{\beta\sqrt{\lambda\ln\lambda}} . \qquad x = O(1) .$$

$$n = \tfrac{1}{\lambda}\hat{n} . \qquad p = \lambda\hat{p} .$$

$$J_n = \tfrac{\ln\lambda}{\lambda}\hat{J}_n . \qquad J_p = \lambda\ln\lambda\hat{J}_p .$$

$$\psi = \ln\lambda\,\hat{\psi} .$$

The following highest order equations for the system are obtained,

$$-\hat{p} + 1 = 0 . \tag{5.1}$$

$$\hat{J}_n = -\hat{n}\frac{\partial\hat{\psi}}{\partial\hat{x}} . \tag{5.2}$$

$$-\frac{\hat{J}_p}{\mu} = \hat{p}\frac{\partial\hat{\psi}}{\partial\hat{x}} . \tag{5.3}$$

$$\frac{\partial \hat{n}}{\partial \hat{t}} = 0 . \tag{5.4}$$

$$\frac{\partial \hat{p}}{\partial \hat{t}} = 0 . \tag{5.5}$$

In addition, to next order,

$$\frac{\partial \hat{n}}{\partial \hat{x}} = 0 , \tag{5.6}$$

and,

$$\frac{\partial^2 \hat{\psi}_0}{\partial x^2} = 0 . \tag{5.7}$$

These equations can now easily be solved. From equation (5.1),

$$\hat{p} = 1 .$$

Equations (5.4) and (5.6) imply,

$$\hat{n} = 1 .$$

From equation (5.7) the voltage is found to be linear,

$$\hat{\psi} = A\hat{x} + B .$$

But $\hat{\psi} = 0$ at $x = a$, giving,

$$B = -aA .$$

It can be seen the electron and hole currents are purely functions of $\bar{t}$,

$$\hat{J}_n = f(\bar{t}) , \qquad \hat{J}_p = g_p(\bar{t}) ,$$

where,

$$f(\bar{t}) = \frac{g_p(\bar{t})}{\mu} .$$

The solution to this system of equations is therefore,

$$\hat{\psi} = \frac{g_p(\bar{t})}{\mu}(a - x) .$$

$$\hat{n} = 1 .$$

$$\hat{p} = 1 .$$

$$\hat{J}_n = \frac{g_p(\bar{t})}{\mu} .$$

$$\hat{J}_p = g_p(\bar{t}) .$$

5.3 The minority diffusion layer

$$t = \frac{\breve{t}}{\beta\sqrt{\lambda \ln \lambda}} . \qquad x = \frac{1}{(\lambda \ln \lambda)^{\frac{1}{4}}} \breve{x} .$$

$$\psi = \frac{\ln \lambda a g_p}{\mu} + (\lambda)^{-\frac{1}{4}} (\ln \lambda)^{\frac{3}{4}} \breve{\psi} .$$

$$n = \frac{1}{\lambda} \breve{n} . \qquad J_p = \lambda \ln \lambda \breve{J}_p .$$

$$p = \lambda \breve{p} . \qquad J_n = (\lambda)^{-\frac{3}{4}} (\ln \lambda)^{\frac{1}{4}} \breve{J}_n .$$

With these scalings, the highest order equations are,

$$\breve{p} = 1 . \tag{5.8}$$

$$\breve{J}_n = \frac{\partial \breve{n}}{\partial \breve{x}} . \tag{5.9}$$

$$-\frac{\breve{J}_p}{\mu} = \breve{p} \frac{\partial \breve{\psi}}{\partial \breve{x}} . \tag{5.10}$$

$$\frac{\partial \breve{J}_p}{\partial \breve{x}} = 0 . \tag{5.11}$$

$$\frac{\partial \breve{n}}{\partial \breve{t}} - \frac{\partial \breve{J}_n}{\partial \breve{x}} = 0 . \tag{5.12}$$

In addition, to the next order,

$$\frac{\partial^2 \breve{\psi}}{\partial \breve{x}^2} = 0 . \tag{5.13}$$

From equation (5.13),

$$\breve{\psi} = \frac{g_p(\bar{t})}{\mu} (a - x) .$$

From equations (5.8) and (5.11) it can be deduced the hole concentration and current remain unchanged,

$$\breve{p} = 1 , \qquad \breve{J}_p = g_p(\bar{t}) .$$

Combining equations (5.8) and (5.9) it is found,

$$\frac{\partial \breve{n}}{\partial \breve{t}} = \frac{\partial^2 \breve{n}}{\partial \breve{x}^2} .$$

The boundary conditions for this equation now need to be determined. From the overall boundary conditions,

$$n = \frac{1}{\lambda}\,, \qquad \text{at } t = 0\,, \qquad \Rightarrow \breve{n} = 1\,.$$

Approaching the depletion layer,

$$\breve{x} \sim O\left(\frac{(\ln\lambda)^{\frac{3}{4}}}{\lambda^{\frac{1}{4}}}\right)\,,$$

and,

$$\breve{n} \to (\lambda \ln\lambda)^{-\frac{1}{4}}\,.$$

Therefore, to highest order, the boundary conditions are,

$$\breve{n} = 1 \text{ at } \breve{t} = 0,$$

$$\breve{n} = 0 \text{ on } \breve{x} = 0.$$

This equation can now be solved by finding a similarity solution, using the method of stretchings.

$$T = \epsilon^{\alpha}\breve{t}, \qquad X = \epsilon^{\beta}\breve{x}, \qquad N = \epsilon^{\gamma}\breve{n}.$$

The choice of solution must also leave the boundary conditions unchanged. Therefore,

$$\epsilon^{-\gamma}N = \frac{1}{\lambda} \qquad \text{at } \breve{t} = 0\,, \qquad \Rightarrow \quad \gamma = 0\,.$$

Transforming the above equation using the stretchings provided gives,

$$\epsilon^{\alpha}\frac{\partial N}{\partial T} = \epsilon^{2\beta}\frac{\partial^2 N}{\partial X^2}\,, \qquad \Rightarrow \quad \alpha = 2\beta\,.$$

Therefore, if $n(x,t)$ is a solution, then so is $N(X,T)$, since the transformation leaves the original equation invariant. $N\left(\epsilon^{\beta}\breve{x}, \epsilon^{\alpha}\breve{t}\right)$ is then a solution. To reduce the equation to an ordinary differential equation,

$$\epsilon^{\alpha t} = 1\,, \qquad \Rightarrow \qquad \epsilon = t^{-\frac{1}{\alpha}}\,.$$

Substituting this new variable into the equation gives a second order ordinary differential equation in terms of ν, where $\nu = \breve{x}\breve{t}^{-\frac{1}{2}}$,

$$\frac{d^2N}{d\nu^2} + \frac{1}{2}\nu\frac{dN}{d\nu} = 0, \qquad \Rightarrow \qquad \frac{d}{d\nu}\left(\frac{\partial N}{\partial \nu}e^{\frac{1}{4}\nu^2}\right) = 0.$$

Therefore,

$$\frac{dN}{d\nu}e^{\frac{1}{4}\nu^2} = A.$$

$$N = A\int_B^{\nu} e^{-\frac{1}{4}u^2}du.$$

The boundary conditions must also be transformed in terms of this new variable.

$$\breve{t} = 0\,, \qquad \Rightarrow \quad \nu \to \infty\,,$$

and

$$\breve{x} = 0\,, \qquad \Rightarrow \quad \nu = 0\,,$$

giving,

$$N \to 1\,, \qquad \text{as} \quad \nu \to \infty\,,$$
$$N = 0\,, \qquad \text{at} \quad \nu = 0\,,$$

for the boundary conditions. The second boundary condition gives immediately $B = 0$. Applying the other boundary condition gives,

$$1 = A\int_0^{\infty} e^{-\frac{1}{4}u^2}du.$$

However, using the following substitution,

$$s = \frac{1}{2}u,$$

it is found,

$$1 = A\int_0^{\infty} 2e^{-s^2}ds\,, \qquad \Rightarrow\ A = \frac{1}{\sqrt{\pi}}\,.$$

However, $\nu = \frac{\breve{x}}{\sqrt{\breve{t}}}$, giving,

$$\breve{n}\left(\breve{x},\breve{t}\right) = erf\left(\frac{\breve{x}}{2\sqrt{\breve{t}}}\right),$$

for the concentration. Now the electron concentration, $\breve{J}_n$, is found. Referring to equation (5.9),

$$\breve{J}_n = \frac{\partial \breve{n}}{\partial \breve{x}},$$

and substituting for $\breve{n}$, it is found,

$$\begin{aligned}\breve{J}_n &= \frac{2}{\sqrt{\pi}}\frac{\partial}{\partial \breve{x}}\left(\int_0^{\frac{\breve{x}}{2\sqrt{\breve{t}}}} e^{-u^2}du\right)\,. \\ &= \frac{2}{\sqrt{\pi}}\frac{1}{2\sqrt{\breve{t}}}e^{-\left(\frac{\breve{x}^2}{4\breve{t}}\right)}\,.\end{aligned}$$

Thus, the solutions in this layer are,

$$\begin{aligned}
\breve{\psi} &= \frac{g_p(\bar{t})}{\mu}(a-x) \ . \\
\breve{n}\left(\breve{x},\breve{t}\right) &= erf\left(\frac{\breve{x}}{2\sqrt{\breve{t}}}\right) \ . \\
\breve{p} &= 1 \ . \\
\breve{J}_n &= \frac{1}{\sqrt{\pi\bar{t}}} e^{\left(-\frac{\breve{x}^2}{4\bar{t}}\right)} \ . \\
\breve{J}_p &= g_p(\bar{t}) \ .
\end{aligned}$$

5.4 The Transition Layer

$$\begin{aligned}
t &= \tfrac{1}{\beta\sqrt{\ln\lambda}}\bar{t} \ . & x &= \sqrt{\tfrac{\ln\lambda}{\lambda}}s + \tfrac{1}{\sqrt{\lambda}}\bar{x} \ . \\
\psi &= \tfrac{ag_p}{\mu}\ln\lambda + \bar{\psi} \ . & & \\
n &= \lambda^{-\frac{5}{4}}(\ln\lambda)^{\frac{1}{4}}\bar{n} \ . & J_n &= \lambda^{-\frac{3}{4}}(\ln\lambda)^{\frac{1}{4}}\bar{J}_n \ . \\
p &= \lambda\bar{p} \ . & J_p &= \lambda\ln\lambda\bar{J}_p \ .
\end{aligned}$$

The first order equations are,

$$\frac{\partial^2\bar{\psi}}{\partial\bar{x}^2} = -\bar{p}+1 \ . \tag{5.14}$$

$$\bar{J}_n = \frac{\partial\bar{n}}{\partial\bar{x}} - \bar{n}\frac{\partial\bar{\psi}}{\partial\bar{x}} \ , \tag{5.15}$$

$$0 = \frac{\partial\bar{p}}{\partial\bar{x}} + \bar{p}\frac{\partial\bar{\psi}}{\partial\bar{x}} \ , \tag{5.16}$$

$$0 = \frac{\partial\bar{J}_n}{\partial\bar{x}} \ , \tag{5.17}$$

$$0 = \frac{\partial\bar{J}_p}{\partial\bar{x}} - \frac{\partial\bar{p}}{\partial\bar{x}}\frac{ds}{dt} \ . \tag{5.18}$$

In obtaining the above equations care is taken transforming from the unscaled variables to the scaled ones, since the x variable contains a function of time $s = s(\bar{t})$. For example, the hole concentration,

$$P = P(x(\bar{x}, \bar{t}), \bar{t}) \ ,$$

is related to,

$$p(\bar{x}, \bar{t}) \ ,$$

by,

$$\frac{\partial p(\bar{x}, \bar{t})}{\partial \bar{t}} = \frac{\partial P(x, \bar{t})}{\partial \bar{t}} + \frac{\partial P(x, \bar{t})}{\partial x} \frac{\partial x}{\partial \bar{t}} \ ,$$

where,

$$\frac{\partial x}{\partial \bar{t}} = \sqrt{\frac{\ln \lambda}{\lambda}} \frac{ds}{d\bar{t}} \ ,$$

Therefore,

$$\frac{\partial P}{\partial \bar{t}} = \frac{\partial \bar{p}}{\partial \bar{t}} - \sqrt{\ln \lambda} \frac{\partial \bar{p}}{\partial \bar{x}} \frac{ds}{d\bar{t}}.$$

Considering $\bar{p}$ to be a function of $\bar{\psi}$ and $\bar{t}$, then,

$$\frac{\partial \bar{p}}{\partial \bar{x}} = \frac{\partial \bar{p}}{\partial \bar{\psi}} \frac{\partial \bar{\psi}}{\partial \bar{x}}.$$

Transforming equation (5.16), it is found,

$$\begin{aligned} 0 &= \frac{\partial \bar{\psi}}{\partial \bar{x}} \frac{\partial \bar{p}}{\partial \bar{\psi}} + \bar{p} \frac{\partial \bar{\psi}}{\partial \bar{x}} \ , \\ &= \frac{\partial \bar{\psi}}{\partial \bar{x}} \left(\frac{\partial \bar{p}}{\partial \bar{\psi}} + \bar{p} \right) \ , \qquad \text{where } \tfrac{\partial \bar{\psi}}{\partial \bar{x}} \neq 0 \ , \\ \Rightarrow \qquad & \frac{\partial \bar{p}}{\partial \bar{\psi}} = -\bar{p} \ . \end{aligned}$$

Therefore,

$$-\ln \bar{p} = \bar{\psi} + A.$$

To match into the neutral layer $\bar{\psi} \to 0$, and $\bar{p} \to 1$. Thus, $A = 0$ and,

$$\bar{p} = e^{-\bar{\psi}}.$$

Equation (5.18) can be re-written,

$$\frac{\partial}{\partial \bar{x}} \left(\bar{J}_p - \bar{p} \frac{ds}{d\bar{t}} \right) = 0 \ .$$

Integrating with respect to $\bar{x}$ gives,

$$\bar{J}_p - \bar{p}\frac{ds}{d\bar{t}} = f(\bar{t}) .$$

Matching into the neutral layer $\bar{\psi} \to 0$, $\bar{p} \to 1$ and $\bar{J}_p \to g_p(\bar{t})$ giving,

$$f(\bar{t}) = g_p(\bar{t}) - \frac{ds}{d\bar{t}} ,$$

for the arbitrary function. The hole current is therefore,

$$\bar{J}_p = (\bar{p} - 1)\frac{ds}{d\bar{t}} + g_p(\bar{t}) .$$

Referring to (5.14) and noting $\bar{p} = e^{-\hat{\psi}}$ it is found,

$$\frac{\partial^2 \bar{\psi}}{\partial \bar{x}^2} = -e^{\bar{\psi}} + 1 .$$

Integrating with respect to x gives,

$$\frac{1}{2}\frac{\partial \bar{\psi}}{\partial \bar{x}}^2 = e^{-\bar{\psi}} + \bar{\psi} + C .$$

Matching into the neutral region $\bar{\psi} \to 0$, and $\frac{\partial \bar{\psi}}{\partial \bar{x}} \to 0$, giving $C = -1$. Re-arranging the above integral gives,

$$-\left(\sqrt{2}\bar{x} - \sqrt{2}\bar{x}_1\right) = \int_{\bar{\psi}(\bar{x}_1)}^{\bar{\psi}} \frac{dy}{\sqrt{(e^{-y} + y - 1)}} .$$

The negative root is chosen since the gradient is known to be negative. Referring to equation (5.15), $\bar{n}$ is found from,

$$\sqrt{\frac{1}{\pi \bar{t}}} = \frac{\partial \bar{n}}{\partial \bar{x}} - \bar{n}\frac{\partial \bar{\psi}}{\partial \bar{x}} .$$

This is a straight forward integrating factor equation, giving,

$$\frac{\partial}{\partial \bar{x}}\left(e^{-\bar{\psi}}\bar{n}\right) = \sqrt{\frac{1}{\pi \bar{t}}}e^{-\bar{\psi}} .$$

On integrating,

$$e^{-\bar{\psi}}\bar{n} = \sqrt{\frac{1}{\pi \bar{t}}}\int_{C_*}^{\bar{x}} e^{-\bar{\psi}} dx , \qquad \Rightarrow \bar{n} = \sqrt{\frac{1}{\pi \bar{t}}}e^{\bar{\psi}(\bar{x})}\int_{C_*}^{\bar{x}} e^{-\bar{\psi}(x)} dx .$$

Matching into the depletion layer C_* is found. In summary, the solution to the transition layer system is,

$$
\begin{aligned}
-\sqrt{2}\bar{x} + \sqrt{2}\bar{x}_1 &= \int_{\bar{\psi}(\bar{x}_1)}^{\bar{\psi}} \frac{dy}{\sqrt{(e^{-y} + y - 1)}} \, . \\
\bar{n} &= \sqrt{\frac{1}{\pi \bar{t}}} e^{\bar{\psi}(\bar{x})} \int_{C_*}^{\bar{x}} e^{-\bar{\psi}(x)} dx \, . \\
\bar{p} &= e^{-\bar{\psi}} \, . \\
\bar{J}_n &= g_p(\bar{t}) \, . \\
\bar{J}_p &= (\bar{p} - 1) \frac{ds}{d\bar{t}} + g_p(\bar{t}) \, .
\end{aligned}
$$

5.5 Depletion Layer

$$
t = \tfrac{1}{\beta\sqrt{\lambda \ln \lambda}} \grave{t} \, . \qquad x = \sqrt{\tfrac{\ln \lambda}{\lambda}} \grave{x}
$$

$$
\psi = \ln \lambda \grave{\psi} \, .
$$

$$
n = \lambda^{-\frac{5}{4}} (\ln \lambda)^{-\frac{1}{4}} \grave{n}. \qquad p = \lambda e^{\ln \lambda \phi_p} \, .
$$

$$
J_n = \lambda^{\frac{-3}{4}} (\ln \lambda)^{\frac{1}{4}} J_n. \qquad J_p = \lambda \ln \lambda e^{\ln \lambda \phi_p} j_p \, .
$$

The highest order equations are,

$$
1 = \frac{\partial^2 \grave{\psi}}{\partial \grave{x}^2} \, . \tag{5.19}
$$

$$
\grave{J}_n = -\grave{n} \frac{\partial \grave{\psi}}{\partial \grave{x}} \, . \tag{5.20}
$$

$$
0 = \frac{\partial \phi_P}{\partial \grave{x}} + \frac{\partial \grave{\psi}}{\partial \grave{x}} \, . \tag{5.21}
$$

$$
0 = \frac{\partial \phi_P}{\partial \bar{t}} + \frac{\partial \phi_P}{\partial \grave{x}} j_p \, . \tag{5.22}
$$

$$
0 = \frac{\partial \grave{J}_n}{\partial \grave{x}} \, . \tag{5.23}
$$

From equation (5.23),

$$\grave{J}_n = g_p(\bar{t}) \ .$$

To match into the transition layer, $\grave{J}_n$ must be given by,

$$\grave{J}_n = \sqrt{\frac{1}{\pi \bar{t}}} \ ,$$

From equation (5.19) the voltage is found to quadratic,

$$\grave{\psi} = \frac{1}{2}\grave{x}^2 + a\grave{x} + b \ .$$

Substituting the voltage and electron current solutions into equation (5.20),

$$\grave{n} = \frac{-1}{\grave{x} + a}\sqrt{\frac{1}{\pi \bar{t}}} \ ,$$

is found to be the electron concentration. Using equation (5.21) gives,

$$\frac{\partial}{\partial \grave{x}}\left(\phi_P + \grave{\psi}\right) = 0 \ , \qquad \Rightarrow \quad \phi_P + \grave{\psi} = f(\bar{t}) \ .$$

Matching into the other layers ϕ_P and j_p are found. The solution to the system is given by,

$$\begin{aligned}
\grave{\psi} &= \frac{1}{2}\grave{x}^2 + a\grave{x} + b \ . \\
\grave{n} &= \frac{-1}{\grave{x} + a}\sqrt{\frac{1}{\pi \bar{t}}} \ . \\
p &= \lambda e^{\ln \lambda \phi_P} \ . \\
\grave{J}_n &= g_p(\bar{t}) \ . \\
\grave{J}_p &= \lambda \ln \lambda e^{\ln \lambda \phi_P} j_p \ .
\end{aligned}$$

5.6 Inversion Layer

$$t = \frac{1}{\beta\sqrt{\lambda \ln \lambda}}\grave{t} \; . \qquad\qquad x = \sqrt{\frac{1}{\lambda \ln \lambda}}\tilde{x} \; .$$

$$\psi = \psi(0) + \tilde{\psi} \; .$$

$$n = \lambda^{-\frac{3}{4}}(\ln \lambda)^{\frac{1}{4}}\tilde{n} \; . \qquad\qquad p = \lambda e^{\ln\lambda\left(\frac{ag_p}{\mu} - \frac{\psi}{\ln\lambda}\right)} \; .$$

$$J_n = \lambda^{\frac{-3}{4}}(\ln \lambda)^{\frac{1}{4}}\tilde{J}_n \; . \qquad J_p = \lambda \ln \lambda e^{-\frac{1}{2}s^2 \ln\lambda} j_p \; .$$

The highest order equations are,

$$0 = \frac{\partial^2 \tilde{\psi}}{\partial \tilde{x}^2} \; . \tag{5.24}$$

$$0 = \frac{\partial \tilde{n}}{\partial \tilde{x}} - \tilde{n}\frac{\partial \tilde{\psi}}{\partial \tilde{x}} \; . \tag{5.25}$$

$$0 = \frac{\partial \tilde{n}}{\partial \tilde{t}} - \frac{\partial \tilde{J}_n}{\partial \tilde{x}} \; . \tag{5.26}$$

$$0 = \frac{\partial p}{\partial \tilde{t}} + \frac{\partial J_p}{\partial \tilde{x}} \; . \tag{5.27}$$

$$0 = \frac{\partial p}{\partial \tilde{x}} + p\frac{\partial \tilde{\psi}}{\partial \tilde{x}} \; . \tag{5.28}$$

From equation (5.24) the voltage is found to be linear,

$$\tilde{\psi} = a\tilde{x} \; .$$

In the depletion layer,

$$\grave{\psi} = \frac{1}{2}\grave{x}^2 - s\grave{x} + \left(\frac{1}{2}s^2 + \frac{\epsilon g}{\mu}\right) \; .$$

Replacing these variables with the inversion layer variables, and simplifying, it is found,

$$\frac{\psi(0)}{\ln\lambda} + \frac{\tilde{\psi}}{\ln\lambda} = \frac{1}{2}\frac{\tilde{x}^2}{(\ln\lambda)^2} - \frac{s\tilde{x}}{\ln\lambda} + \frac{1}{2}s^2 + \frac{\epsilon g}{\mu} \; .$$

For these regions to match,

$$\psi(0) = \ln\lambda\left(\frac{1}{2}s^2 + \frac{\epsilon g}{\mu}\right) \; ,$$

and,

$$a = -s \ .$$

Expressing the boundary condition,

$$\frac{\partial \psi(0)}{\partial x} = h\sqrt{\frac{\lambda}{\ln \lambda}}\left(\psi(0) - v \ln \lambda\right) \ ,$$

in terms of the inversion layer variables,

$$\sqrt{\lambda \ln \lambda}\frac{\partial \tilde{\psi}(0)}{\partial \tilde{x}} = h\sqrt{\frac{\lambda}{\ln \lambda}}\left(\psi(0) - v \ln \lambda\right) \ ,$$

implies,

$$\frac{\partial \tilde{\psi}}{\partial \tilde{x}} = h\left(\frac{1}{2}s^2 + \frac{a g_p}{\mu} - v\right) \ .$$

When matching this layer into the depletion region g_p is found to be $\frac{ds}{d\bar{t}}$, also $\frac{\partial \tilde{\psi}}{\partial \tilde{x}} = -s$, giving,

$$-s = h\left(\frac{1}{2}s^2 + \frac{a}{\mu}\frac{ds}{d\bar{t}} - v\right) \ ,$$

which is the equation satisfied by $s(\bar{t})$ in the simplified depletion-neutral layer problem at the beginning of the chapter.

Since,

$$p = \lambda e^{\ln \lambda\left(\frac{a g_p}{\mu} - \frac{\psi}{\ln \lambda}\right)} \ ,$$

and,

$$\psi = \ln \lambda\left(\frac{1}{2}s^2 + \frac{a g_p}{\mu}\right) - s\tilde{x} \ ,$$

then,

$$p = \lambda e^{-\frac{1}{2}s^2 \ln \lambda} e^{s\tilde{x}} \ .$$

Equation (5.27) becomes, to highest order,

$$-s\frac{ds}{d\bar{t}}e^{s\tilde{x}} + \frac{\partial j_p}{\partial \tilde{x}} = 0/; \ , \qquad \Rightarrow \quad \tilde{J}_p = e^{s\tilde{x}}\frac{ds}{d\bar{t}} + h(\bar{t}) \ .$$

However, at $\tilde{x} = 0$, $\tilde{J}_p = 0$, giving,

$$h(\bar{t}) = -\frac{ds}{d\bar{t}} \ .$$

The hole current is therefore,

$$J_p = \lambda \ln \lambda e^{-\frac{1}{2}s^2 \ln \lambda}\frac{ds}{d\bar{t}}\left(e^{s\tilde{x}} - 1\right) \ .$$

Next the electron current and concentration are solved. From equation (5.25),

$$0 = \frac{\partial \tilde{n}}{\partial \tilde{x}} - \tilde{n}\frac{\partial \tilde{\psi}}{\partial \tilde{x}} ,$$

but,

$$\frac{\partial \tilde{\psi}}{\partial \tilde{x}} = -s ,$$

therefore,

$$\frac{\partial \tilde{n}}{\partial \tilde{x}} = -\tilde{n}s , \qquad \Rightarrow \qquad \tilde{n} = A(\bar{t})\, e^{-s\tilde{x}} .$$

Substituting the electron concentration into equation (5.26) gives,

$$\frac{dA}{d\bar{t}} e^{-s\bar{t}} - A\frac{ds}{d\bar{t}}\tilde{x}e^{-s\tilde{x}} = \frac{\partial \tilde{J}_n}{\partial \tilde{x}} .$$

This can be integrated, and the electron current is given by,

$$-\frac{1}{s}\frac{dA}{d\bar{t}}e^{-s\bar{t}} + A\frac{ds}{d\bar{t}}\frac{\tilde{x}}{s}e^{-s\tilde{x}} + A\frac{ds}{d\bar{t}}\frac{1}{s^2}e^{-s\tilde{x}} - B(\bar{t}) = \tilde{J}_n .$$

Imposing the boundary condition,

$$\tilde{J}_n = 0 , \qquad \text{at} \quad \tilde{x} = 0 , \qquad \Rightarrow \qquad B(\bar{t}) = -\frac{dA}{d\bar{t}}\frac{1}{s} + A\frac{ds}{d\bar{t}}\frac{1}{s^2} .$$

Matching into the depletion layer the function $A(\bar{t})$ is found. The solution to the inversion layer system is,

$$\tilde{\psi} = -s\tilde{x} .$$

$$\tilde{n} = A(\bar{t})\, e^{-s\tilde{x}} .$$

$$p = \lambda e^{-\frac{1}{2}s^2 \ln\lambda} e^{s\tilde{x}} .$$

$$\tilde{J}_n = -\frac{1}{s}\frac{dA}{d\bar{t}}e^{-s\bar{t}} + A\frac{ds}{d\bar{t}}\frac{\tilde{x}}{s}e^{-s\tilde{x}} + A\frac{ds}{d\bar{t}}\frac{1}{s^2}e^{-s\tilde{x}} + \frac{dA}{d\bar{t}}\frac{1}{s} - A\frac{ds}{d\bar{t}}\frac{1}{s^2} .$$

$$J_p = \lambda \ln\lambda e^{-\frac{1}{2}s^2 \ln\lambda}\frac{ds}{d\bar{t}}\left(e^{s\tilde{x}} - 1\right) .$$

5.7 Matching The Solutions

5.7.1 The Transition and Depletion Layers

The voltage in the transition layer is described by,

$$-\sqrt{2}\bar{x} + \sqrt{2}\bar{x}_1 = \int_{\bar{\psi}(\bar{x}_1)}^{\bar{\psi}} \frac{dy}{\sqrt{(e^{-y} + y - 1)}} .$$

Approaching the depletion layer from the transition region it can be shown,

$$\bar{\psi} \to \infty ,$$

and the integral equation's highest order behaviour is,

$$\int_{\bar{\psi}(\bar{x}_1)}^{\bar{\psi}} \frac{dy}{\sqrt{(e^{-y} + y - 1)}} \sim \int_{\bar{\psi}(\bar{x}_1)}^{\bar{\psi}} \frac{dy}{\sqrt{y}} + O(1) ,$$

$$\Rightarrow \quad -\sqrt{2}\bar{x} = 2\sqrt{\bar{\psi}} ,$$

to highest order. Therefore, approaching the depletion layer $\bar{\psi}$, to highest order,

$$\bar{\psi} = \frac{1}{2}\bar{x}^2 .$$

In the depletion layer $\grave{\psi}$ is quadratic,

$$\grave{\psi} = \frac{1}{2}\grave{x}^2 + a\grave{x} + b .$$

Expressing these variables in terms of the transition variables,

$$\bar{\psi} = \frac{1}{2}\bar{x}^2 + \bar{x}\left(\sqrt{\lambda}\delta s + a\sqrt{\ln\lambda}\right) + \frac{1}{2}\lambda\delta^2 s^2 + a\sqrt{\lambda \ln\lambda}\delta s + \ln\lambda\left(b - \frac{\epsilon g}{\mu}\right) .$$

To ensure the solutions match the co-efficients of $\bar{x}$ are equated. Co-efficients of $\bar{x}$,

$$\sqrt{\ln\lambda}\,(\delta s + a) = 0 , \quad \Rightarrow \quad \delta\sqrt{\frac{\lambda}{\ln\lambda}}s + a = 0 .$$

Letting $\delta = \sqrt{\frac{\ln\lambda}{\lambda}}$, gives,

$$a = -s .$$

Co-efficients of $\bar{x}_0$,

$$\ln\lambda\left(\frac{1}{2}s^2 + as + b - \frac{ag_p}{\mu}\right) = 0 , \quad \Rightarrow \quad \frac{1}{2}s^2 + as + b - \frac{ag_p}{\mu} = 0 ,$$

giving,

$$b = \frac{1}{2}s + \frac{ag_p}{\mu} .$$

The electron concentration is now matched. In the depletion region,

$$\grave{n} = \frac{1}{s - \grave{x}}\sqrt{\frac{1}{\pi \bar{t}}} .$$

Approaching the transition layer the depletion region solution is expressed in terms of the transition layer variables. Since,

$$\grave{x} = s + \frac{1}{\sqrt{\ln \lambda}}\bar{x} , \qquad \grave{n} = \sqrt{\ln \lambda}\bar{n} ,$$

the depletion layer solution is given by,

$$\bar{n} = \frac{1}{\bar{x}}\sqrt{\frac{1}{\pi \bar{t}}} , \tag{5.29}$$

in this overlap region. In the transition layer,

$$\bar{n} = \sqrt{\frac{1}{\pi \bar{t}}} e^{\bar{\psi}(\bar{x})} \int_{C_*}^{\bar{x}} e^{-\bar{\psi}(x)} dx .$$

Approaching the depletion region $\bar{\psi} \to \infty$, and the highest order behaviour of the above equation for $\bar{n}$ is found. Since,

$$-\sqrt{2}\bar{x} = \int^{\bar{\psi}} \frac{e^{-y}}{\sqrt{e^{-y} + y - 1}} dy ,$$

the equation for $\bar{n}$ is expressed in terms of $\bar{\psi}$.

$$\bar{n} = \sqrt{\frac{1}{\pi \bar{t}}} \frac{-1}{\sqrt{2}} \int_A^{\bar{\psi}} \frac{e^{-y}}{\sqrt{e^{-y} + y - 1}} dy .$$

The integral can be re-written,

$$\begin{aligned} \int_A^{\bar{\psi}} \frac{e^{-y}}{\sqrt{e^{-y} + y - 1}} dy &= \int_A^{\infty} \frac{e^{-y}}{\sqrt{e^{-y} + y - 1}} dy \\ &- \int_{\bar{\psi}}^{\infty} \frac{e^{-y}}{\sqrt{e^{-y} + y - 1}} dy . \end{aligned}$$

But in the limit as $\bar{\psi} \to \infty$,

$$\int_{\bar{\psi}}^{\infty} \frac{e^{-y}}{\sqrt{e^{-y} + y - 1}} dy \sim \int_{\bar{\psi}}^{\infty} \frac{e^{-y}}{\sqrt{y - 1}} dy = \frac{2}{e} \int_{(\bar{\psi}-1)^{\frac{1}{2}}}^{\infty} e^{-u^2} du .$$

It can be shown that in the limit as $\bar{\psi} \to \infty$,

$$\frac{2}{e}\int_{\left(\bar{\psi}-1\right)^{\frac{1}{2}}}^{\infty} e^{-u^2}du \sim \left[-\frac{e^{-u^2}}{2u}\right] = \frac{e^{-\left(\bar{\psi}-1\right)}}{\sqrt{2\left(\bar{\psi}-1\right)}} .$$

Therefore, approaching the depletion layer from the transition region, the electron concentration is, to highest order,

$$\bar{n} = -\sqrt{\frac{1}{2\pi\bar{t}}}e^{\bar{\psi}}\left(\int_A^{\infty}\frac{e^{-y}}{\sqrt{e^{-y}+y-1}}dy - \frac{e^{-\bar{\psi}}}{\sqrt{\bar{\psi}-1}}\right) .$$

In this overlap region,

$$\sqrt{\bar{\psi}-1} \sim \sqrt{\bar{x}} .$$

Therefore,

$$\bar{n} \sim -\sqrt{\frac{1}{2\pi\bar{t}}}e^{\bar{\psi}}\left(\int_A^{\infty}\frac{e^{-y}}{\sqrt{e^{-y}+y-1}}dy - \frac{e^{-\bar{\psi}}}{\frac{\bar{x}}{\sqrt{2}}}\right) .$$

To match into the depletion region this equation is equated with equation (5.29), giving $A = \infty$. This corresponds to $C_* = -\infty$.

The hole concentrations are now matched. In the depletion layer,

$$p = \lambda e^{\ln\lambda\left(-\grave{\psi}+f\right)} .$$

and in the transition layer,

$$p = \lambda e^{-\bar{\psi}} .$$

Expressing $\grave{\psi}$ in terms of $\bar{\psi}$,

$$\grave{\psi} = \frac{ag_p}{\mu} + \frac{\bar{\psi}}{\ln\lambda} ,$$

and substituting into the equation for the depletion layer hole concentration it is found,

$$p = \lambda e^{\ln\lambda\left(\frac{-ag_p}{\mu}-\frac{\bar{\psi}}{\ln\lambda}+f\right)} .$$

For the two regions to match,

$$f = \frac{ag_p}{\mu} .$$

The hole current is now matched. In the depletion layer,

$$\frac{\partial\phi_p}{\partial\bar{t}} + j_p\frac{\partial\phi_p}{\partial\grave{x}} = 0 , \tag{5.30}$$

where,

$$\phi_p = f\left(\bar{t}\right) - \grave{\psi} .$$

However,

$$f(\bar{t}) = \frac{ag_p}{\mu} ,$$

and $\grave{\psi}$ is quadratic in the depletion region, giving,

$$\phi_p = -\frac{1}{2}\grave{x}^2 + s\grave{x} - \frac{1}{2}s^2 .$$

Using this in equation (5.30) the above equation for ϕ_p is,

$$\frac{ds}{d\bar{t}}\grave{x} - s\frac{ds}{d\bar{t}} + \grave{j}_p(-\grave{x} + s) = 0 , \qquad \Rightarrow \quad \grave{j}_p = \frac{ds}{d\bar{t}} .$$

The hole current in the depletion region is therefore,

$$\grave{J}_p = e^{\ln\lambda\left(\frac{ag_p}{\mu} - \grave{\psi}\right)}\grave{j}_p .$$

Expressing the depletion layer variables in terms of the transition layer variables,

$$\bar{J}_p = e^{-\bar{\psi}}\frac{ds}{d\bar{t}} .$$

However, in the transition layer,

$$\bar{J}_p = \left(e^{-\bar{\psi}} - 1\right)\frac{ds}{d\bar{t}} + g_p .$$

For these two regions to match,

$$g_p = \frac{ds}{d\bar{t}} .$$

5.7.2 The Inversion and Depletion Layers

In the depletion layer the hole current is given by,

$$J_p = \lambda \ln\lambda e^{\ln\lambda\left(\frac{ag_p}{\mu} - \grave{\psi}\right)}\frac{ds}{d\bar{t}} ,$$

where $\grave{\psi}$ is,

$$\grave{\psi} = \frac{1}{2}\grave{x}^2 - s\grave{x} + \frac{1}{2}s^2 + \frac{ag_p}{\mu} .$$

Expressing the depletion layer voltage in terms of the inversion layer voltage,

$$\grave{\psi} = \frac{1}{2}s^2 + \frac{ag_p}{\mu} - \frac{s\tilde{x}}{\ln\lambda} + O\left(\frac{1}{(\ln\lambda)^2}\right) ,$$

the hole current is,

$$J_p \rightarrow \lambda \ln \lambda e^{-\frac{1}{2}s^2 \ln \lambda} e^{s\tilde{x}} \frac{ds}{d\bar{t}} .$$

In the inversion layer the hole current is,

$$J_p = \lambda \ln \lambda e^{-\frac{1}{2}s^2 \ln \lambda} \left(e^{s\tilde{x}} - 1 \right) \frac{ds}{d\bar{t}} ,$$

and approaching the depletion layer, ($\tilde{x} \rightarrow \ln \lambda \grave{x}$), the hole current becomes,

$$J_p \sim \lambda \ln \lambda e^{-\frac{1}{2}s^2 \ln \lambda} e^{s\tilde{x}} ,$$

which matches with the depletion layer. The electron current in the depletion region is,

$$\grave{J}_n = \sqrt{\frac{1}{\pi \bar{t}}} ,$$

and the equation for the electron current in the inversion layer is,

$$-\frac{1}{s}\frac{dA}{d\bar{t}} e^{-s\tilde{x}} + A\frac{ds}{d\bar{t}}\frac{\tilde{x}}{s} e^{-s\tilde{x}} + A\frac{ds}{d\bar{t}}\frac{1}{s^2} e^{-s\tilde{x}} = \tilde{J}_n + B(\bar{t}) .$$

Approaching the depletion layer from the inversion layer, ($\tilde{x} \rightarrow \infty$), it is found,

$$\tilde{J}_n \rightarrow -B(\bar{t}) ,$$

where,

$$B(\bar{t}) = \frac{dA}{d\bar{t}}\frac{1}{s} - A\frac{ds}{d\bar{t}}\frac{1}{s^2} .$$

For the two layers to match,

$$\frac{1}{s}\frac{dA}{d\bar{t}} - \frac{A}{s^2}\frac{ds}{d\bar{t}} = \sqrt{\frac{1}{\pi \bar{t}}} .$$

Thus,

$$\frac{d\left(\frac{A}{s}\right)}{d\bar{t}} = \sqrt{\frac{1}{\pi \bar{t}}} . \qquad \Rightarrow \quad A = 2s\sqrt{\frac{\bar{t}}{\pi}} .$$

The solution for the electron concentration in the inversion layer cannot be matched directly into the depletion region and an intermediate layer is needed. This layer is very thin and a distance x_1 into the depletion region. Between these two regions is another layer that is essentially a depletion region but with a larger electron concentration. This layer is referred to as the essentially depleted region. The scalings for x and ψ are,

$$x = \sqrt{\frac{\ln \lambda}{\lambda}} \bar{x_1} + \frac{1}{\sqrt{\lambda \ln \lambda}} \check{x} , \quad \psi = \psi(x_1) + \check{\psi} ,$$

where it is found $\bar{x_1} = s - \sqrt{s^2 - \left(1 + \frac{\ln(\ln\lambda)}{\ln\lambda}\right)}$. To highest order the equation for the electron concentration is,

$$\check{J}_n = \frac{\partial \check{n}}{\partial \check{x}} - \check{n}\frac{\partial \check{\psi}}{\partial \check{x}} , \tag{5.31}$$

where,

$$\check{J}_n = \sqrt{\frac{1}{\pi \bar{t}}} , \qquad \text{and} \qquad \frac{\partial \check{\psi}}{\partial \check{x}} = \bar{x_1} - s .$$

Substituting these values into equation (5.31) the electron concentration becomes,

$$\check{n} = \frac{1}{s - \bar{x_1}}\sqrt{\frac{1}{\pi \bar{t}}} + C(\bar{t})\, e^{-(s-\bar{x_1})\check{x}} .$$

The region between the inversion and intermediate layers is essentially a depletion region but the electron concentration is scaled,

$$n = \lambda^{-\frac{5}{4}}(\ln\lambda)^{-\frac{1}{4}} e^{\ln\lambda \alpha_p} .$$

To highest order the equation for the electron concentration in this region becomes,

$$\frac{\partial \alpha_p}{\partial \grave{x}} - \frac{\partial \grave{\psi}}{\partial \grave{x}} = 0 , \qquad \Rightarrow \quad \alpha_p = \grave{\psi} + v(\bar{t}) ,$$

where,

$$\grave{\psi} = \frac{1}{2}\grave{x}^2 - s\grave{x} + \frac{1}{2}s^2 + \frac{a g_p}{\mu} .$$

The arbitrary function is found by matching into the inversion layer. Approaching the inversion region,

$$e^{\ln\lambda\left(\grave{\psi} + v(\bar{t})\right)} \rightarrow e^{\ln\lambda\left(\frac{1}{2}s^2 + \frac{a g_p}{\mu} + v(\bar{t})\right)} e^{-s\tilde{x}} .$$

However,

$$e^{\ln\lambda\left(\grave{\psi} + v(\bar{t})\right)} = \sqrt{\lambda \ln\lambda}\,\tilde{n} ,$$

giving,

$$\grave{n} = \frac{1}{\sqrt{\lambda \ln\lambda}} e^{\ln\lambda\left(\frac{1}{2}s^2 + \frac{a g_p}{\mu} + v(\bar{t})\right)} e^{-s\tilde{x}} .$$

For the two layers to match,

$$e^{\ln\lambda v(\bar{t})} = 2s\sqrt{\frac{\bar{t}}{\pi}} e^{\ln\lambda\left(\frac{1}{2} + \frac{1}{2}\frac{\ln(\ln\lambda)}{\ln\lambda} - \frac{1}{2}s^2 - \frac{a g_p}{\mu}\right)} .$$

This solution is matched into the thin intermediate layer. Approaching this layer from the essentially depleted region end,

$$e^{\ln\lambda\left(\grave{\psi} + v(\bar{t})\right)} \rightarrow e^{\psi(\bar{x_1}) + \ln\lambda v(\bar{t})} e^{-(s-\bar{x_1})\check{x}} .$$

The intermediate layer solution is given by,

$$\check{n} = \frac{1}{s - \bar{x_1}} \sqrt{\frac{1}{\pi \bar{t}}} + C\left(\bar{t}\right) e^{-(s-\bar{x_1})\check{x}} ,$$

and approaching the inversion layer ($\check{x} \to -\ln\lambda\left(\bar{x_1} - \grave{x}\right)$), to highest order,

$$\check{n} = C\left(\bar{t}\right) e^{-(s-\bar{x_1})\check{x}} .$$

For the solutions to match,

$$C = e^{\psi(\bar{x_1}) + \ln\lambda v(\bar{t})} ,$$

where,

$$e^{\ln\lambda v(\bar{t})} = 2s\sqrt{\frac{\bar{t}}{\pi}} e^{\ln\lambda\left(\frac{1}{2} + \frac{1}{2}\frac{\ln(\ln\lambda)}{\ln\lambda} - \frac{1}{2}s^2 - \frac{agp}{\mu}\right)} .$$

This gives an equation to find both C and x_1. Since,

$$e^{\ln\lambda v(\bar{t})} = 2s\sqrt{\frac{\bar{t}}{\pi}} e^{\ln\lambda\left(\frac{1}{2} + \frac{1}{2}\frac{\ln\ln\lambda}{\ln\lambda} - \frac{1}{2}s^2 - \frac{agp}{\mu}\right)} ,$$

and,

$$e^{\psi(\bar{x_1})} = e^{\ln\lambda\left(\frac{1}{2}\bar{x_1}^2 - s\bar{x_1} + \frac{1}{2}s^2 + \frac{agp}{\mu}\right)} .$$

then,

$$C = 2s\sqrt{\frac{\bar{t}}{\pi}} , \qquad \text{and} \quad \frac{1}{2}\bar{x_1}^2 - s\bar{x_1} + \frac{1}{2}\left(1 + \frac{\ln(\ln\lambda)}{\ln\lambda}\right) = 0 .$$

From this quadratic $\bar{x_1}$ is found to be,

$$s - \sqrt{s^2 - \left(1 + \frac{\ln\ln\lambda}{\ln\lambda}\right)} .$$

Chapter 6

Conclusions.

It is the purpose of this chapter to bring together the results developed and presented earlier in this thesis. The first part of this chapter reviews the results of the problems investigated in the previous chapters. These descriptions are qualitative in nature in order that the reader can acquire a general physical understanding of the processes involved. At the end of this chapter there is a section outlining some possible avenues of future research that are relevant to the problem areas studied in this document.

In Chapter 3 it was found, by the use of matched asymptotic expansions, that the electric potential across the MOS capacitor in equilibrium has an inversion-depletion-transition-neutral layer structure. In the neutral layer the space charge and corresponding electric field are small. In the depletion region the electric field is large and repels the holes into the neutral layer and attracts the electrons towards the semiconductor-oxide interface. The remaining fixed dopant ions in this region give rise to the large space charge. The analysis demonstrated that the depletion and neutral layers are separated by a very thin transition region. This layer is similar in nature to the transition layer in [21]. Its presence enables the electric potential in the depletion and neutral regions to be smoothly matched. Across the transition layer the hole concentration changes rapidly from a large value in the neutral layer to a small value in the depletion region. This concentration gradient gives rise to a hole diffusion current. In equilibrium throughout the device the drift-diffusion currents balance to give no net movement of charge. The electric field present in the transition region gives rise to an equal but opposite drift of holes into the neutral region which balances with the diffusion current out of the neutral layer. In the classical delta-depletion approximation of these devices the continuity of the hole concentration breaks down at the neutral-depletion layer interface as well as the balance in the drift-diffusion currents. The asymptotic analysis reveals that the results of the depletion layer approximation are valid, in that the behaviour

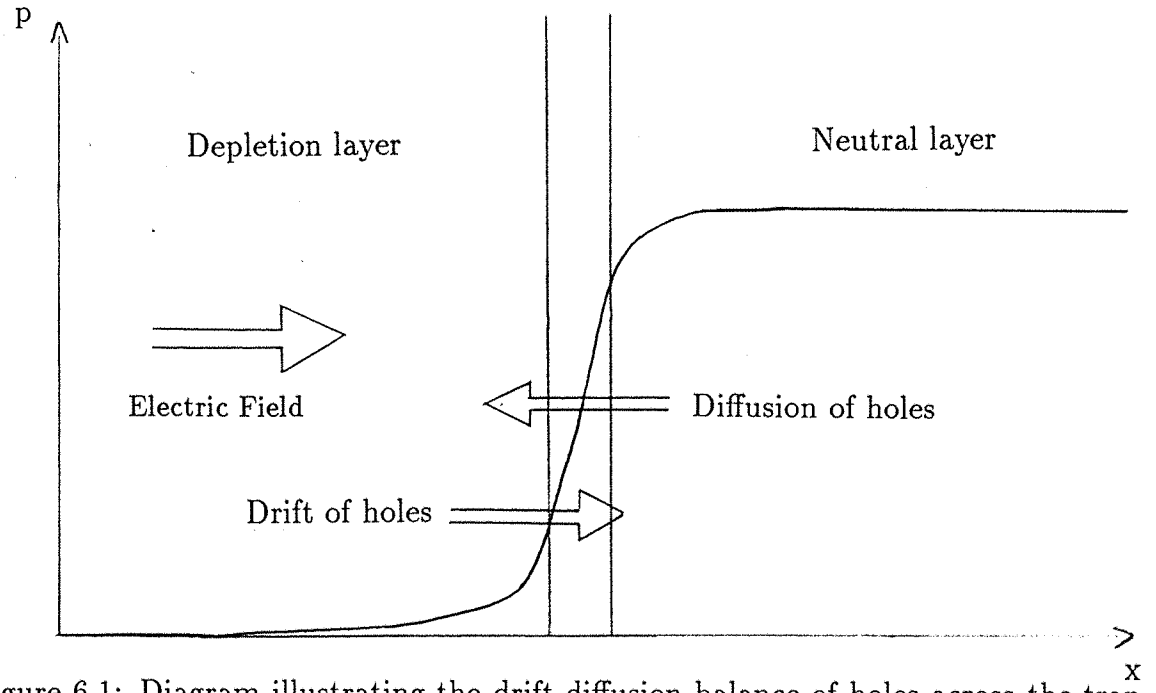

Figure 6.1: Diagram illustrating the drift-diffusion balance of holes across the transition layer.

in the depletion and neutral layers is correct, but that care should be taken in interpreting the behaviour of the neutral-depletion interface. Finally, at the semiconductor-oxide interface there is a thin inversion layer. The electric field attracts the electrons across the device towards this layer. If the gate electric potential is large enough the concentration of electrons in this region is greater than the bulk hole concentration. The asymptotic analysis shows that this inversion layer is narrow compared to the depletion layer and hence the convention of neglecting its width is valid. Again care should be taken in interpreting the depletion layer approximation near this region.

The analysis of the steady fully ionised MOS device is therefore in agreement with the conventional depletion layer approximation but gives additional details of the behaviour throughout the device.

In Chapter 4, the conditions on the MOS device are relaxed to allow for partial ionisation of the dopant atoms. The resulting structure of the solution is similar to that of Chapter 3. The degree of ionisation can be reduced by considering the single dopant energy level to move away from the band edges. The main change is that the transition region of the completely ionised problem spreads out under partial ionisation and can become wider than the depletion region. In this transition region a large proportion of dopant atoms are not ionised and they therefore possess no net charge. Here, the growth of the electric potential is slow. However, a point is reached when the occupation of the dopant energy level changes rapidly. This very thin 'ionisation' layer is where the majority of dopant atoms are ionised through the

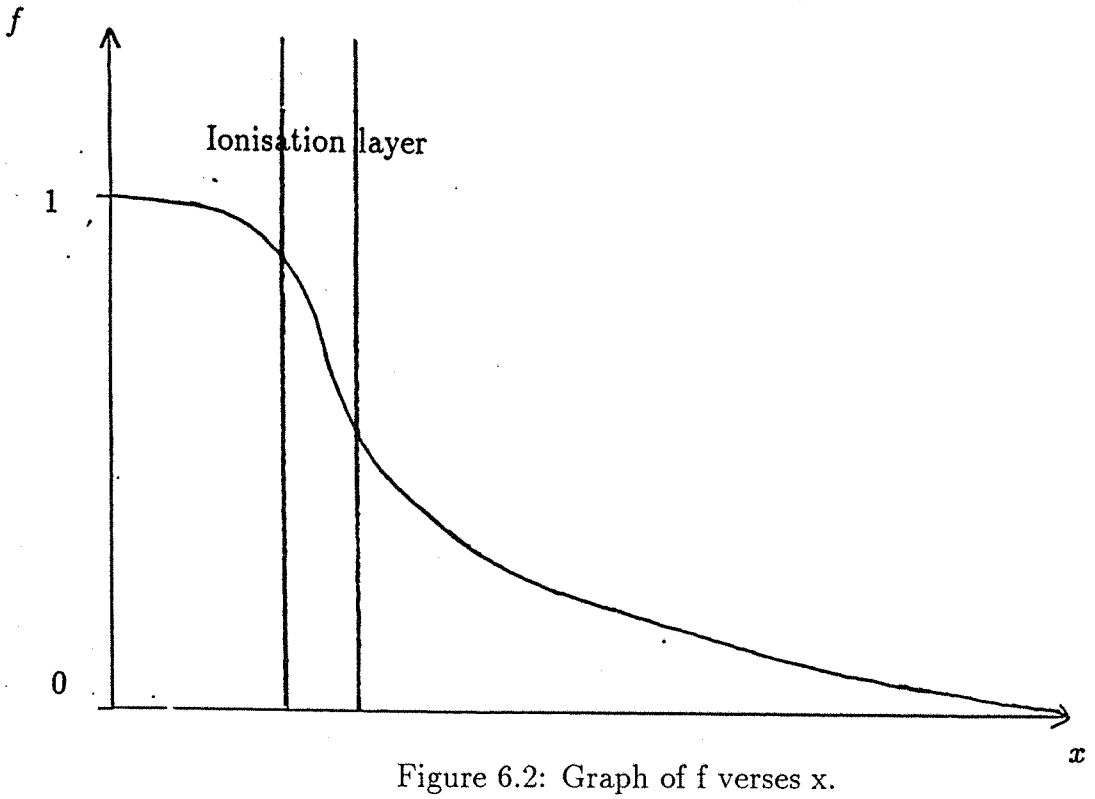

Figure 6.2: Graph of f verses x.

release of carriers and sits between the transition and depletion layers. Figure 6.2 shows qualitatively how the dopant occupancy function changes as a function of distance from the semiconductor-oxide interface. In the depletion and inversion layers the dopant is fully ionised, to highest order, and their characteristics are similar in nature to the depletion and inversion layers of the fully ionised problem.

Finally, in Chapter 5, the fully ionised MOS device of Chapter 3 is considered during a voltage transient. The inversion-depletion-transition-neutral layer structure is found to persist but there is an extra region separating the neutral and transition layers, (the minority diffusion region). Because of the transient nature of the problem the transition layer, centered about $s(t)$, is found to move as the depletion layer extends into the device, (see figure 6.3). In the neutral layer the electric potential is linear in x, the hole and electron concentrations are at their equilibrium levels, and the currents are purely time dependent. An electron concentration gradient is present between the neutral layer, where the concentration is relatively small, and the transition layer, where it is extremely small. This gradient is accommodated in a region between the neutral and transition layers, called the 'minority diffusion' layer, (see figure 6.4), where the electrons diffuse towards the transition region and an electron diffusion current results. When the electrons have diffused into the transition layer the large electric field sweeps them across and into layer at the semiconductor-oxide interface. On the time-scale considered here the electron current is relatively small and so the electron concentration remains small. As a result in the electric potential is unaffected by the electron current and the inversion layer is not present in the manner described in Chapter 3. The depletion layer therefore grows to a greater thickness than its steady-state value. This

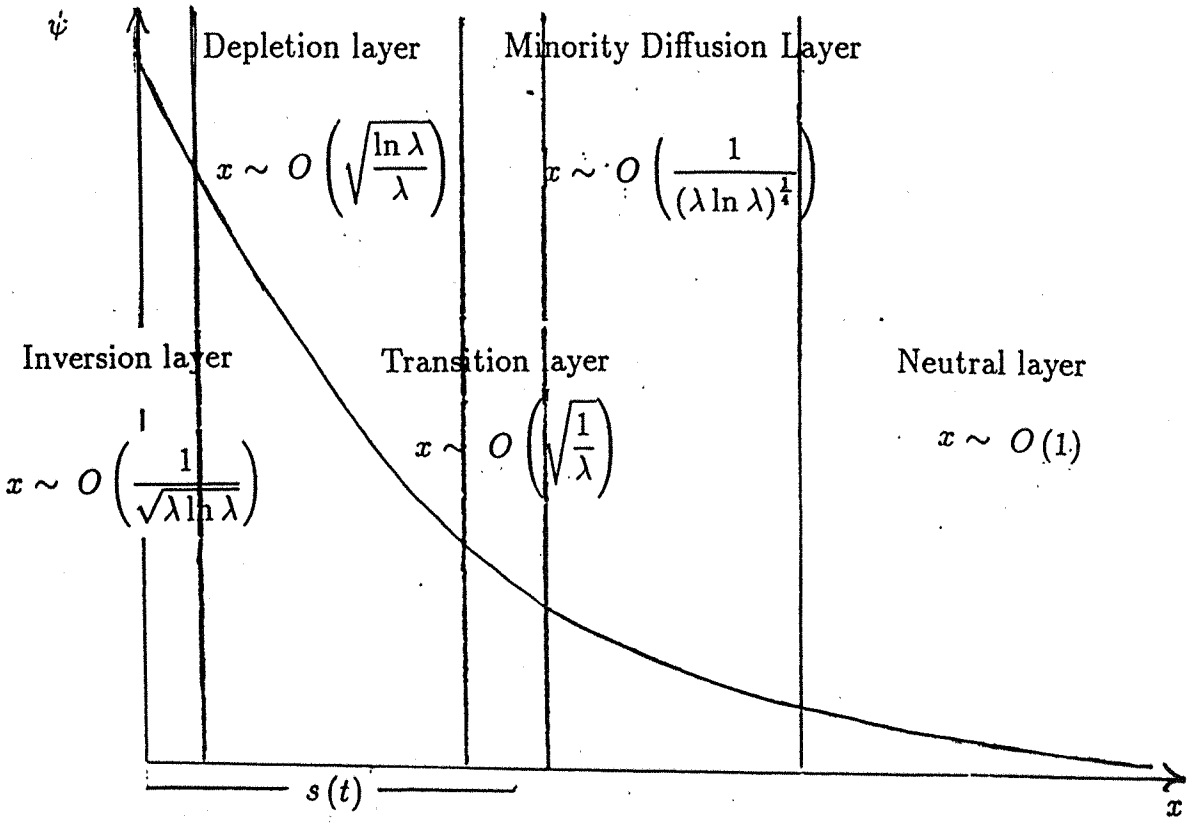

Figure 6.3: Sketch of the five layers found in the transient problem.

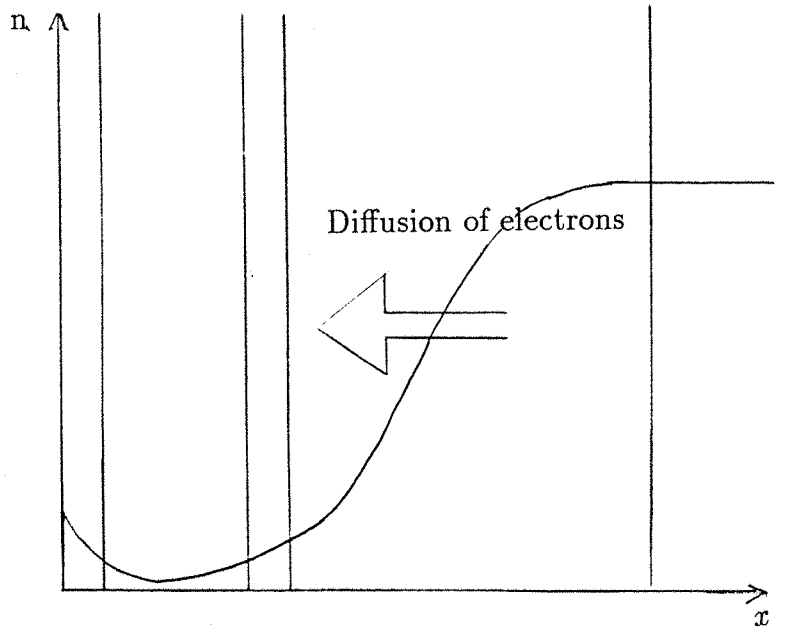

Figure 6.4: Illustration of the diffusion of electrons.

behaviour is called deep depletion. To return to steady-state it would be necessary to consider the problem on a time-scale where the electron concentration becomes comparable to, and then exceeded , the hole concentration so the inversion layer appeared. The full details of the electron potential, and more importantly the electron concentration, show why deep depletion occurs and how long it might last.

The research performed in this document compares favourably to the delta-depletion approximation. This approximation is a very simple but effective description of the structure of the MOS capacitor. However, the existence of the transition layer is needed to ensure that the solution is continuous everywhere.

Future Research.

Considering the full transient amorphous system of equations, when a continuous distribution of states is coupled into the device equations, is an extremely complicated problem. It seems sensible to continue to consider some of the simpler cases to gain further insight into how to approach and solve the full amorphous system.

The research undertaken in this document can be categorised into two cases namely steady-state and transient. Below is an outline of how the research might proceed.

1)Steady-state Case.

The major simplification of the steady-state case is that the trap occupancy is an algebraic function of the carrier concentration.

Chapters 3 and 4 investigated both the full and partial ionisation of the single dopant energy level in the steady-state case, respectively. As a first step the trap concentrations were taken to be sufficiently small for the recombination of carriers to be negligible. This made all currents zero to first order and the problem of the occupancy of traps was decoupled. However, the behaviour of the traps has not been analyzed.

It will be necessary to determine an appropriate trap distribution for further analysis to proceed. As described in the defect pool model of Chapter 2 the usual sort of distribution consists of two exponential tail band states extending out of the conduction and valence bands and a Gaussian distribution of states located near to the middle of the band gap.

Subsequently, the assumption of small trap concentrations could be relaxed and the behaviour with recombination could be approached.

2)Transient Case.

The major simplification in the transient case has been to decouple the problem for the trap occupancy by assuming small trap concentrations. This meant, to first order, no recombination of carriers. In addition, the complete ionisation of the dopant energy level was assumed. As in the steady-state case above, investigations into the behaviour of the traps has not been undertaken.

A first relatively simple problem to study is the long time behaviour of the deeply depleted MOS device. Electrons to fill the inversion layer could be considered to appear from the existing minority diffusion layer or the model could be expanded to allow for some small recombination.

Before approaching the full problem of recombination the the partial ionisation of the dopant atoms could be considered, as in the steady-state case of Chapter 4.

APPENDIX A

Below is a list of the variables used in the full amorphous silicon problem.

t	–	time , (s) .
$\psi(x)$	–	the voltage at a point x within the semiconductor substrate , (V) .
n	–	the electron concentration , (cm^{-3}) .
p	–	the hole concentration , (cm^{-3}) .
J_n	–	the electron current density , (A cm^{-2}) .
J_p	–	the hole current density , (A cm^{-2}) .
f_a	–	the probability an acceptor type trap is occupied by an electron.
f_d	–	the probability a donor type trap is occupied by an electron.
E_C	–	the energy of the lower edge of the conduction band , (eV) .
E_V	–	the energy of the upper edge of the valence band , (eV) .
E_i	–	the intrinsic Fermi level , (eV) .
$N_{ta}(E)$	–	the concentration of acceptor type traps at energy E , (cm^{-3}) .
$N_{td}(E)$	–	the concentration of donor type traps at energy E (cm^{-3}) .
μ_n	–	the electron mobility , $\left(cm^{-2}V^{-1}s^{-1}\right)$.
μ_p	–	the hole mobility , $\left(cm^{-2}V^{-1}s^{-1}\right)$.
ϵ	–	the permeativity of the semiconductor , (F) .

σ_{na} – the electron capture cross-section for an acceptor type trap , (cm^2) .

σ_{nd} – the electron capture cross-section for a donor type trap , (cm^2) .

σ_{pa} – the hole capture cross-section for an acceptor type trap , (cm^2) .

σ_{pd} – the hole capture cross-section for a donor type trap , (cm^2) .

v_{th} – the thermal velocity of carriers , ($cm\ s^{-1}$) .

q – electronic charge , (C) .

APPENDIX B

Below is a table comparing the range of parameter sizes for crystalline and amorphous silicon.

Parameter	Crystal range	Amorphous range
λ	$10^4 - 10^9$	$10^8 - 10^{14}$
β	1.2×10^9	90
α	$10^2 - 10^4$	10^{14}
μ	0.3	0.1
γ	20	40
σ_1	1	1
σ_2	0.1	0.1
σ_3	1	1

Bibliography

[1] P.G. LeComber, W.E. Spear, and A. Ghaith. Amorphous Silicon Field Effect Device and Possible Application. Electron Lett., vol 15, pp. 179-181, 1979.

[2] Robert F. Pierrot. Field Effect Devices. Addison-Wesley, 1990.

[3] S.M. Sze. Semiconductor Devices: Physics and Technology. Wiley and Sons, New York, 1986.

[4] S.M. Sze. Physics of Semiconductor Devices. Wiley and Sons, New York, 1981.

[5] P. A. Markowich. The Semiconductor Device Equations. Wien-New York, Springer 1982.

[6] J.E. Carrol Physical Models for Semiconductor Devices. 1974.

[7] M.J. Powell. The Physics of Amorphous Silicon Thin Film Transistors. I.E.E.E Transactions on Electron Devices. p. 2753-2763, Vol.36, No: 12, DEC. 1989.

[8] M. Thompson. The Physics and Applications of Amorphous Silicon Thin Film Transistors and Image Sensors. Proc. of the Int. Workshop on Amorphous Semiconductors, pp. 289-298. 1987.

[9] W. Shockely and W.T. Hall Statistics of Recombinations of Holes and electrons. Phys.Rev, Vol.87, pp 835-842, SEPT. 1952.

[10] J. Furlan. Charge Carrier Dynamic Nonequilibrium in Amorphous Semiconductors. I.E.E.E. Transactions on Electron Devices. Vol.39, No:2, p. 448-450, FEB. 1992.

[11] G.W. Taylor and J.G. Simmons. Basic Equations For Statistics, Recombination Processes, and Photoconductivity in Amorphous Insulators and Semiconductors. J.Non-Crys. Solids. **8-10**, 1972, p. 940-946.

[12] G.W. Taylor and J.G. Simmons. Theory of steady State Photoconductivity in Amorphous Semiconductors. J.Non-Crys. Solids. **8-10**, 1972, p. 945-953.

[13] J.G. Simmons and G.W. Taylor. Nonequilibrium Steady-State Statistics and Associated Effects for Insulators and Semiconductors Containing an Arbitrary Distribution of Traps. Phys.Rev. vol.4, No.2, p. 502-511 JUL. 1971.

[14] J.G. Shaw, M. Hack, P.G. Lecomber, and M. Willlums. Density of States and Transient Simulations of Amorphous-Silicon devices. J.Non.Crys. Solids. 137-138, (1991) p. 1233-1236.

[15] F.R. Shapiro and Y. Bar-Yam. Microscopic Transient Simulation of Semiconductors and Insulators. J.Non.Crys. Solids. **64**, p. 2185-2188, AUG. 1988.

[16] R. Sokel and R.C. Hughes. J.Appl.Phys. **53**, 7414 (1982).

[17] G. Seynhaeve, R.P. Barclay, and G.J. Adriaenssens, J.Non.Crys. Solids, 97-98, p. 706, (1987).

[18] C. van Berkel. Deep Trapping Controlled Switching Characteristics in Amorphous Silicon Thin Film Transistors. J.Non.Crys. Solids. **66**, p. 4488-4494, NOV. 1989.

[19] J.M. Marshall. Transient Photoconductivity and Thermalization in Amorphous Semiconductors. Philosophical Magazine B, 1983, Vol.47, No.5, p. 471-480.

[20] M.G. Hack, A.G. Lewis, and J.G. Shaw. Influence of Traps on the Characteristics of Thin Film transistors. J.Non.Crys. Solids 137-138, p. 1229-1232, (1991).

[21] C.P. Please. An Analysis of Semiconductor P-N Junctions. I.M.A. J.Appl.Maths. 28, p. 301-318, (1982).

[22] C. van Berkel and M.J. Powell. Resolution of Amorphous Silicon Thin Film Transistor Instability Mechanisms Using Ambipolar Transistors Appl.Phys.Lett. **51** (14), p. 1094-1096, OCT. 1987.

[23] M.J. Powell. Bias Dependence of Instability Mechanisms in Amorphous Silicon Thin Film Transistors. Appl.Phys.Lett. **51** (16), p. 1242-1244, OCT. 1987.

[24] S.C. Deane, M.J. Powell, J.R. Hughes, and I.D. French. Thermal Bias Evidence for the Defect Pool in Amorphous Silicon Thin Film Transistors. Appl.Phys.Lett. **57** (14), p.1416-1418, OCT. 1990.

[25] M.J. Powell, C. van Berkel, and J.R. Hughes. Time and Temperature Dependence of Instability Mechanisms in Amorphous Silicon Thin Film Transistors. Appl.Phys.Lett. **54** (14), p. 1323-1325, APR. 1989.

[26] K. Winer. Defect Formation in a-Si:H Phys.Rev.B, Vol.41, No.17, JUN. 1990.

[27] K. Winer. Defect Pool Model of Defect Formation in a-Si:h. J.Non.Crys. Solids 137-138, (1991), p. 157-162.

[28] R.A Street and K. Winer. Defect Equilibria in Undoped a-Si:H. Phys.Rev.B, Vol.40, No.9, p. 6237-6249.

[29] M.J Powell, C. van Berkel, and A.R. Franklin. Defect Pool in Amorphous Thin Film Transistors. Phys.Rev.B, Vol.45, No.8, p. 4160-4170.

[30] W.B. Jackson. Role of Band Tail Carriers in Metastable Defect Formation and Annealing in Hydrogenated Amorphous silicon. Phys.Rev.B, vol.41, No.2, 1990, p. 1059-1074.

[31] P.A. Markowich and C. Schmeiser. Uniform Asymptotic Representation of the basic Semiconductor Device Equations. I.M.A. J.App.Maths, 1986, **36**, p. 43-57.

[32] M.J. Ward, F.M. Odeh, and D.S. Cohen. Asymptotic Methods for Metal Oxide Semiconductor Field Effect Transistor Modelling. SIAM J.Appl.Math. Vol.50, No.4, pp. 1099-1125, AUG. 1990.

[33] M.J. Ward. Singular Perturbation and a Free Boundary Problem in the Modelling of Field Effect Transistors. SIAM J.Appl.Math. vol.52, No.1, pp. 112-139, FEB. 1992.

[34] A.S. Grove. Physics and Technology of Semiconductor Devices. Wiley. 1967.

[35] Z. Smith and S. Wagner. Phys.Rev.Lett. 59, p. 688, (1987).

[36] M. Stutzmann, Philos.Mag.B **56**, p. 63, (1987).

[37] C. Ringhofer. An Asymptotic Analysis Of A Transient p-n-Junction Model. SIAM J. Appl Math. Vol. 47, No. 3, JUN 1987 .

[38] W.B. Jackson. Role of Band-Tail Carriers in Metastable Defect Formation and Annealing in Hydrogenated Amorphous Silicon. Phys.Rev.B, Vol.41, No.2, p.1059-1075, JAN. 1990.

[39] X. Xu, A. Okumura, A. Morimoto, M. Kumeda, and T. Shimizu. Phys.Rev.B, **38**, p. 8371, (1988).

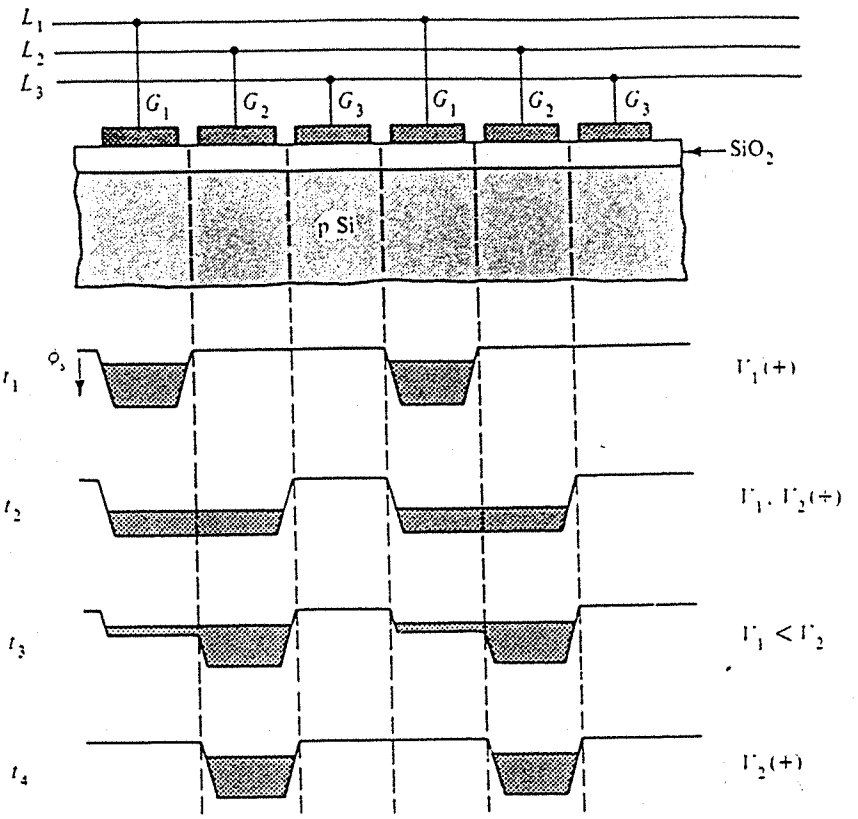

Figure 1.13: Operation of a CCD.

longer than the charge storage times involved in CCD operation. If now, a large positive clock pulse is applied to the gate electrode, a deep potential well is first created. Before inversion occurs by thermal generation, the depletion width is greater than it is at equilibrium. This is known as deep depletion. Injecting electrons into this potential well, electrically or optically, enables them to be stored there. The storage is temporary, however, because the electrons must move out to another location before thermal generation becomes appreciable. What is needed is a method for allowing charge to flow from one potential well to another quickly without losing much charge. The operation of a CCD is outlined with reference to figure 1.13. At time t_1 a positive voltage, V_1, is applied to the G_1 electrode and a charge packet is stored in corresponding G_1 potential well. At time t_2 a potential is also applied to the G_2 electrode, V_2, and the charge equalises across the common $G_1 - G_2$ well. This continues at t_3 when V_1 is reduced and thus decreases the well under G_1. More charge flows into the G_2 well and the process is completed at time t_4 when V_1 is zero. In this way charge can be injected using an input diode, transported down the line and detected at the other end.

CCD's have applications in memories, logic functions and signal processing. They are also used in imaging, where an array of photosensors are used to form charge packets proportional to the light intensity. These packets are then shifted to a detector point for readout.